creative commons
COMMONS DEED

저작자표시-비영리-변경금지 2.0 대한민국

이용자는 아래의 조건을 따르는 경우에 한하여 자유롭게

- 이 저작물을 복제, 배포, 전송, 전시, 공연 및 방송할 수 있습니다.

다음과 같은 조건을 따라야 합니다:

저작자표시. 귀하는 원저작자를 표시하여야 합니다.

비영리. 귀하는 이 저작물을 영리 목적으로 이용할 수 없습니다.

변경금지. 귀하는 이 저작물을 개작, 변형 또는 가공할 수 없습니다.

- 귀하는, 이 저작물의 재이용이나 배포의 경우, 이 저작물에 적용된 이용허락조건을 명확하게 나타내어야 합니다.
- 저작권자로부터 별도의 허가를 받으면 이러한 조건들은 적용되지 않습니다.

저작권법에 따른 이용자의 권리는 위의 내용에 의하여 영향을 받지 않습니다.

이것은 이용허락규약(Legal Code)을 이해하기 쉽게 요약한 것입니다.

Disclaimer

dCollection

Ph.D. Dissertation in Agricultural Biotechnology

Engineering of bacteriophage endolysins and their applications to control and detect foodborne pathogens

식중독균의 제어 및 검출을 위한 박테리오파지 엔도라이신의 엔지니어링 및 응용에 관한 연구

February, 2019

The Graduate School
Seoul National University
Department of Agricultural Biotechnology

Bokyung Son

Engineering of bacteriophage endolysins and their applications to control and detect foodborne pathogens

Advisor: Sangryeol Ryu

Submitting a Ph.D. Dissertation
in Agricultural Biotechnology

February, 2019

The Graduate School
Seoul National University
Department of Agricultural Biotechnology

Bokyung Son

Confirming the Ph.D. Dissertation written by
Bokyung Son
February, 2019

Chair	_____(Seal)
Vice Chair	_____(Seal)
Examiner	_____(Seal)
Examiner	_____(Seal)
Examiner	_____(Seal)

Abstract

Son, Bokyung

Department of Agricultural Biotechnology

The Graduate School

Seoul National University

As the incidence of antibiotic-resistant bacteria has become increased, phage endolysins have received considerable attention as one of the promising alternatives to antibiotics. However, the discovery of potent endolysin is challenging because it requires labor-intensive work and has difficulties in getting soluble form with high lytic activity. In this respect, modular structure of endolysin consisted of enzymatic active domain (EAD) and cell wall binding domain (CBD) provides an opportunity to develop novel endolysins by rearrangement or random mutagenesis of domains. Most staphylococcal phage endolysins consist of an N-terminal cysteine, histidine-dependent amidohydrolases/peptidase (CHAP) domain, a central amidase domain, and a CBD. Despite extensive studies using truncated staphylococcal endolysins, the precise function of the each domain, especially amidase domain, has not been determined. Understanding an

exact function of each domain is the most important factor to be considered for successful modular engineering of endolysins. For these reasons, a functional analysis of each domain of endolysins from *S. aureus* phage was performed. I found that the CHAP domain conferred the main catalytic activity of the endolysin, while the central amidase domain showed no enzymatic activity in degrading the intact *S. aureus* cell wall. However, the endolysins lacking the amidase domain had reduced hydrolytic activity compared to the full-length endolysins. The comparison of cell wall binding affinity of a CBD and an amidase plus CBD fused with a green fluorescent protein revealed that the major function of the amidase domain is to enhance the cell wall binding affinity of CBD, leading to the maximal lytic activity of endolysin. These results suggest an auxiliary role of the amidase domain of staphylococcal endolysins in cell wall binding, and can be useful information for designing effective antimicrobial and diagnostic agents against *S. aureus*. Based on these results, a random domain swapping of *S. aureus* endolysins was conducted to obtain the engineered endolysins with higher lytic activity than their parental endolysins. In random libraries, the novel chimeric endolysin, Lys109 which consists of a LysSA12 CHAP domain, a LysSA97 amidase domain and a LysSA97 CBD was selected and characterized for its staphylolytic activity. Lys109 exhibited bacterial cell lysis activity higher than its parental endolysins against *Staphylococcus*

species. In addition, the staphylococcal biofilm was effectively removed by the treatment of Lys109. The bactericidal activity of Lys109 was evaluated in foods and on stainless steel. In milk, *S. aureus* was completely destroyed within 45 min when treated with 900 nM of Lys109. The treatment of 50 nM Lys109 on the surface of pork and beef for 1 h resulted in 3-log/cm^2 and 2-log/cm^2 reduction of *S. aureus* cells, respectively. A complete bacterial elimination was observed after 1 h treatment with 100 nM of Lys109 on the stainless steel. These results propose that a novel chimeric endolysin with higher activity and solubility can be developed by a random domain swapping of endolysins and that the chimeric endolysin has a great potential as an antimicrobial agent. Next, I constructed fusion proteins consisting of two different endolysins to test their activity and stability for simultaneous control of *S. aureus* and *B. cereus*. This is the first study to generate fusion proteins with two endolysins targeting different bacterial genus. The full-length or C-terminally truncated LysB4 (LysB4EAD), an endolysin from *B. cereus*-infecting phage B4, were fused to LysSA11, an endolysin of *S. aureus*-infecting phage SA11, via a helical linker in both orientation. The fusion proteins maintained the lytic activity of their parental endolysins against both *S. aureus* and *B. cereus*, showing successfully extended antimicrobial spectrum. Among them, LysB4EAD-LysSA11 showed significantly increased thermal stability compared with its parental

endolysins and was selected for further study. LysB4EAD-LysSA11 showed high lytic activity at pH 8.0-9.0 against *S. aureus* and at pH 5.0-10.0 against *B. cereus*, but the lytic activity of the protein was decreased in the presence of 50 mM NaCl. The strong lytic activity of LysB4EAD-LysSA11 was also observed in boiled rice contaminated with *S. aureus* and *B. cereus*. In addition, the treatment of LysB4EAD-LysSA11 in the contaminated boiled rice showed the same or higher lytic activity against *S. aureus* and *B. cereus* compared to that of two parental endolysins. These results indicate that LysB4EAD-LysSA11 can be used as an effective antimicrobial agent targeting multiple pathogens. This study will be helpful to design highly specific but multifunctional antimicrobials. Lastly, CBD of LysPBC1 from *Bacillus cereus*-infecting phage PBC1 was engineered by a phage display technique to enhance its cell wall binding affinity. LysPBC1_CBD was successfully displayed on the M13 filamentous phage via pIII coat protein and the displayed protein retained its binding ability to *B. cereus*. A random mutation library of LysPBC1_CBD on phage was constructed and selected for better binding to *B. cereus* cells. Among the 10 clones selected from the library, a LysPBC1_CBD Q47H mutant showed approximately 2-fold increase in cell wall binding ability compared to LysPBC1_CBD. These results indicate that the phage display technique enables engineering CBDs to have a higher cell wall binding affinity and thus has a great potential to be

utilized in the development of effective CBD-based bioprobes. However, this approach was insufficient to reduce the number of clones nonspecifically binding to *B. cereus* at the panning steps. In order to successfully identify CBD with high cell wall binding affinity through a phage display system, further optimization of the experimental conditions is required. In this study, I engineered endolysins through multiple strategies for control and detection of foodborne pathogens and demonstrated their potentials as biocontrol agents and as bioprobes.

Keywords: *Staphylococcus aureus*, bacteriophage, endolysin, protein engineering, biocontrol, detection

Student Number: 2015-30475

Contents

List of Figures

List of Tables

I. Introduction

I.1. *Staphylococcus aureus*

Staphylococcus aureus is a human commensal and potentially lethal opportunistic pathogen that can cause wide range of infections, from superficial skin infections to life threatening diseases such as bacteremia, necrotizing pneumonia, and endocarditis (Tong, Davis, Eichenberger, Holland, & Fowler, 2015). In addition, this organism has emerged as a major pathogen for both community-associated and hospital-acquired infections (Baba et al., 2002). The rise in incidence of infection has been accompanied by emergence of antibiotic-resistant strains, in particular, methicillin-resistant *S. aureus* (MRSA) (Enright et al., 2002). There are clear medical needs for vaccines and immune therapeutics that can address the public health crisis of MRSA infections.

S. aureus is also a common causes of food poisoning causing an estimated 241,000 illnesses per year in the United States (Bennett, Walsh, & Gould, 2013) and the symptoms includes mainly abdominal cramps, nausea, and vomiting. Food-poisoning outbreaks caused by *S. aureus* have been reported in many types of food such as ice-cream, raw milk cheese, and ham products (Atanassova, Meindl, & Ring, 2001; Fetsch et al., 2014; Jørgensen, Mørk, & Rørvik, 2005). These outbreaks are due to the production of one or

more enterotoxins by the bacteria during growth. Besides, cross-contamination during food preparation and processing was another risk factor in foodborne outbreaks caused by *S. aureus* (Syne, Ramsubhag, & Adesiyun, 2013). The symptoms include mainly nausea, vomiting, abdominal cramping with or without diarrhea.

MRSA isolates have become resistant to more than 20 different antibiotics including last-resort therapeutics, vancomycin. Resistance is associated with therapeutic failure and increased mortality. Therefore, there is an urgent need for creating new antimicrobials to combat MRSA.

I.2. Bacteriophage

Bacteriophages (or phages) which specifically infect and kill bacteria are the most abundant microorganisms on the planet and are known to outnumber bacteria by an estimated ten-fold (Brüssow & Hendrix, 2002; Oliveira et al., 2013). Most phages consist of tails and icosahedral heads containing DNA or RNA. The infection starts with binding of the phage virion to specific receptors on the bacterial surface, and followed by inserting and replicating their nucleic acid into the bacterial cell (Chan, Abedon, & Loc-Carrillo, 2013). Infections are terminated by killing the host bacterial cells that they have infected. Depending on their life cycles, phages can be classified into two groups. The lytic phages repeats the cycles of self-proliferation, synchronously destroying host bacteria. In their lysogenic cycle, the phage genome is integrated into the bacterial genome, and the phage genome replicates cooperatively with the host bacteria without destroying it (Matsuzaki et al., 2005).

The emerging antibiotic-resistant bacteria has renewed the interest in phages as a natural antimicrobial agent since phages have a number of advantages over antibiotics (Carlton, 1999). Phages can be reproduced rapidly in their lysis process and can lyse only in their host range, indicating

that they do not inhibit the growth of commensal bacteria other than the host bacteria. In addition, phage products such as ListShield (Intralytix, Inc., Baltimore, MD, USA), Listex P100 (Micreos Food Safety, Wageningen, The Netherlands), EcoShield (Intralytix) and SalmoFresh (Intralytix) were approved by the US Food and Drug Administration (FDA) as GRAS (Generally Recognized as Safe) (Bai, Kim, Ryu, & Lee, 2016). However, in the view of the safety concerns, the possibility to transfer the antibiotic resistance genes, toxin genes, or virulence factors should be considered for the successful application of phages to therapeutic agents or biocontrol agents (Sulakvelidze, Alavidze, & Morris, 2001).

I.3. Bacteriophage endolysin

Endolysins are phage-derived peptidoglycan (PG) hydrolases, which are synthesized at the end of the phage replication cycles (Schmelcher, Donovan, & Loessner, 2012) and are responsible for liberating the phage progeny from the host bacteria. In this process of 'lysis from within', holin proteins are required for endolysins to cross the cytoplasmic membrane and to gain access to the PG. Holins are generally small hydrophobic proteins and they form large holes enough to allow endolysin contact to the PG at the appropriate time (Catalao, Gil, Moniz-Pereira, Sao-Jose, & Pimentel, 2013; Young, 2013). Then, endolysins rapidly degrade the PG of the host bacteria followed by osmotic cell lysis and subsequently release of progeny phage particles. When endolysins are added exogenously, immediate osmotic lysis occurs followed by the death of target cells. In addition, endolysins have a narrow host specificity and a low probability for the development of bacterial resistance (Borysowski, Weber-Dąbrowska, & Górski, 2006). For these reasons, endolysins have been considered to be one of the most promising alternatives to antibiotics.

However, the activity of endolysin is limited only to Gram-positive bacteria that can contact directly with PG. Therefore, the potential of

endolysins as alternatives to antimicrobials for controlling Gram-positive bacteria has been extensively studied. In case of Gram-negative bacteria, an outer membrane prevents an access of endolysins (Fischetti, 2010). Many researchers have made efforts to use endolysins in Gram-negative bacteria, such as combining endolysins with an outer membrane permeabilizer or a physical treatment and protein modification of endoylsins (Briers & Lavigne, 2015). In respect to protein modification, engineered endolysins, called as 'Artilysins' have been reported that they pass through the outer membrane and eventually kill the bacteria. Fusion of an outer membrane permeabilizing peptide and endolysin induced local distortion of the LPS layer and promoted uptake followed by PG degradation (Briers et al., 2014).

Endolysins from Gram-positive-infecting phages typically have the modular domain structure, comprising two or more separated domains: an enzymatically active domain (EAD) at an N-terminal region and a cell wall binding domain (CBD) at a C-terminal region (Schmelcher & Loessner, 2016). EAD is responsible for degrading PG and CBD confers substrate specificity. The domains were connected by short and flexible linker regions. Sometimes, some endolysins have multiple EADs. Phage endolysins are classified into different groups depending on their target bonds of EADs within the PG (Oliveira et al., 2013). Glucosaminidases, muramidases, and transglycosulases hydrolaze the bonds between *N*-acetylmuramic acid and

N-acetylglucosamine in the sugar moieties. Contrast to these proteins, endopeptidases cleave within the peptide stem of PG and the amide bonds between the sugar and peptide moieties in PG were cleaved by amidases.

The effect of CBD on the lytic activity of endolysins is variable. Loessner el al. hypothesized that the strong binding of the CBD to cell wall of bacteria may prevent the lysis of other host cells (Loessner, Kramer, Ebel, & Scherer, 2002), indicating endolysins of the phages from Gram-negative bacteria do not need CBD since outer membrane of Gram-negative bacteria protects host bacteria from free endolysins after cell lysis (Briers et al., 2007; Schmelcher, Powell, Becker, Camp, & Donovan, 2012). Therefore, the importance of CBD has been found in various examples with endolysins from the phages infecting Gram-positive bacteria. An endolysin of Φ11 *S. aureus* phage showed significant reduction of hydrolytic activity after deletion of its CBD (Sass & Bierbaum, 2007). The loss of CBD from a Twort phage endolysin (PlyTW) resulted in 10-fold decrease in activity compared to full-length PlyTW (Becker et al., 2015). Furthermore, fusing CBD from bacteriocin lysostaphin to CHAP domain of HydH5, a staphylococcal phage vB_SauS-phiIPLA88 virion-associated peptidoglycan hydrolase, improved the lytic activity of CHAP domain against *S. aureus* (Rodríguez-Rubio, Martínez, Rodríguez, Donovan, & García, 2012). However, there are reported endolysins fully active in the absence of their

CBD (Cheng & Fischetti, 2007; Donovan, Foster-Frey, et al., 2006). Low et al. reported that positively charged EADs could exert lytic activity without CBD (Low, Yang, Perego, Osterman, & Liddington, 2011). There is also another case that C-terminal domain has an inhibitory role when a specific ligand is absent in the cell wall (Low, Yang, Perego, Osterman, & Liddington, 2005). Although the presence of CBD of PlyL endolysin from *B. anthracis* prophage inhibited its lytic activity of EAD against *B. cereus* species, it was required to show lytic activity against *B. cereus*.

The potential of endolysins for biotechnological applications has been considered. The rare or no probability to develop resistance to endolysin is one of the most favorable characteristics of endolysins. Because endolysins target the cell wall components which are essential for viability and fitness of bacteria, mutations caused by resistance could be highly harmful to the bacterial cells, thereby making resistance to rarely occur (Fischetti, 2006; Gutiérrez, Fernández, Rodríguez, & García, 2018). In addition, endolysin might bypass the possible resistance mechanisms by acting on the cell wall without entering the bacterial cells (Spratt, 1994; Viertel, Ritter, & Horz, 2014).

Unlike antibiotics, endolysins have the possibility to trigger an immune response, interfering with the lytic activity of endolysisns. To address this issue, Loeffler et al. elucidated that the lytic activity of Cpl-1

endolysin from a pneumococcal phage was not neutralized in hyper-immune rabbit serum (Loeffler, Djurkovic, & Fischetti, 2003). The immune response of MV-L endolysin from ΦMR11 *S. aureus* phage has been tested and resulted that the immunized serum did not inactivate the endolysin (Rashel et al., 2007). These results suggest the potential for the therapeutic use of endolysins.

Food contamination by bacterial pathogens is a challenge in both the food industry and healthcare systems, causing foodborne illness. Despite intensive efforts to improve hygienic conditions, the outbreaks of foodborne diseases has gradually increased. To solve this problem, several studies have been reported for the successful application of endolysins in foods. LysH5 endolysin from *S. aureus* phage phi-SauS-IPLA88 showed the lytic activity in milk when treated with nisin (García, Martínez, Rodríguez, & Rodríguez, 2010). Well characterized LysK endoysin from *S. aureus* phage K also has been attempt to kill staphylococcal strains in milk (Mao, Schmelcher, Harty, Foster-Frey, & Donovan, 2013). The moderate lytic activity against clostridial cells were observed by addition of ctp1L endolysin from *Clostridium tyrobutyricum* virulent phage (Mayer, Payne, Gasson, & Narbad, 2010). Nanoparticles-immobilized Ply500 endolysin from *Listeria* phage A500 showed antilisterial activity on lettuce (Solanki et al., 2013). LysZ5 from the genome of the *L. monocytogenes* phage FWLLm3 effectively

controlled listerial cells in soya milk, suggesting the potential for the use of endolysin as a biocontrol agent (Zhang, Bao, Billington, Hudson, & Wang, 2012).

Endolysins have been studied on medical application in animal models (Loessner, 2005). The therapeutic efficacy of endolysins has been confirmed with PlyG endolysin from the *B. anthracis* γ phage which showed the curative effect when intraperitoneally injected (Schuch, Nelson, & Fischetti, 2002). Also, the treatment of Cpl-1 lysozyme and Pal amidase effectively rescued the mice challenged with antibiotic-resistant *S. pnemoniae* clinical isolate (Jado et al., 2003). In addition to these studies, the efficacy of endolysin against *S. aureus* has been demonstrated previously (O'flaherty, Coffey, Meaney, Fitzgerald, & Ross, 2005; Rashel et al., 2007).

I.4. Engineering of phage endolysin

Endolysins have evolved optimally for causing efficient lysis of the host bacteria from within (Schmelcher, Donovan, et al., 2012). However, there is still potential for improvement when it comes to application in complex environments, concerns about the cell physiology, and dynamics of protein architecture (Van Tassell, Daum, Kim, & Miller, 2016). The modular design of endolysins allows them amenable to engineering for 'tailor-made' antimicrobials. Therefore, the properties of endolysins can be optimized for specific application through various endolysin engineering strategies (Schmelcher, Donovan, et al., 2012). There are several types of modification. First, many researchers have been tried to truncate domains of endolysins to figure out the function of each domain and create more effective proteins than full-length of proteins (Becker et al., 2015; Fenton et al., 2010).

Domain swapping is one of the effective molecular engineering methods. A previous study showed that an exchange of CBDs results in the switched cell wall specificity or increased lytic activity. Chimeirc endolysins consisting of individual EAD and CBD modules from PlyPSA and Ply118 endolysins from *Listeria* phages showed swapped properties with different binding specificity and catalytic activity (Schmelcher, Tchang, & Loessner,

2011). The replacement of CBD of a streptococcal LambdaSa2 endolysin by staphylococcal SH3b domains presented a 5-fold increase in staphylolytic activity, maintaining significant lytic activity against streptococcal strains (Becker, Foster-Frey, Stodola, Anacker, & Donovan, 2009). When a CHAP domain of Ply187 endolysin from *S. aureus* phage 187 and a SH3b domain of LysK were fused to generate chmeric endolysins, significantly improved lytic activity of the fusion protein was observed compared to its parental endolysins (Mao et al., 2013).

Novel chimeric endolysins with desired properties could be created by screening in random domain swapping library. Recently, Yang et al. reported a chimeric endolysin with extended antimicrobial spectrum and higher lytic activity compared to its parental endolysins (Yang et al., 2015). In an effort to treat bovine mastitis, proteins with high antimicrobial activity against *S. aureus* were screened in a random library in the presence of milk. As a result, a fusion protein with a CHAP domain of LysK and a CBD of lysostaphyin showed the most effective activity in milk (Verbree et al., 2018).

In other studies, fusion of two full-length enzymes has been conducted and a CBD or EAD was added to a full-length enzyme (Becker, Foster-Frey, et al., 2009; Donovan, Dong, et al., 2006). Two heterologous CBDs were combined to extend binding spectrum of endolysins and duplicated CBDs showed increased cell wall affinity and enhanced lytic

activity at high NaCl concentrations (Schmelcher et al., 2011).

In some studies, random or site directed mutagenesis was introduced to improve lytic activity of endolysin. Chen and Feschetti identified endolysins that have greater lytic activity on group B streptococci than wild-type after random mutagenesis (Cheng & Fischetti, 2007). Altered net charge of the catalytic domain of Cpl-7 resulted in change of CBD-dependence (Díez-Martínez et al., 2013).

I.5. Purpose of this research

In response to increasing concern over antibiotic-resistant bacteria, the development of novel antimicrobials has been called for, with bacteriophage endolysins having received considerable attention as alternatives to antibiotics. However, the discovery of potent endolysin is still challenging because the current trial-and-error strategies are time-consuming and labor-intensive. The modular structure of endolysins can provide an opportunity to develop novel endolysins with desired properties by various engineering strategies such as rearrangement of domains or random mutagenesis.

Therefore, this study aims to (i) elucidate the exact function of each domain of endolysins from *S. aureus* phages, (ii) develop a random screening strategy using random domain swapping method and identify novel chimeric endolysins, (iii) construct and characterize the fusion proteins to control *S. aureus* and *B. cereus* simultaneously, and (iv) improve cell wall binding affinity of CBD using phage display technology.

II. The auxiliary role of the amidase domain in cell wall binding and exolytic activity of staphylococcal phage endolysins

II.1. Introduction

Staphylococcus aureus is a Gram-positive facultative anaerobe that frequently colonizes the nose, skin, or gastrointestinal tract (Lindsay & Holden, 2004). *S. aureus* has long been recognized as an important pathogen causing a wide range of infections, from superficial skin infections to life threatening diseases such as bacteremia, necrotizing pneumonia, and endocarditis (Tong et al., 2015). Although these infections were historically treatable with standard antibiotics, the emergence and spread of multidrug-resistant forms of *S. aureus* have greatly limited treatment options. Therefore, new approaches to controlling *S. aureus* are urgently required (Furuno et al., 2005; Lindsay & Holden, 2004; Seybold et al., 2006).

Bacteriophages produce highly evolved lytic enzymes, called endolysins, which disrupt host bacterial cell walls to release their progeny (Loessner, 2005). Due to the strong lytic activity, high specificity and low probability of resistance development, use of endolysins has been proposed as an alternative antimicrobial for treatment of staphylococcal infections (Borysowski et al., 2006). Endolysins of Gram-positive bacteria generally have a modular structure consisting of a catalytic domain (s) and a cell wall binding domain (CBD), while approximately 75% of the endolysins of

staphylococcal phages have three distinct domains: an N-terminal cysteine-, histidine-dependent amidohydrolase/peptidase (CHAP) domain, a central N-acetylmuramoyl-L-alanine amidase (Ami_2 or Ami_3) domain, and a C-terminal SH3b domain as a CBD (Chang & Ryu, 2017). Several truncation studies of *S. aureus* endolysins have reported that the CHAP domains confer most of the lytic activity of the endolysin by cleaving the multiple peptide bonds of peptidoglycan (Becker, Dong, et al., 2009; Navarre, Ton-That, Faull, & Schneewind, 1999; Rodríguez-Rubio et al., 2013).

On the other hand, the central amidase domains of *S. aureus* endolysins showed little or no lytic activity by themselves (Becker, Dong, et al., 2009; Kashani, Schmelcher, Sabzalipoor, Hosseini, & Moniri, 2018; Navarre et al., 1999; Sass & Bierbaum, 2007). Although it is common for one catalytic domain of endolysins to have dominant activity and the silent domain can act in a cooperative manner to cleave multiple peptidoglycan bonds (Abaev et al., 2013; Becker, Dong, et al., 2009; Sass & Bierbaum, 2007), the exact role of the amidase domains of *S. aureus* endolysins is still unclear.

Here, I elucidated the role of the amidase domains of three *S. aureus* phage endolysins (LysSA12, LysSA97 and LysSAP4). The amidase domains of both endolysins help CBDs bind to host cells more efficiently and thereby enhance the overall lytic activity of the endolysin. This is, to the

best of my knowledge, the first study elucidating the auxiliary role of amidase in cell wall binding.

II.2. Materials and Methods

II.2.1. Bacterial strains, media, and growth conditions

All tested *S. aureus* cells were grown in tryptic soy broth (TSB) medium (Difco, Detroit, MI) at 37℃ with shaking. *Escherichia coli* DH5α and BL21 (DE3) star were grown in LB broth (Difco, Detroit, MI) at 37℃ with aeration and used in the cloning and expression of proteins, respectively.

II.2.2. *In silico* analysis of staphylococcal endolysins

The sequences of LysSA12 and LysSA97 were analyzed. Their domain composition was investigated using the BLAST (http://blast.ncbi.nlm.nih.gov/Blast.cgi), Interproscan 5 (http://www.ebi.ac.uk/interpro), and Pfam 28.0 programs (http://pfam.xfam.org) (Altschul, Gish, Miller, Myers, & Lipman, 1990; Altschul et al., 1997; Finn et al., 2013). Amino acid sequence alignments of the endolysins were performed using ClustalX2.1 (Larkin et al., 2007). The molecular weight and isoelectric point of the proteins were calculated using the Compute pI/Mw program (http://www.expasy.ch/tools/pi_tool.html) (Gasteiger et al., 2005).

II.2.3. Cloning, expression, and purification of *S. aureus* endolysin derivatives and EGFP fusion proteins

To clone the endolysins and their derivatives, genes were amplified from the genome of the bacteriophages SA12 (GenBank accession no. KC677663) and SA97 (GenBank accession no. KJ716334) using the oligonucleotides listed in Table 1 (Chang & Ryu, 2017; Chang et al., 2015; Chang, Yoon, Kang, Chang, & Ryu, 2017). The PCR product was cloned into pET28a (Novagen, Madison, WI) carrying an N-terminal His-tag sequence. All plasmids used in this study are listed in **Table II-1**. The correctly cloned plasmid was transformed into competent *E. coli* BL21 (DE3). Expression of the recombinant proteins was induced with 0.5 mM IPTG (isopropyl-β-D-thiogalactopyranoside) at OD_{600} (optical density at 600 nm) = 0.7, followed by incubation for additional 20 h at 18℃. Bacterial cells were suspended in lysis buffer (50 mM sodium phosphate, 300 mM sodium chloride and 30% glycerol; pH 8.0) and disrupted by sonication at a duty cycle of 25% and output control of 5 (Sonifier 250, Branson, Danbury, CT). After centrifugation (20,000 x g, 30 min), the supernatant was passed through Ni-NTA agarose (Qiagen, Hilden, Germany), and purification of the recombinant proteins was performed according to the manufacturer's

instructions. After the buffer was changed to storage buffer (50 mM sodium phosphate, 300 mM NaCl, and 30% glycerol; pH 8.0) using PD Miditrap G-25 (GE healthcare), the purified protein was stored at –80℃ until use. To generate EGFP fusion proteins, the endolysin derivatives were cloned into EGFP-harboring pET28a (M. Kong et al., 2015). Each protein was expressed and purified as described above.

II.2.4. Construction of LSA12AMICBD mutants

The H206E, A236L, H313E and C321A mutant of LSA12AMICBD were constructed via an overlapping extension PCR protocol (Nelson & Fitch, 2012). To construct pET28a_LSA12AMICBD H206E, the LSA12AMICBD gene was amplified from the pET28a_ LSA12AMICBD vector in two parts, using two sets of primers (pET28a-F and LysSA12_H206E_overl_R for the front part; LysSA12_H206E_overl_F and pET28a-R for the rear part). Two overlapping PCR fragments were used for the second PCR step generating the LSA12AMICBD (H206E) gene. The resultant PCR product was inserted between the BamHI and SalI restriction sites of pET28a and pET28a-EGFP to construct LSA12AMICBD H206E-containing plasmid vectors (pET28a_ LSA12AMICBD H206E and pET28a-EGFP_LSA12AMICBD H206E, respectively). For the construction of pET28a_LSA12AMICBD A236L,

pET28a_LSA12AMICBD H313E, pET28a_LSA12AMICBD C321A, pET28a_EGFP_LSA12AMICBD A236L, pET28a_EGFP_ LSA12AMICBD H313E, pET28a_EGFP_ LSA12AMICBD C321A, two corresponding sets of primers were used. The sequences of primers used in this study are listed in Table 1.

Table II-1. Plasmids and primers used in this chapter

Plasmids		
	Description	**Reference**
pET28a	Kan^r, T7 promoter, His-tagged expression vector	Novagen, Wisconsin, SA
pET28a-EGFP	pET28a with EGFP	This study
pET28a-LysSA12	pET28a with LysSA12 (56 kDa)	(Chang, Yoon, et al., 2017)
pET28a-LSA12CBD	pET28a with LSA12CBD	This study
pET28a-LSA12CHAP	pET28a with LSA12CHAP (20 kDa)	This study
pET28a-LSA12CHAPCBD	pET28a-LSA12CBD with LSA12CHAP (32 kDa)	This study
pET28a-LSA12AMICBD	pET28a with LSA12AMICBD (44 kDa)	This study
pET28a-LysSA97	pET28a with LysSA97 (56 kDa)	(Chang, Yoon, et al., 2017)
pET28a-LSA97CBD	pET28a with LSA97CBD	This study
pET28a-LSA97CHAPCBD	pET28a-LSA97CBD with LSA97CHAP (33 kDa)	This study
pET28a-LSA97AMICBD	pET28a with LSA97AMICBD (38 kDa)	This study
pET28a-EGFP_LSA12CBD	pET28a-EGFP with LSA12CBD (42 kDa)	This study
pET28a-EGFP_LSA12AMICBD	pET28a-EGFP with LSA12AMICBD (66 kDa)	This study
pET28a-EGFP_LSA12AMI	pET28a-EGFP with LSA12AMI (54 kDa)	This study
pET28a-EGFP_LSA97CBD	pET28a-EGFP with LSA97CBD (42 kDa)	(Chang & Ryu, 2017)
pET28a-EGFP_LSA97AMICBD	pET28a-EGFP with LSA97AMICBD (65 kDa)	This study

pET28a-EGFP_LSA97AMI	pET28a-EGFP with LSA97AMI (52 kDa)	This study
pET28a-EGFP_LSAP4CBD	pET28a-EGFP with LSAP4CBD (42 kDa)	This study
pET28a-EGFP_LSAP4AMICBD	pET28a-EGFP with LSAP4AMICBD (65 kDa)	This study
pET28a-EGFP_LSAP4AMI	pET28a-EGFP with LSAP4AMI (52 kDa)	This study
	Primers (5′→3′)[a]	
	Sequence	**Purpose**
BamH1_LSA12CHAP_F	AAA GGA TCC ATGC AAG CAA AAC TAA CTA AAA A	pET28a-LSA12CHAP and pET28a-LSA12CHAPCBD construction
LSA12CHAP_Sal1_R	TTT GTC GAC TGA TCG TGG AGC TGT TTC GCT T	pET28a-LSA12CHAP construction
LSA12CHAP_EcoR1_R	TTT GAA TTC TGA TCG TGG AGC TGT TTC GCT T	pET28a-LSA12CHAPCBD construction
BamH1_LSA12AMI_F	AAA GGA TCC GTA CAA TCT CCT ACG CAA GCA	pET28a-LSA12AMI, pET28a-LSA12AMICBD, pET28a-EGFP_LSA12AMI and pET28a-EGFP_LSA12AMICBD construction
LSA12AMI_Sal1_R	TTT GTC GAC ACT TGA AGC GCT TGA CTC ATT AG	pET28a-LSA12AMI and pET28a-EGFP_LSA12AMI construction
EcoR1_LSA12CBD_F	AAA GAA TTC TCA AGT AAT ACA GTT AAA CCA GT	pET28a-LSA12CBD construction
LSA12CBD_Sal1_R	TTT GTC GAC ACT GAT TTC TCC CCA TAA GT	pET28a-LSA12CBD, pET28a-LSA12AMICBD and pET28a-EGFP_LSA12AMICBD construction
pET28a_F	GAAGAACGGCATCAAGGTGAACTTCAA GATC	pET28a-LSA12AMICBD (H206E, H313E, A236L, C321A) and pET28a_EGFP-

		LSA12AMICBD (H206E, H313E, A236L, C321A) construction
pET28a_R	GGA GCG GGC GCT AGG GCG CTG GCA AGT GTA G	pET28a-LSA12AMICBD (H206E, H313E, A236L, C321A) and pET28a_EGFP-LSA12AMICBD (H206E, H313E, A236L, C321A) construction
LysSA12_H206E_overl_F	TAT AGT TAT TGA AAA CGA CGC AGG	pET28a-LSA12AMICBD H206E and pET28a_EGFP-LSA12AMICBD H206E construction
LysSA12_H206E_overl_R	CCT GCG TCG TTT TCA ATA ACT ATA	pET28a-LSA12AMICBD H206E and pET28a_EGFP-LSA12AMICBD H206E construction
LysSA12_H313E_overl_F	CAA TCC GAT TAG AAA ACG AAT TCA	pET28a-LSA12AMICBD H313E and pET28a_EGFP-LSA12AMICBD H313E construction
LysSA12_H313E_overl_R	GTG AAT TCG TTT TCT AAT CGG ATT G	pET28a-LSA12AMICBD H313E and pET28a_EGFP-LSA12AMICBD H313E construction
LysSA12_A236L_overl_F	GAG GCA GGT ATT CTG CAT AAGT TAC	pET28a-LSA12AMICBD A236L and pET28a_EGFP-LSA12AMICBD A236L construction
LysSA12_A236L_overl_R	CGT AAC TAT GCA GAA TAC CTG CCT C	pET28a-LSA12AMICBD A236L and pET28a_EGFP-LSA12AMICBD A236L construction
LysSA12_C321A_overl_F	ACT TCA ACA TCA GCG CCA CAC AGA	pET28a-LSA12AMICBD C321A and

		pET28a_EGFP-LSA12AMICBD C321A construction
LysSA12_C321A_overl_R	TTC TGT GTG GCG CTG ATG TTG AAG T	pET28a-LSA12AMICBD C321A and pET28a_EGFP-LSA12AMICBD C321A construction
BamH1_LSA97CHAP_F	AAA GGA TCC ATG CCG TCG GTT AGG ACA TAC AG	pET28a-LSA97CHAP and pET28a-LSA97CHAPCBD construction
LSA97CHAP_Sal1_R	TTT GTC GAC TTC TTT TGC GTA GAA TGG ACG GAT	pET28a-LSA97CHAPconstruction
LSA97CHAP_EcoR1_R	TTT GAA TTC TTC TTT TGC GTA GAA TGG ACG GAT	pET28a-LSA97CHAPCBD construction
BamH1_LSA97AMI_F	AAA GGA TCC CAA GAT AAG TTA TCA AAA GGT AAA	pET28a-LSA97AMICBD, pET28a-EGFP_LSA97AMICBD and pET28a-EGFP_LSA97AMI construction
LSA97AMI_Sal1_R	TTT GTC GAC ACT ACT TGG CGC ATC AAT TTG TC	pET28a-EGFP_LSA97AMI construction
EcoR1_LSA97CBD_F	AAA GAA TTC AGT AGT AAG CCA AGC GCT GAC AA	pET28a-LSA97CBD construction
LSA97CBD_Sal1_R	TTT GTC GAC TTA AGC CCA CTC AAT CGT GCC CCA	pET28a-LSA97CBD, pET28a-LSA97AMICBD and pET28a-EGFP_LSA97AMICBD construction
BamH1_LSAP4AMI_F	AAA GGA TCC A AAG TAA GTG TTG GAG ATA AAG C	pET28a-EGFP_LSAP4AMICBD and pET28a-EGFP_LSAP4AMI construction
LSAP4AMI_Sal1_R	TTT GTC GAC TTG GTT TTT AGC TGA TGT TTT AAC	pET28a-EGFP_LSAP4AMI construction

LSAP4CBD_Sal1_R	TTT GTC GAC CTA AAT CGT GCT AAA CTT ACC AAA	pET28a-EGFP_LSA97AMICBDand pET28a-_EGFP_LSA97AMICBD construction
Nde1_EGFP_F	AAA CAT ATG ATG GTG AGC AAG GGC GAG GA	
EGFP_BamH1_R	TTT GGA TCC CTT GTA CAG CTC GTC CAT GCC G	pET28a-EGFP construction

II.2.5. Lytic activity assay

The lysis activity of endolysins and their derivatives was assessed using a turbidity reduction assay (B. Son et al., 2012). Bacterial cells grown to the exponential phase were resuspended in reaction buffer (50 mM sodium phosphate, 300 mM NaCl; pH 8.0). Purified endolysins and their derivatives were then added to the cell suspension at a final concentration of 0.3 μM, and the OD reduction of cells was measured over time using a SpectraMax i3 multimode microplate reader (Molecular Devices, Sunnyvale, CA). The assay on peptidoglycan was performed as described above. Purified peptidoglycan was prepared by a method described by Kuroda et al (Kuroda & Sekiguchi, 1990).

II.2.6. EGFP fusion protein binding assay.

The binding of each EGFP fusion protein to *S. aureus* cells was measured as previously described (Loessner et al., 2002). Bacterial cells, cultivated to early exponential phase, were harvested and re-suspended in Dulbecco's phosphate-buffered saline (PBS). The cells were incubated with EGFP fusion protein for 5 min at room temperature. The mixture was washed twice with PBS to remove unbound protein and was transferred to a 96-well plate to measure fluorescence using a SpectraMax i3 multimode

microplate reader with excitation at 485 nm and emission at 535 nm. The OD_{600} of cells was measured, and fluorescence was normalized by calculating the whole-cell fluorescence per OD_{600}. Relative binding capacity was derived by comparing to the highest measured value and is presented as relative fluorescence intensity (RFI). In addition, target bacteria labelled with EGFP fusion protein were examined by fluorescence microscopy (DE/Axio Imager A1 microscope, Carl Zeiss, Oberkochen, Germany) using a GFP filter set (470/40 nm excitation, 495 nm dichroic, 525/50 nm emission).

II.3. Results and discussion

II.3.1. Modular structure of LysSA12

Bioinformatics analysis revealed that the endolysin of phage SA12, LysSA12 (Genbank accession No. AGO49867.1), consists of an N-terminal CHAP (PF05257) domain (LSA12CHAP), a central amidase_2 (PF01510) domain (LSA12AMI), and a C-terminal CBD (LSA12CBD) with homology to the SH3 domain (PF08460) (Chang, Lee, Shin, Heu, & Ryu, 2013; Chang, Yoon, et al., 2017). LysSA12 showed an overall 98% amino acid identity with endolysin LysH5, an endolysin (Genbank accession No. EU 573240.1) from *S. aureus* phage phi-SauS-IPLA88. (García et al., 2010), and a 96% identity with endolysin phi11 (Genbank accession No. NC_004615.1) found in genomic DNA of *S. aureus* NCTC8325 (Sass & Bierbaum, 2007). LysK (Genbank accession No. AAO47477.2), an endolysin from staphylococcal phage K, showed only limited amino acid sequence similarity (37% identity) to LysSA12 (O'flaherty et al., 2005). LysSA12 has a conserved Cys-His-Asn catalytic triad in its CHAP domain, and these residues are conserved in LysH5, phi11, and LysK (Figure II-1Figure II-1. Modular structure of LysSA12 and LysSA97.)

(A)

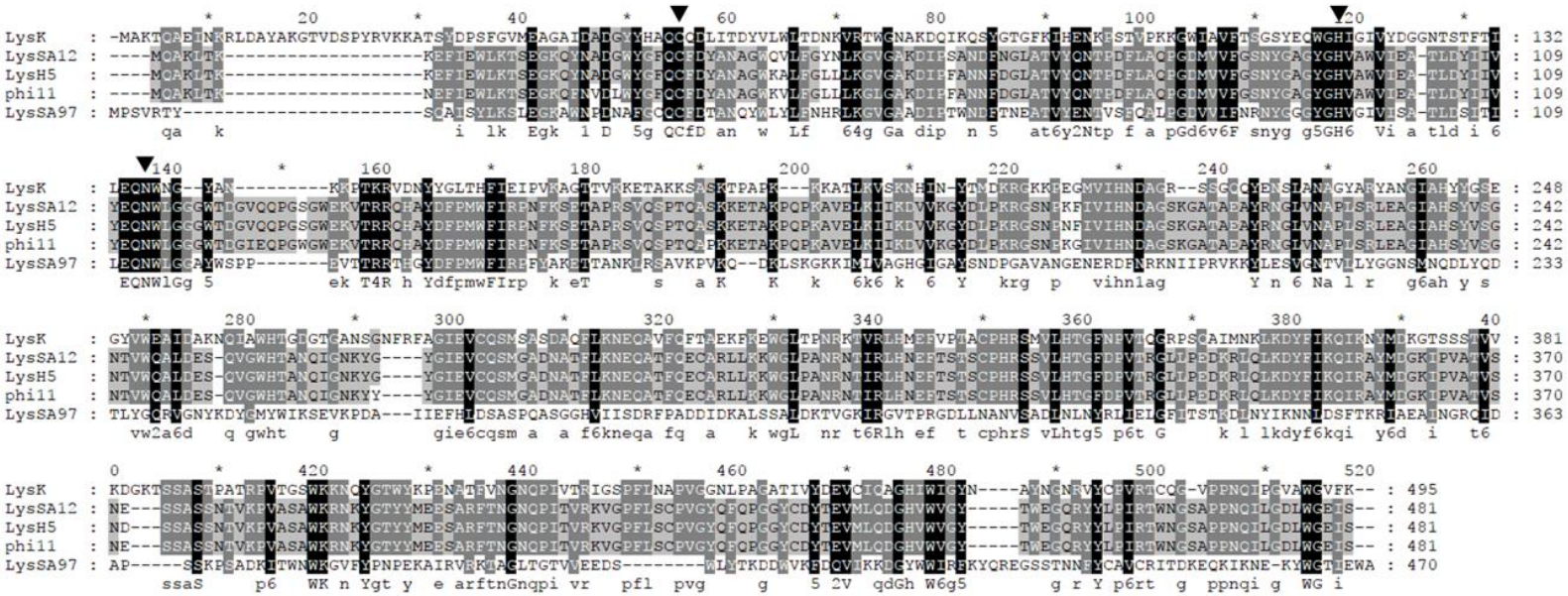
LysK
LysSA12
LysH5
phi11
LysSA97

(B)

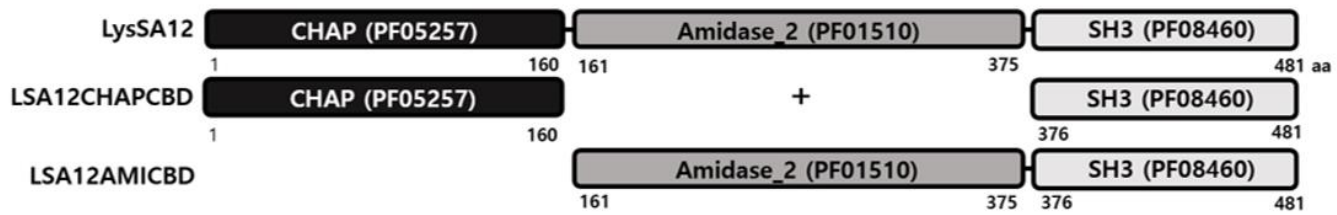
LysSA12
CHAP (PF05257)
Amidase_2 (PF01510)
SH3 (PF08460)
1
160
161
375
481 aa
LSA12CHAPCBD
CHAP (PF05257)
+
SH3 (PF08460)
1
160
376
481
LSA12AMICBD
Amidase_2 (PF01510)
SH3 (PF08460)
161
375
376
481

Figure II-1. Modular structure of LysSA12 and LysSA97.

(A) Sequence alignment of LysSA12 and LysSA97 with other related endolysins. LysK, *S. aureus* phage K endolysin; LysH5, *S. aureus* phage vB_SauS-phiIPLA88 endolysin; phi11, *S. aureus* phage phi11 endolysin. Conserved and identical residues are shaded in gray (dark gray, >70% conserved; light gray, >40% conserved) and black, respectively. The conserved Cys-His-Asn triad is indicated by triangles. (B) Schematic representations of LysSA12, LysSA97, and their deletion constructs. The numbers indicate the initial and final amino acids in the domains as determined using the Pfam domain database. CHAP domain, black box; amidase domain, dark grey box; CBD, light grey box.

II.3.2. Expression and purification of LysSA12 derivatives

Since a defined function for the amidase domain in endolysins containing both CHAP and amidase domains is not known, the influence of the amidase domain on enzymatic activity or on binding ability of endolysin was studied by comparing the lytic activities and binding abilities of various combinations of the three domains of LysSA12. The truncated proteins consisting of LSA12CHAP, LSA12AMI, LSA12CHAP plus LSA12AMI (LSA12CHAPAMI), LSA12CHAP plus LSA12CBD (LSA12CHAPCBD), and LSA12AMI plus LSA12CBD (LSA12AMICBD) were constructed based on domain composition (Figure II-1), and their enzymatic activities were compared with those of intact LysSA12. In addition, three EGFP fusion proteins containing LSA12AMI, LSA12AMICBD, and LSA12CBD, were constructed to test their binding ability. The proteins were overexpressed in *E. coli* using the pET-28a vector, and the purified proteins migrated as a single band of the expected molecular mass on SDS-PAGE (Figure II-2).

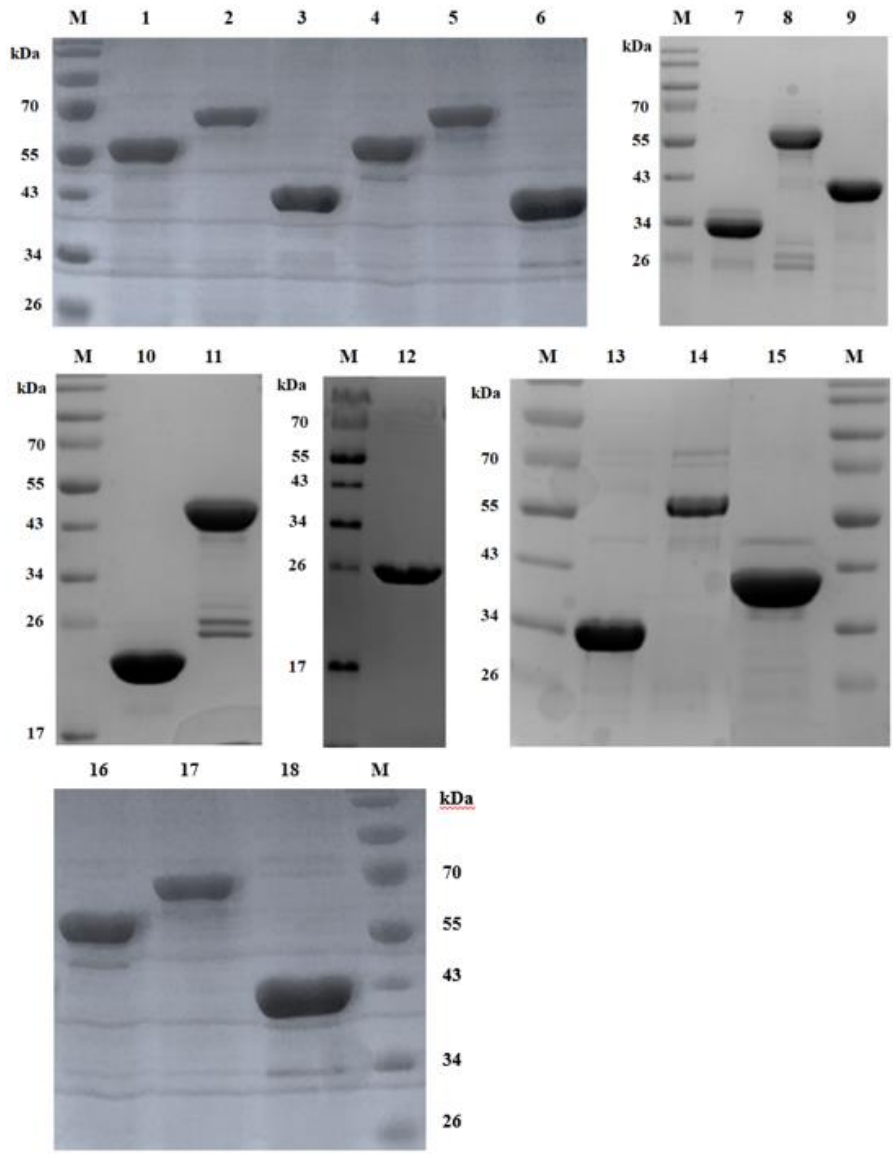

Figure II-2. SDS-polyacrylamide gel electrophoresis analysis of LysSA12, LysSA97, and their derived proteins.

Proteins were purified by nickel-nitrilotriacetic acid affinity chromatography and analyzed using 12 % SDS-polyacrylamide gel

electrophoresis. Lane M, protein ladder; lane 1, EGFP_LSA12AMI; lane 2, EGFP_LSA12AMICBD; lane 3, EGFP_LSA12CBD; lane 4, EGFP_LSA97AMI; lane 5, EGFP_LSA97AMICBD; lane 6, EGFP_LSA97CBD; lane 7, LSA12 CHAPCBD; lane 8, LysSA12; lane 9, LSA12AMICBD; lane 10, LSA12CHAP; lane 11, LSA12CHAPAMI; lane 12, LSA12AMI; lane 13, LSA97CHAPCBD; lane 14 LysSA97; lane 15, LSA97AMICBD; lane 16, LSAP4AMI; lane 17, LSAP4AMICBD; lane 18, LSAP4CBD.

II.3.3. Lytic activities of LysSA12 and its truncated proteins on live *S. aureus* cells

Turbidity reduction assays with LysSA12 and its truncated proteins were conducted against the exponentially growing *S. aureus* cells. LSA12AMICBD and LSA12AMI did not inhibit the growth of cells, but rather caused a slight increase in the OD values (Figure II-3). It has been reported that the negatively charged teichoic acid and lipoteichoic acid on the surface of *S. aureus* cells can interact with positively charged proteins to increase the OD value (Takano et al., 2000). The calculated pI values of the truncated proteins of LysSA12 with no lytic activity are 5.3 for LSA12CHAP, 8.73 for LSA12CHAPAMI, 9.18 for LSA12AMICBD, and 9.38 for LSA12AMI, suggesting that the positively charged LSA12AMICBD and LSA12AMI with high pI values caused an increase in OD value as reported by Takano et al. (Takano et al., 2000). LSA12CHAP, LSA12AMI, and LSA12CHAPAMI barely lysed the intact *S. aureus* cells, whereas LSA12CHAPCBD and the full-length LysSA12 resulted in clear lysis, suggesting that the both CHAP and a C-terminal CBD are necessary to exert the lytic activity of LysSA12. Consistent with these results, the CHAP domain is known to be responsible for the major catalytic activity of the endolysin in degrading cell wall peptidoglycan, exhibiting both amidase and

endopeptidase activity (Becker, Dong, et al., 2009; Schmelcher, Donovan, et al., 2012). Sometimes, there is an inactive domain among two different EADs in the same endolysin (Becker, Foster-Frey, & Donovan, 2008; Kashani et al., 2018). For example, the isolated amidase domain of Φ11 endolysin (Sass & Bierbaum, 2007), the glycosidase domains from the λ Sa2 prophage endolysin (Donovan & Foster-Frey, 2008) or B30 endolysin (Donovan, Foster-Frey, et al., 2006), and the amidase domain in LysK (Becker, Dong, et al., 2009) are unable to hydrolyze bacterial cells. These findings raised questions about the function of the central amidase domain of endolysins.

LSA12CHAPCBD showed 2-fold reduced activity compared with wild-type LysSA12 at equimolar concentrations. These findings demonstrate that the highest exolytic activity of LysSA12 requires the amidase domain. Moreover, this phenomenon was confirmed in other *S. aureus* strains other than *S. aureus* RN4220 and *S. aureus* ATCC 13301 (Figure II-4). Similar results have been reported for LysK; amidase deletion reduced the activity of LysK as measured in the turbidity reduction assay using equimolar amount of proteins (Becker, Dong, et al., 2009).

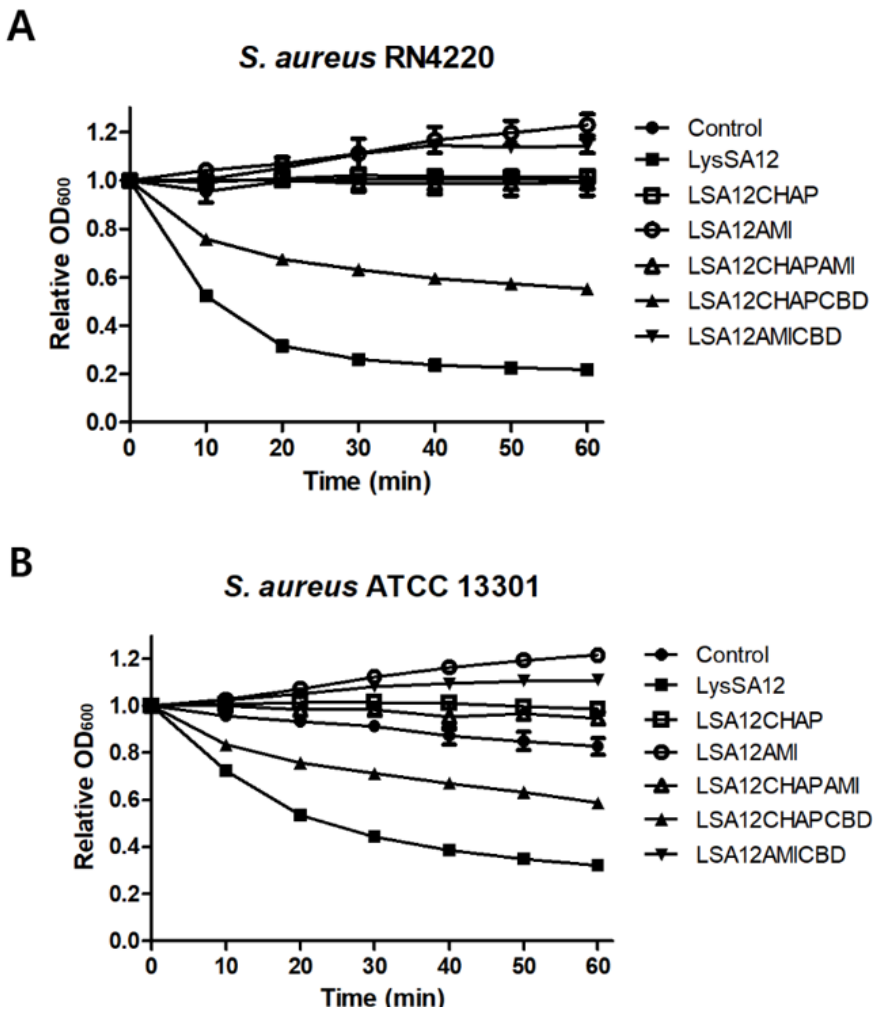

Figure II-3. Lytic activity comparison of LysSA12 and its derivate domains against *S. aureus* RN4220 and *S. aureus* 13301.

Equimolar concentrations (0.3 μM) of the purified enzymes expressed from the full length and truncated proteins were added to a 1 mL suspension of (A) *S. aureus* RN4220 and (B) *S. aureus* ATCC 13301.

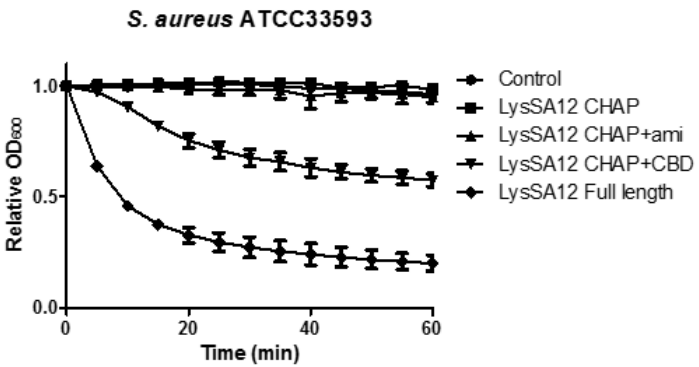
S. aureus ATCC33593
Relative OD600
1.0
0.5
0.0
0
20
40
60
Time (min)
Control
LysSA12 CHAP
LysSA12 CHAP+ami
LysSA12 CHAP+CBD
LysSA12 Full length

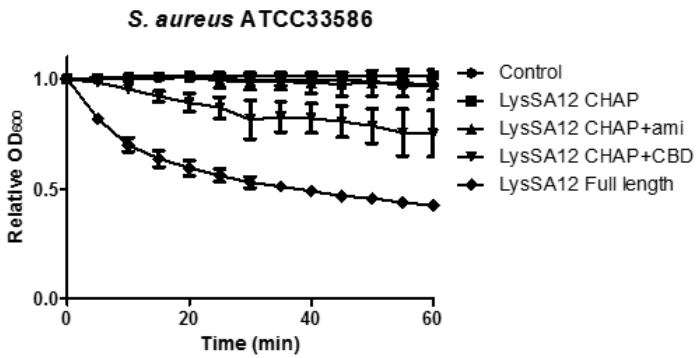
S. aureus ATCC33586
Relative OD600
1.0
0.5
0.0
0
20
40
60
Time (min)
Control
LysSA12 CHAP
LysSA12 CHAP+ami
LysSA12 CHAP+CBD
LysSA12 Full length

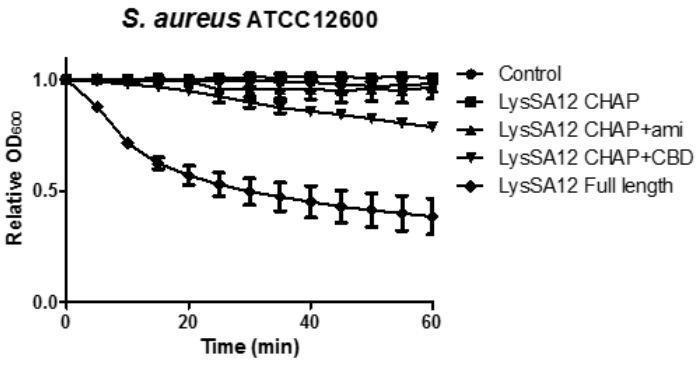
S. aureus ATCC12600
Relative OD600
1.0
0.5
0.0
0
20
40
60
Time (min)
Control
LysSA12 CHAP
LysSA12 CHAP+ami
LysSA12 CHAP+CBD
LysSA12 Full length

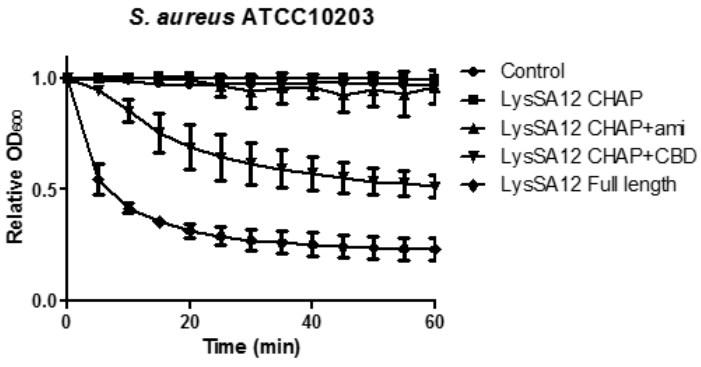
S. aureus ATCC10203
Relative OD600
1.0
0.5
0.0
0
20
40
60
Time (min)
Control
LysSA12 CHAP
LysSA12 CHAP+ami
LysSA12 CHAP+CBD
LysSA12 Full length

Figure II-4. Activity comparison of LysSA12 and its derivate domains against various *S. aureus* strains.

Equimolar concentrations (0.3 μM) of the purified enzymes expressed from the full length and truncated proteins were added to a 1 mL suspension of *S. aureus* ATCC 33593, *S. aureus* ATCC 33586, *S. aureus* ATCC 12600 and *S. aureus* ATCC 10203.

II.3.4. Lytic activities of LysSA12 and its truncated proteins on the purified peptidoglycan

Turbidity reduction assay was also conducted with LysSA12 and its truncated proteins on the purified *S. aureus* peptidoglycan (Figure II-5). In contrast to results against *S. aureus* intact cells, LSA12AMICBD showed the ability to degrade purified peptidoglycan of *S. aureus* even though the effect was not as much as LysSA12 and LSA12CHAPCBD. This discrepancy, which has also been reported in several other studies (Pritchard, Dong, Kirk, Cartee, & Baker, 2007; Sass & Bierbaum, 2007), was possibly due to the absence of secondary cell wall polymers, including teichoic acids and cell wall polysaccharides, and/or wall associated proteins in the purified peptidoglycan (Bhavsar & Brown, 2006; Eugster & Loessner, 2012; Schlag et al., 2010). I propose that the lack of LSA12AMICBD lytic activity against the intact cells might result from steric interference of the secondary cell wall structure.

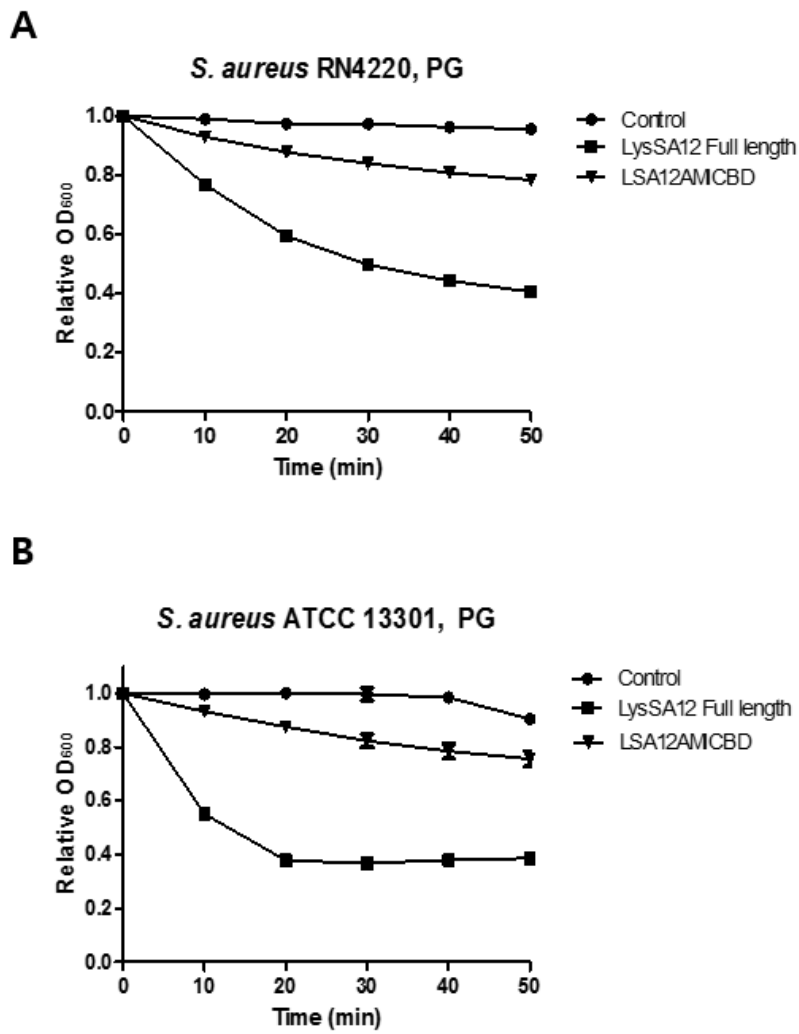

Figure II-5. Activity of the LysSA12 and LSA12AMICBD against purified peptidoglycan of *S. aureus* RN4220 and *S. aureus* ATCC 13301. Equimolar concentrations (0.3 μM) of the purified enzymes were added to a 1 ml purified peptidoglycan of (A) *S. aureus* RN4220 and (B) *S. aureus* ATCC 13301.

II.3.5. Amidase domain helps CBD bind to intact cells

To elucidate the role of the amidase domain in exolysis of target bacteria, the binding activities of EGFP_LSA12AMI, EGFP_LSA12CBD, and EGFP_LSA12AMICBD were examined by measuring the RFI of *S. aureus* after mixing bacterial cells with the EGFP fusion proteins (Figure II-6). Among the EGFP fusion proteins tested, EGFP_LSA12AMICBD showed the highest ability to bind to *S. aureus*, while EGFP_LSA12AMI had negligible binding to the *S. aureus* cells. EGFP_LSA12AMICBD exhibited approximately 2-fold enhanced binding capacity to *S. aureus* cells relative to EGFP_LSA12CBD (Figure II-6 A and B). These results were confirmed by fluorescent microscopy images, which clearly showed that EGFP_LSA12AMICBD displayed greater binding to the *S. aureus* cells relative to EGFP_LSA12CBD (Figure II-6 C and D). I also compared the binding activities of LSA12AMICBD and LSA12CBD at various concentrations (0.5, 1, 5, and 10 μM). Compared to EGFP_LSA12CBD, EGFP_LSA12AMICBD showed more than 2-fold stronger binding activity at all concentrations tested, implying that the amidase domain increases the binding activity of CBD (Figure II-7). Taken together, these findings indicate that the amidase domain of LysSA12 increases the lytic activity of the CHAP domain by enhancing accessibility of the CHAP domain to the

target bacteria even though the results obtained with the two endolysins in this study might not be extended to all staphylococcal endolysins.

Several studies have shown that the central amidase domain of endolysins has little or no activity and have proposed potential roles of the amidase domain. Donovan and Foster-Frey pointed out that the apparent lack of activity of the amidase domain may be due to inherent differences in cleavage between lysis from within and lysis from without (Donovan & Foster-Frey, 2008). Furthermore, Becker and colleagues speculated that cofactors produced during the phage lytic cycle or peptidoglycan fragments created by the initial CHAP digestion may be required for the amidase domain to exert its optimal activity (Becker, Dong, et al., 2009). This study demonstrated that two different amidase domains of *S. aureus* phage endolysins facilitate binding of each CBD to host cell walls, leading to maximal lytic activity of these endolysins. Considering that the amidase domain alone did not show any cell binding capacity, it could be that the amidase domains help with and stabilize the folding of the CBD or act as a spacer between the CHAP domain and CBD, enabling the CBD to interact with their cognate target cells efficiently. Further structural and biophysical studies will be needed to fully understand the molecular mechanism of enhanced binding activity provided by the amidase domain.

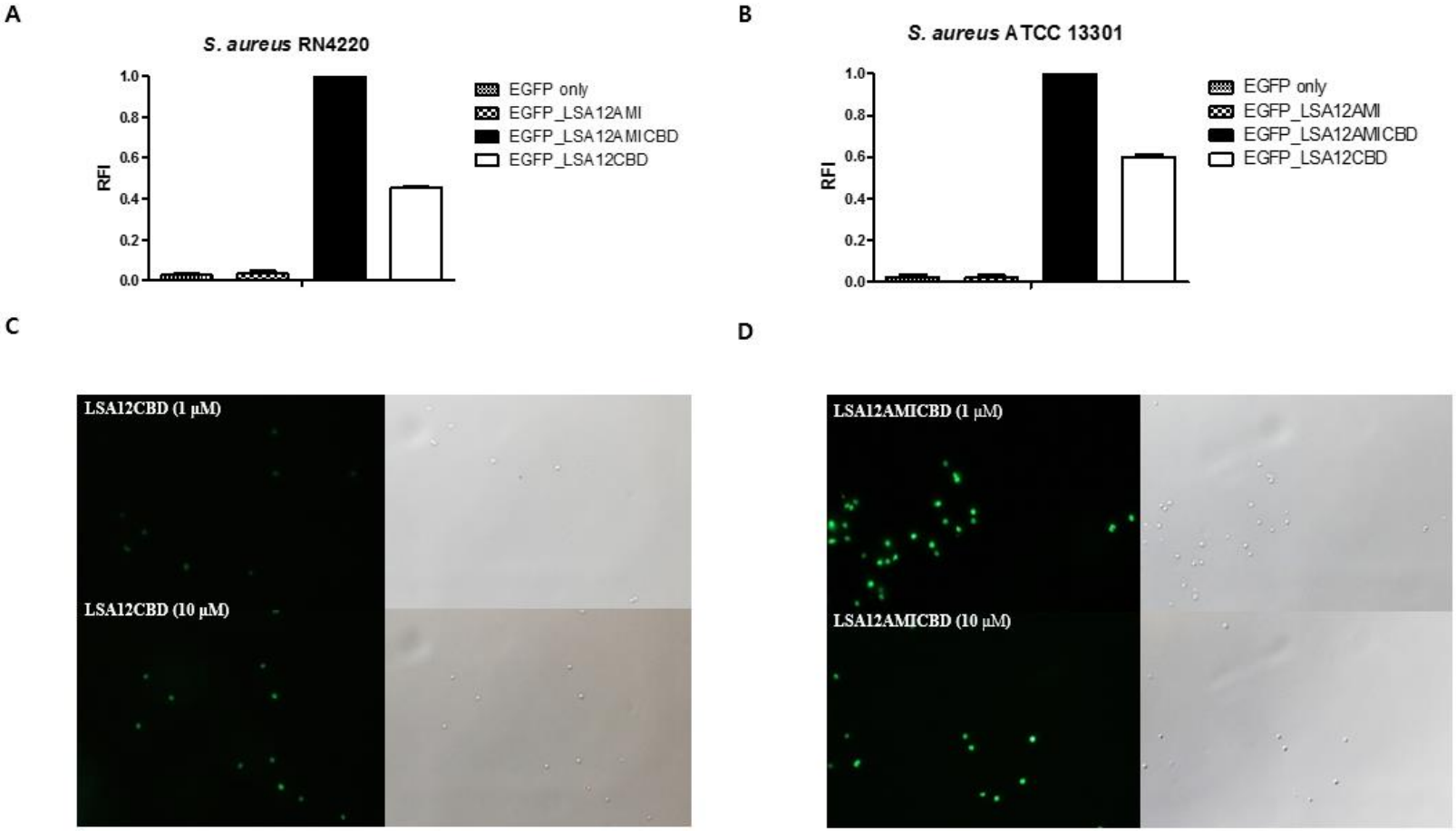
A
S. aureus RN4220
RFI
1.0
0.8
0.6
0.4
0.2
0.0
EGFP only
EGFP_LSA12AMI
EGFP_LSA12AMICBD
EGFP_LSA12CBD
B
S. aureus ATCC 13301
RFI
1.0
0.8
0.6
0.4
0.2
0.0
EGFP only
EGFP_LSA12AMI
EGFP_LSA12AMICBD
EGFP_LSA12CBD
C
LSA12CBD (1 μM)
LSA12CBD (10 μM)
D
LSA12AMICBD (1 μM)
LSA12AMICBD (10 μM)

Figure II-6. Binding activity comparison among EGFP-fused LysSA12 derivatives.

Relative cell binding activities of 1 μM of EGFP_LSA12AMI, EGFP_LSA12AMICBD, and EGFP_LSA12CBD toward (A) *S. aureus* RN4220 and (B) *S. aureus* ATCC 13301. Optical and florescent images of *S. aureus* RN4220 after the addition of (C) EGFP_LSA12CBD and (D) EGFP_LSA12AMICBD at 1 μM (top) and 10 μM (bottom). The data shown are the mean values from three independent measurements and the error bars represent the standard deviations. The scale bar represents 2 μm.

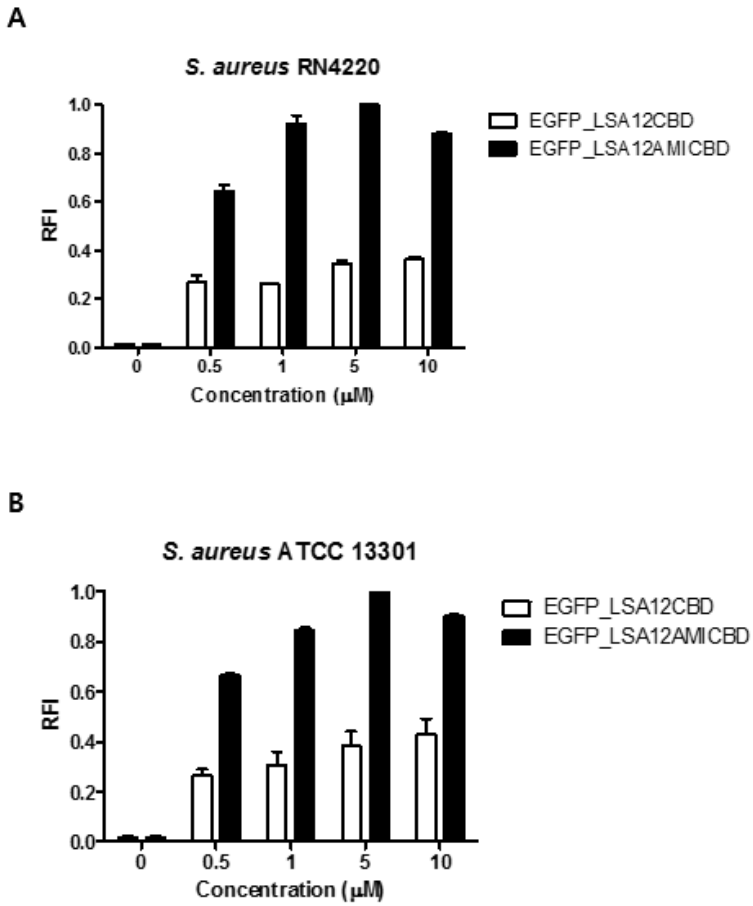

Figure II-7. Binding activity comparison at different concentrations.

Relative cell binding activities of EGFP_LSA12CBD and EGFP_LSA12AMICBD were measured with (E) *S. aureus* RN4220 and (F) *S. aureus* ATCC 13301 at different concentrations. EGFP did not show binding to *S. aureus*. The data shown are the mean values from three independent measurements and the error bars represent the standard deviations.

II.3.6. Active site analysis of LSA12AMICBD

According to the result from BLASTP analysis of LSA12AMICBD, four residues (His-206, Ala-236, His-313 and Cys-321) were predicted to the catalytic site of LSA12AMICBD and mutated. LSA12AMICBD H206, A236L, H313E and C321A were examined for their lytic activity on the purified PG and cell wall binding activity to intact cells. As a result, it was revealed that the lytic activity disappeared when the three residues (His-206, His-313, and Cys-321) were mutated. In the case of H313E and C321A, the amidase domain still helped increase the cell wall binding of CBD, but H206E did not increase cell wall binding of CBD. The results show that the active sites of the amidase domain are His-206, His-313 and Cys-321, of which the His-206 residue plays an important role in helping to increase cell wall binding of CBD. Additional structural studies are required based on these results to reveal the exact mechanism of action.

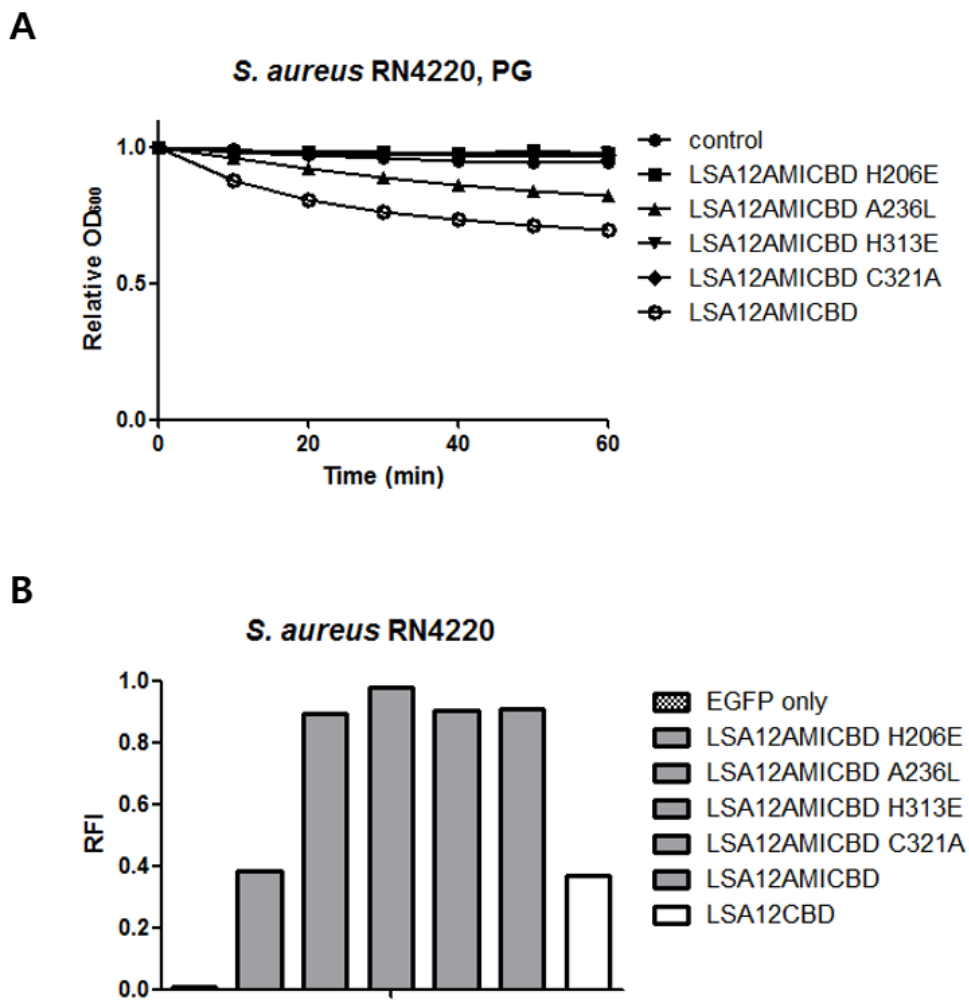

Figure II-8. The lytic activity and cell wall binding activity of LSA12AMICBD mutants.

Equimolar concentrations (0.3 μM) of the purified enzymes were added to a 1 ml purified peptidoglycan of *S. aureus* RN4220 (A) and relative cell binding activities of the mutants were measured with *S. aureus* RN4220 (B).

II.3.7. Role of the LysSA97 amidase domain

To further investigate the role of the amidase domain in other *S. aureus* endolysins, the LysSA97 endolysin (Genbank accession No. AHZ95694.1) isolated from staphylococcal phage SA97 was studied [20]. Bioinformatics analysis predicted that LysSA97 would be an N-acetylmuramoyl-L-alanine amidase composed of CHAP, amidase_3, and a novel CBD not homologous to any of the reported CBDs. These findings indicate that LysSA12 and LysSA97 belong to different staphylococcal endolysin groups based on their domain compositions (Figure II-1). As in the analysis of LysSA12 and its truncated proteins, LSA97AMICBD did not have any lytic activity against intact *S. aureus* cells, and LSA97CHAPCBD showed reduced lytic activity compared to the full-length LysSA97 (Figure II-9).

The binding assay revealed that EGFP_LSA97AMICBD exhibited the highest cell binding activity among the constructs tested (Figure II-10), which was approximately 15-fold higher than LSA97CBD at 1.0 μM (Figure II-11). The enhancing effect of the amidase domain on cell wall binding was more evident in LysSA97 endolysin than in LysSA12 endolysin due to the relatively low binding capacity of LSA97CBD. In other words, these results suggest that the amidase domain of LysSA97 also improves the

weak binding of CBD and thereby enhances the lytic activity of the endolysin.

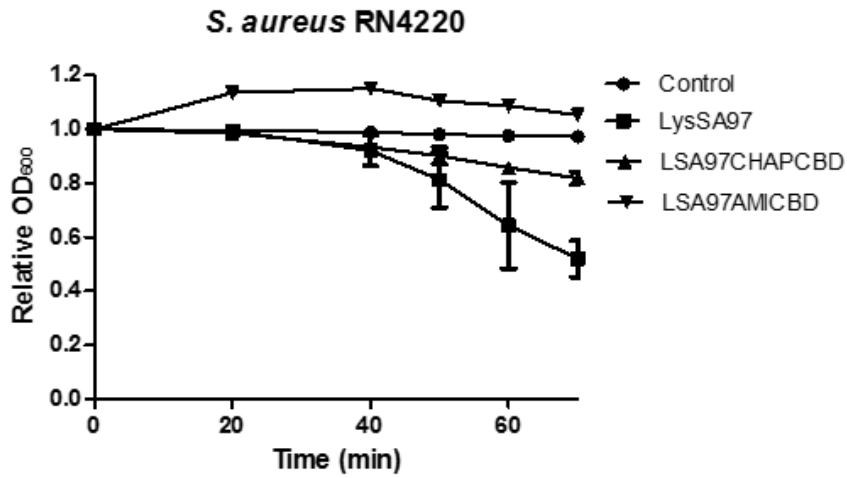

Figure II-9. Lytic activity comparison of LysSA97 and its derivate domains against *S. aureus* RN4220.

Equimolar concentrations (2.0 μM) of the purified enzymes expressed from the full length and truncated proteins were added to a 1 mL suspension of *S. aureus* RN4220.

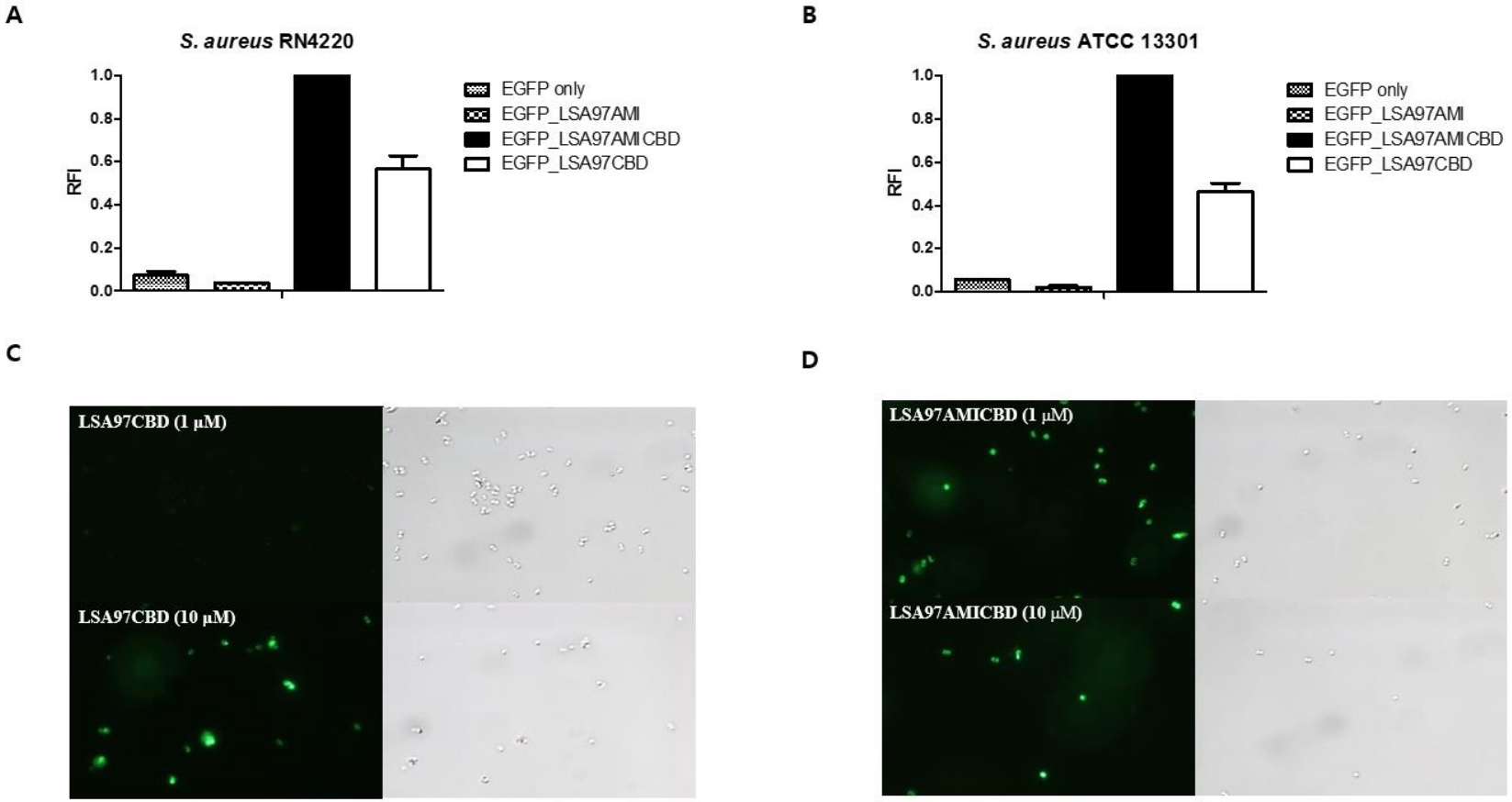
A
S. aureus RN4220
RFI
1.0
0.8
0.6
0.4
0.2
0.0
EGFP only
EGFP_LSA97AMI
EGFP_LSA97AMICBD
EGFP_LSA97CBD
B
S. aureus ATCC 13301
RFI
1.0
0.8
0.6
0.4
0.2
0.0
EGFP only
EGFP_LSA97AMI
EGFP_LSA97AMICBD
EGFP_LSA97CBD
C
LSA97CBD (1 μM)
LSA97CBD (10 μM)
D
LSA97AMICBD (1 μM)
LSA97AMICBD (10 μM)

Figure II-10. Binding activity comparison among EGFP-fused LysSA97 derivatives.

Relative cell binding activities of 10 μM of EGFP_LSA97AMI, EGFP_LSA97AMICBD, and EGFP_LSA97CBD with (A) *S. aureus* RN4220 and (B) *S. aureus* ATCC 13301. Optical and florescence images of *S. aureus* RN4220 after the addition of (C) EGFP_LSA97CBD and (D) EGFP_LSA97AMICBD at 1 μM (top) and 10 μM (bottom). The data shown are the mean values from three independent measurements and the error bars represent the standard deviations. The scale bar represents 2 μm.

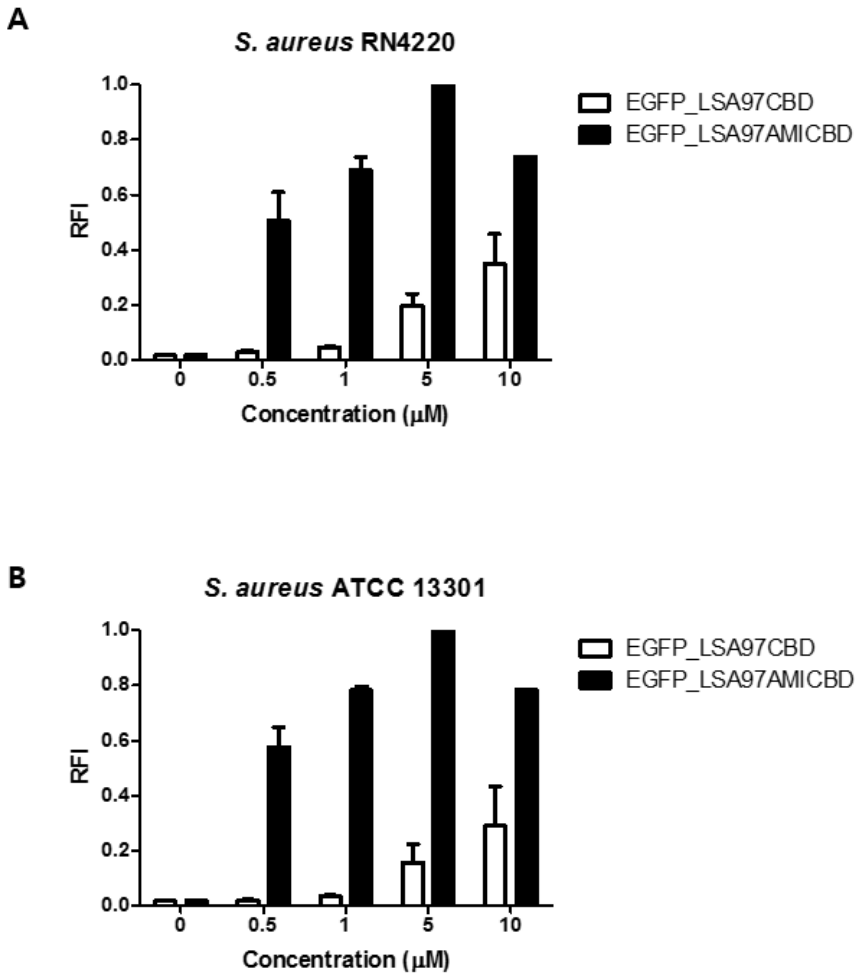

Figure II-11. Binding activity comparison at different concentrations.

At different concentrations, the relative cell binding activities of EGFP_LSA97CBD and EGFP_LSA97AMICBD were measured with (A) *S. aureus* RN4220 and (B) *S. aureus* ATCC 13301. The data shown are the mean values from three independent measurements and the error bars represent the standard deviations.

II.3.8. Role of the LysSAP4 amidase domain

The auxiliary role of the amidase domain in cell wall binding was evaluated with LysSAP4 endolysin from *S. aureus* bacteriophage SAP4 (Park et al., unpublished). Bioinformatics analysis predicted that LysSAP4 is composed of a CHAP domain, an amidase_3 domain, and a SH3b domain. Amino acid sequence alignment revealed that LysSAP4 has 21% overall identity with LysSA12 and 40% with LysSA97. As in the analysis of LysSA12 and LysSA97, EGFP_LSAP4AMICBD exhibited the highest cell binding activity among the proteins tested, showing approximately 4-5-fold higher binding ability than LSAP4CBD with 10.0 μM (Figure II-12).

In conclusion, several truncated derivatives of LysSA12, LysSA97 and LysSAP4 were generated to identify the function of each domain. The amidase domains of both staphylococcal endolysins enhanced the overall exolytic activity of enzymes by helping CBD bind its target cells more efficiently. These molecular studies will be helpful in the creation of novel chimeric proteins for preventing and treating *S. aureus* infections. Furthermore, the newly constructed fusion proteins containing the amidase domain and CBD that have higher binding ability to *S. aureus* can be used as promising materials for the development of diagnostic agents.

A

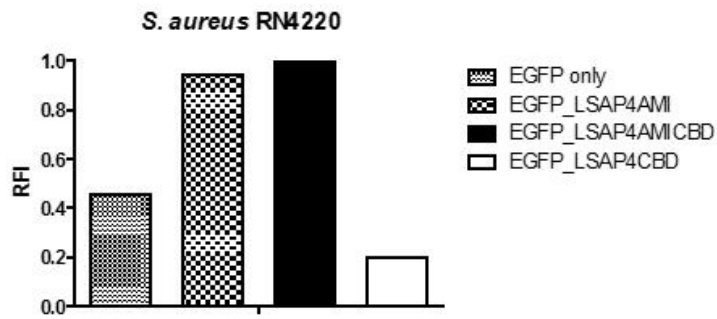
S. aureus RN4220
RFI
1.0
0.8
0.6
0.4
0.2
0.0
EGFP only
EGFP_LSAP4AMI
EGFP_LSAP4AMICBD
EGFP_LSAP4CBD

B

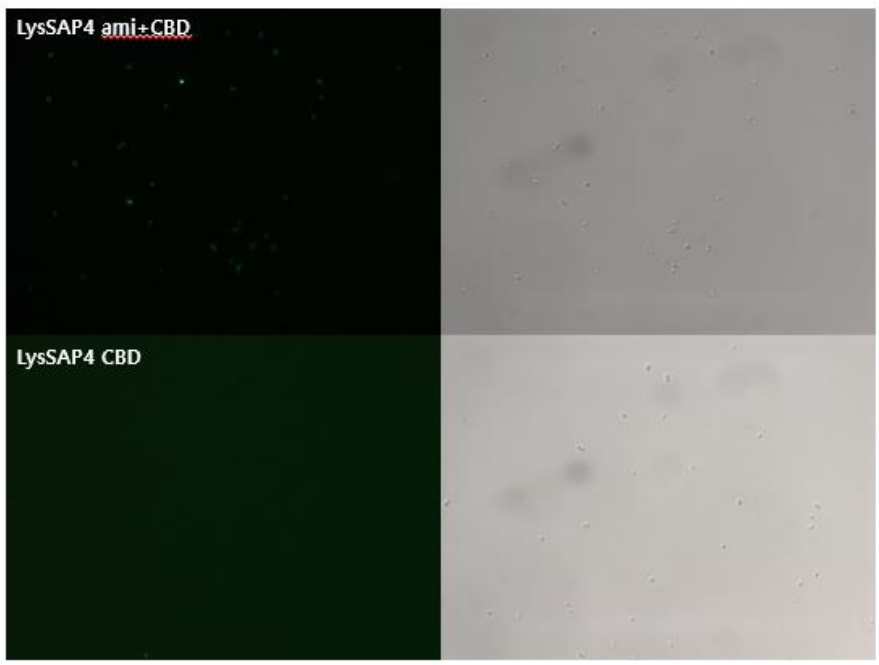
LysSAP4 ami+CBD
LysSAP4 CBD

Figure II-12. Determination of the role of the LysSAP4 amidase domain. (A) Relative cell binding activities of 10 μM of EGFP_LSAP4AMI, EGFP_LSAP4AMICBD, and EGFP_LSAP4CBD with *S. aureus* RN4220. (B) Optical and florescence images of *S. aureus* RN4220 after the addition of EGFP_LSAP4AMICBD (top) and EGFP_LSAP4CBD (bottom) at 10 μM. The scale bar represents 2 μm.

III. Development of a novel chimeric endolysin using random domain swapping

III.1. Introduction

Staphylococcus aureus is a Gram-positive bacterium that has threatened human and animal health, causing staphylococcal food poisoning and wide range of infectious diseases, including skin infections, pneumonia, meningitis, endocarditis, and osteomyelitis (De Lencastre, Oliveira, & Tomasz, 2007; Lowy, 1998). Especially, the global spread of methicillin-resistant *S. aureus* (MRSA) is raising serious concerns because MRSA can easily become resistant to multiple antibiotics, limiting treatment options (Chambers & DeLeo, 2009). Moreover, the strong biofilm-forming ability of *S. aureus* has aggravated problems in a food and medical industry (Lewis, 2001; Otto, 2012). For these reasons, there is an urgent need for creating new antimicrobials to combat *S. aureus* (Foster, 2004).

Endolysins are bacteriophage-encoded peptidoglycan hydrolases produced by bacteriophages at the end of their replication cycles to break down the peptidoglycan of bacterial cell wall resulting in the release of the viral progeny (Schmelcher, Donovan, et al., 2012). Endolysin has been suggested as a promising antibacterial agent, because the purified endolysin protein can rapidly lyse and induce death of Gram-positive bacteria when applied exogenously. Compared to classical antibiotics, endolysins have

several advantages because they have narrow host specificity, high sensitivity, and low probability for developing bacterial resistance (Borysowski et al., 2006). Endolysins from bacteriophages infecting Gram-positive bacteria have a modular architecture with at least two separated functional regions. Generally, an N-terminal domain carrying one or two catalytic domains was attached by a short linker to a C-terminal cell wall-binding domain (CBD) (Fischetti, 2008; Schmelcher, Donovan, et al., 2012). The catalytic domain determines the enzymatic mechanism of endolysin whereas the CBD positions the catalytic domain to the peptidoglycan of target bacteria for efficient lysis of endolysin (Loessner, 2005; Schmelcher et al., 2011).

Most endolysins of staphylococcal phages have three distinct domains: an N-terminal cysteine-, histidine-dependent amidohydrolase/peptidase (CHAP) domain, a central N-acetylmuramoyl-l-alanine amidase (Ami_2 or Ami_3) domain, and a C-terminal SH3b domain as a CBD (Chang & Ryu, 2017). The efficacy of *S. aureus* phage endolysins in killing *S. aureus* and in controlling staphylococcal infection in animal models have been reported in several studies (Fenton et al., 2010; Gu et al., 2011; Kerr et al., 2001; Rashel et al., 2007). Although several *S. aureus* phage endolysins presented promising results, poor expression or the insolubility of the expressed proteins has limited the development of a

highly active staphylococcus-specific phage endolysins (Daniel et al., 2010). In addition, identifying a novel endolysin from *S. aureus* phages is relatively difficult because most *S. aureus*-targeting endolysins have similar domain compositions and display high amino acid sequence identity (Becker, Foster-Frey, et al., 2009; Chang & Ryu, 2017; Oliveira et al., 2013). To circumvent these issues, a number of groups have designed truncated or chimeric versions of lysins (Fernandes et al., 2012; Idelevich et al., 2011; Manoharadas, Witte, & Bläsi, 2009), but the current trial-and-error strategies are time-consuming and labor-intensive to find a novel endolysin with desired properties. In this study, I developed a random domain swapping method and newly identified nineteen chimeras containing different combinations of catalytic and cell wall binding domains from four *S. aureus* phage endolysins. Among them, a novel chimeric endolysin 'Lys109' which showed enhanced lytic activity against *S. aureus* and other multiple staphylococcal species was selected and characterized in buffer conditions, food products and stainless steel. This proof of concept study indicates the potential of the random domain swapping method for developing a novel therapeutic agent for controlling *S. aureus*.

III.2. Materials and Methods

III.2.1. Bacterial strains and growth conditions.

The bacterial strains used in this study are listed in Table 1. Staphylococcal strains were grown in tryptic soy broth (TSB) medium (Difco, Detroit, MI) at 37℃ under aerobic conditions. Baird-Parker agar plates with egg yolk tellurite (BPA; Difco) were used for selective enumeration of *S. aureus. Bacillus cereus, B. subtilis, Listeria monocytogenes,* and *Streptococcus thermophilus* were cultivated in brain heart infusion (BHI) medium (Difco, Detroit, MI). Luria-Bertani (LB) medium (Difco) was used for the growth of Gram-negative strains. *Escherichia coli* DH5α and BL21 (DE3) star strains were used in cloning and expression of proteins, respectively.

III.2.2. Library construction for random domain swapping

The gene encoding SPN1S lysRz (SPN1S_0028 and SPN1S_0029) was amplified from *Salmonella* Typhimurium phage SPN1S (Genbank accession number NC_016761) using the oligonucleotides listed in Table S1. The gene fragment was digested with EcoRI-SalI and inserted into pBAD33 vector (Lim, Shin, Kang, & Ryu, 2012). To confirm the cell lysis efficiency,

the pET28a_EGFP vector (Minsuk Kong & Ryu, 2015) was co-transformed into competent *E. coli* BL21 (DE3) with pBAD33_SPN1S lysRz. The fluorescence of released EGFP was measured by using a SpectraMax i3 multimode microplate reader (Molecular Devices, Sunnyvale, CA) with excitation at 485 nm and emission at 535 nm. Four different *S. aureus* phage endolysin including LysSA12, LysSA97, LysSA11 and LysSAP4 were used in constructing two types of libraries (Chang, Kim, & Ryu, 2017; Chang & Ryu, 2017). For the first library, I tried to generate chimeric endolysins containing two catalytic domains. The genes encoding four CHAP domains and those encoding three amidase domains from the four endolysins were amplified and digested with BamHI/XhoI to be inserted as N-terminal domain of chimeric endolysins. For the central domain of chimeric endolysins, the seven genes were amplified and digested with XhoI/BamHI. All plasmids and primers used in this study are listed in Table III-1. For the second library, all genes encoding CHAPs and amidase domains were amplified and digested with only BamHI to ensure a diversity in the number of catalytic domains to be inserted into endolysins. All gene fragments were randomly ligated into BamHI sites of pET28a vectors (Novagen, Madison, WI) containing one of the genes encoding four different cell wall binding domains from the four endolysins. The vector libraries were co-transformed into competent *E. coli* BL21 (DE3) harboring pBAD33_SPN1S lysRz.

Table III-1. Plasmids and primers used in this chapter

	Description
pET28a	Kan^R, T7 promoter, His-tagged expression vector
pBAD33	Amp^r, araC, P_{BAD}, pBR322 *ori*
pET28a-LSA12CBD	pET28a with LSA12CBD
pET28a-LSA97CBD	pET28a with LSA97CBD
pET28a-LSA11CBD	pET28a with LSA11CBD
pET28a-LSAP4CBD	pET28a with LSAP4CBD
	Sequence
EcoR1_SPN1SlysRz_F	AAA GAA TTC GGA GTG AAA CGA TGG ACA TTA ACC AGT TCC GGC
SPN1SlysRz_Sal1_R	TTT GTC GAC TCA CCT GGT CAG CGA ATC GTA C
BamH1_LSA12CHAP_F	AAA GGA TCC ATGC AAG CAA AAC TAA CTA AAA A
LSA12CHAP_BamH1_R	TTT GGA TCC TGA TCG TGG AGC TGT TTC GCT T
LSA12CHAP_Xho1_R	TTT CTC GAG TGA TCG TGG AGC TGT TTC GCT T

BamH1_LSA12AMI_F	AAA GGA TCC GTA CAA TCT CCT ACG CAA GCA
LSA12AMI_BamH1_R	TTT GGA TCC ACT TGA AGC GCT TGA CTC ATT AG
LSA12AMI_Xho1_R	TTT CTC GAG ACT TGA AGC GCT TGA CTC ATT AG
BamH1_LSA97CHAP_F	AAA GGA TCC ATG CCG TCG GTT AGG ACA TAC AG
LSA97CHAP_BamH1_R	TTT GGA TCC TTC TTT TGC GTA GAA TGG ACG GAT
LSA97CHAP_Xho1_R	AAA CTC GAG ATG CCG TCG GTT AGG ACA TAC AG
BamH1_LSA97AMI_F	AAA GGA TCC CAA GAT AAG TTA TCA AAA GGT AAA
LSA97AMI_BamH1_R	TTT GGA TCC ACT ACT TGG CGC ATC AAT TTG TC
LSA97AMI_Xho1_R	TTT CTC GAG ACT ACT TGG CGC ATC AAT TTG TC
BamH1_LSAP4CHAP_F	AAA GGA TCC GGG AAG CAG TTC AAT CCT GAT TT

LSAP4CHAP_BamH1_R	TTT GGA TCC TTT ATC TGG GAA ATT TAA TCT AA
LSAP4CHAP_Xho1_R	TTT CTC GAG TTT ATC TGG GAA ATT TAA TCT AA
BamH1_LSAP4AMI_F	AAA GGA TCC AAA GTA AGT GTT GGA GAT AAA GC
LSAP4AMI_BamH1_R	TTT GGA TCC TTG GTT TTT AGC TGA TGT TTT AAC
LSAP4AMI_Xho1_R	TTT CTC GAG TTG GTT TTT AGC TGA TGT TTT AAC
BamH1_LSA11CHAP_F	AAA GGA TCC ATG AAA GCA TCG ATG ACT AGA AG
LSA11CHAP_BamH1_R	TTT GGA TCC GTC TTT GAA ATT AGG TTC TAT AA
LSA11CHAP_Xho1_R	TTT CTC GAG GTC TTT GAA ATT AGG TTC TAT AA

III.2.3. Screening of chimeric endolysins by plate lysis method

The resulting clones from random library were screened as described in a previous study with some modifications (Yang et al., 2015). In brief, the clones were picked and grown in 96 well plate with fresh LB broth containing 0.01 mM of IPTG and grown overnight at 37 ℃ to initiate the expression of chimeric endolysins. Afterward, 0.2% of arabinose were added into the wells for expressing SPN1S lysRz. These cultures were dotted onto agar plate overlaid with autoclaved *S. aureus* RN 4220 and incubated for 12 h at 37 °C. The clones exhibiting clear lysis zone against *S. aureus* were screened and picked for sequencing analysis to identify the cloned chimeric endolysin.

III.2.4. Expression, and purification of endolysins

Identified clones were expressed with 0.5 mM IPTG (isopropyl-β-D-thiogalactopyranoside) at OD_{600} (optical density at 600 nm) = 0.7, followed by incubation for additional 20 h at 18 ℃. Bacterial cells were suspended in lysis buffer (50 mM sodium phosphate, 300 mM sodium chloride and 30 % glycerol; pH 8.0) and disrupted by sonication at a duty cycle of 25% and output control of 5 (BRANSON ULTRASONICS). After centrifugation (20,000 x g, 30 min), the supernatant passed through a Ni-nitrilotriacetic

acid (NTA) superflow column (Qiagen), and purification of the recombinant proteins was performed according to the manufacturer's instruction. The purified protein was stored at – 80 ℃ until use after buffer was changed to the storage buffer (50 mM sodium phosphate, 300 mM NaCl and 30 % glycerol; pH 8.0) using PD Miditrap G-25 (GE healthcare).

III.2.5. *In silico* analysis of endolysins

The sequences of chimeric endolysin and its parental endolysins were analyzed. Their domain composition was investigated using the BLAST (http://blast.ncbi.nlm.nih.gov/Blast.cgi), Interproscan 5 (http://www.ebi.ac.uk/interpro), and Pfam 28.0 programs (http://pfam.xfam.org) (Altschul et al., 1990; Altschul et al., 1997; Finn et al., 2013). Amino acid sequence alignments of the endolysins were performed using ClustalX2.1 (Larkin et al., 2007). The molecular weight and isoelectric point of the proteins were calculated using the Compute pI/Mw program (http://www.expasy.ch/tools/pi_tool.html) (Gasteiger et al., 2005).

III.2.6. Lytic activity assay

The lysis of the chimeric endolysins and their original endolysins

was assessed by turbidity reduction assay (B. Son et al., 2012). Bacterial cells grown to exponential phase were re-suspended with the reaction buffer (50 mM Tris-HCl, pH 6.5). Then, purified proteins were added to the cell suspension at a final concentration of 300 nM, and the OD reduction of cells was measured over time by using a SpectraMax i3 multimode microplate reader at 600 nm. The relative lytic activity was calculated after 60 min as follows; (ΔOD_{600} test (endolysin added) - ΔOD_{600} control (buffer only)) /initial OD_{600}. Antimicrobial spectrum was tested by plate lysis assay as previously described (Chang, Kim, et al., 2017). In brief, 10 μL of diluted endolysin (167, 16.7 and 1.67 pmol) was spotted onto a freshly prepared bacterial lawn on TSA agar plates. Spotted plates were air-dried in a laminar flow hood for 15 min and incubated overnight at 37 ℃. Minimum inhibitory concentration (MIC) of the endolysins were determined by serially diluting the endolysins in 1:2 in 96-well plates as described previously (Andrews, 2001; Swift et al., 2015). Exponentially growing *S. aureus* CCARM 3090 was added to each well at a final concentration of 10^5 CFU/well and the plate was incubated at 37 °C for 20 h. The MIC was defined as the lowest concentration of the endolysin producing inhibition of visible growth.

III.2.7. Biofilm reduction assay

A biofilm reduction assay was performed as previously described with some modifications (Wu, Kusuma, Mond, & Kokai-Kun, 2003). Staphylococcal strains incubated in TSB medium supplemented with 0.25 % D-(+)-glucose (Sigma) were prepared and sub-cultured to the same media in a 96-well polystyrene microplate. After incubating the microplate for 24 h at 37 ℃, all wells were washed with PBS. Once the biofilm was formed, the experimental group wells were filled with endolysins. After the incubation for 2 h at 37 ℃, each well was washed once with PBS and stained with 1.0 % crystal violet. Additionally, each well was washed three times with PBS, followed by solubilizing with 33 % acetic acid. The absorbance of the obtained solution was measured at 570 nm and the sessile biomass was presented as an A_{570} value.

III.2.8. Effect of pH and temperature on endolysin activity

For the temperature stability assay of Lys109, the lytic activity was measured at 25℃ for 60 min after enzyme was incubated at various temperatures (4-65℃) for 30 min. To study the effect of temperature on LysSA109 enzymatic activity, 300 nM Lys109 was added into target cell suspension and the mixture was incubated at different temperatures (4–

65℃) for 60 min. To test the effect of pH on the activity of Lys109, 300 nM of Lys109 was added to the *S. aureus* CCARM 3090 cell suspended in the following buffers: 50 mM sodium acetate (pH 4.5 and 5.4), 50 mM Tris–HCl (pH 6.5 -8.0), 50 mM glycine (pH 9.0), and 50 mM N-cyclohexyl-3-aminopropanesulfonic acid (pH 10.0).

III.2.9. Antimicrobial activity assay in food samples

The lytic activity of Lys109 against MRSA CCARM 3090 strain was tested in commercial whole-fat pasteurized milk and meat (pork and beef) as previously described [21]. A milk sample was inoculated with exponentially growing MRSA CCARM 3090 cells (approximately 105 CFU/mL). Before the addition of Lys109 at 0, 30, 300, 900 and 1500 nM, the milk samples were pre-incubated with bacteria at 25℃ for 1 h to allow them to adapt to milk. Each milk sample was then incubated at 25℃ for an additional hour. Viable bacterial cells (CFU/mL) were counted every 15 min after Lys109 addition by plating each sample on a BPA plate. Pork and beef samples were aseptically cut into cubes approximately 2x2 cm3 in volume. MRSA CCARM 3090 cells (approximately 105 CFU/mL) were inoculated onto the surface of each sample by pipetting and were pre-incubated at 25℃ for 1 h to allow the bacteria to adapt to each condition.

Subsequently, each sample was inoculated with 0, 50 and 100 nM of Lys109 and further incubated at 25℃ for an additional hour. After 1 h, S. aureus cells were detached from the surface of the meat products by agitating them in PBS with 0.05 % tween-20 (PBST) for 2 min with a bench-top vortex mixer at maximum speed. Cell suspensions were serially diluted, plated onto BPA plates and incubated at 37℃ for 24h.

III.2.10. Antimicrobial activity assay on stainless steel

The lytic activity of Lys109 against MRSA CCARM 3090 strain was tested on the stainless steel as previously described [21]. A stainless steel coupon with size 2x2 cm3 was sterilized by autoclaving. Exponentially growing MRSA CCARM 3090 bacterial cells were harvested and resuspended in PBS to a final concentration of approximately 105 CFU/ml. Prepared bacterial cells were pipetted onto the stainless steel surfaces and dried for 1 h in clean bench. Subsequently, the stainless steel was treated with Lys109 (0–100 nM) and left for 60 min at 25℃. For the negative control, PBS was used instead of Lys109 solution. S. aureus cells were detached from the surface of the meat products by agitating them in PBST for 2 min with a bench-top vortex mixer at maximum speed. Cell

suspensions were serially diluted and plated onto BPA plates, and incubated at 37 ℃ for 24 h.

III.2.11. Statistical analysis

All experiments were replicated three times. GraphPad Prism (version 5.01) was used to conduct statistical analysis. The one-way analysis of variance (ANOVA) followed by the one-way Tukey's test for all pairwise comparison (95% confidence interval) were performed. The data are presented as means with standard deviations. A P-value <0.05 was considered statistically significant.

III.3. Results and discussion

III.3.1. Development of a random domain swapping method

The overall scheme of random domain swapping method was presented in Figure III-1. The screening of chimeric endolysins was performed with SPN1S-mediated *E. coli* lysis and chimeric endolysin-mediated *S. aureus* lysis. The protocol was established based on a 96 well plate format for the rapid and efficient screening, taking advantage of SPN1S phage endolysin and Rz/Rz1-like protein (SPN1S lysRz). SPN1S lysRz has been reported to cause the host cell lysis and release viral progeny at the end of phage life cycle (Lim et al., 2012). To evaluate the cell lysis efficiency of SPN1S lysRz, the amount of EGFP protein released from lysed *E. coli* was measured. Fluorescence was significantly increased after induction with arabinose, indicating that SPN1S lysRz can cause the rapid lysis of *E. coli* cells from within and thereby can release accumulated proteins in the cytosol (Figure III-2B). In an effort to identify an active chimeric endolysin from large random library, the lytic efficacy of the released proteins was evaluated by their ability to form a clear zone on the agar plate overlaid with the heat-killed *S. aureus* cells. The use of autoclaved *S. aureus* cells as endolysin substrates in screening allowed us to

clearly distinguish active chimeric endolysins among clones. When *E. coli* and *S. aureus* were co-cultured, it gave rise to false positive clones, some of which showed clear zone on the lawn of *S. aureus* but produced insoluble or inactive form of proteins. A previous study described that *E. coli* grows faster than *S. aureus* in mixed culture of *E. coli* and *S. aureus*, indicating that *E. coli* might inhibit the growth of *S. aureus*, forming inhibition-like zone on the *S. aureus* lawn (Fujikawa & Sakha, 2014). As positive controls, four different *S. aureus* phage endolysins (LysSA11, LysSA97, LysSAP4 and LysSA12) were expressed in the presence of pBAD33_SPN1S lysRz. The clear zones were visualized on the agar plate depending on their activities, whereas clones without pBAD33_SPN1S lysRz did not show any clear zone, suggesting that SPN1S lysRz-induced lysis of *E. coli* allowed active chimeric endolysins to form clear zone on the agar plate containing target bacteria (Figure III-2B and C). These results indicate that random domain swapping method has been successfully developed for screening of novel chimeric endolysins.

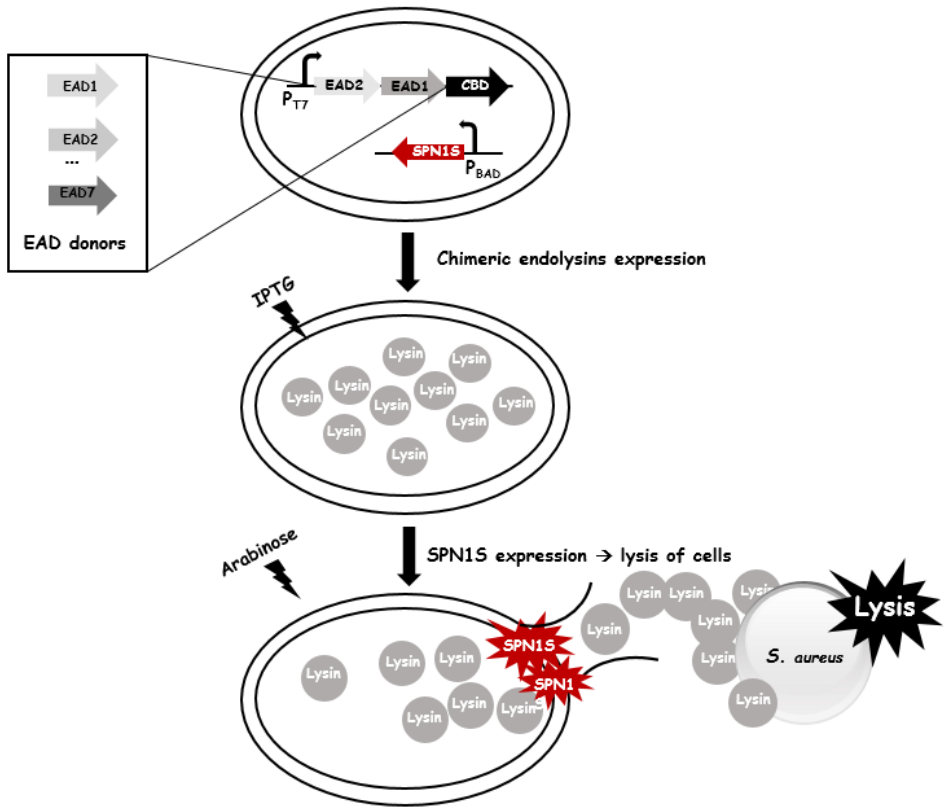

Figure III-1. Scheme of the random domain screening method.

A

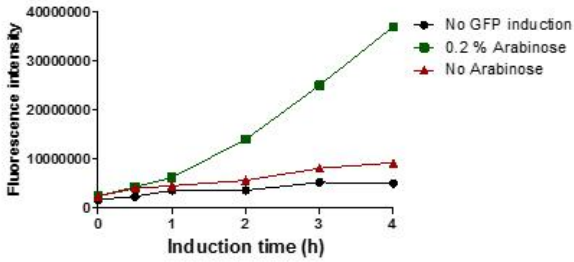

B

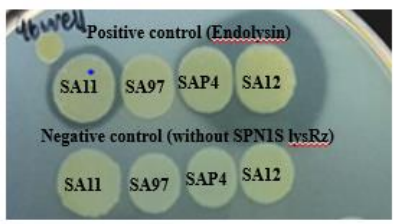

C

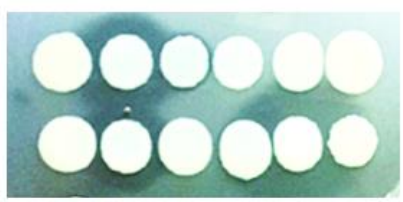

Figure III-2. Development of screening system on 96-well microplate.

(A) EGFP released from SPN1S-induced lysis in host *E. coli* cells. Cells without induction (IPTG for EGFP expression and arabinose for SPN1S lysRz expression) were used as controls. (B) Clones for positive and negative controls were culutred with 0.2% arabinose overnight on the lawn of autoclaved *S. aureus* RN4220. (C) Clones were culutred with 0.2% arabinose overnight on the lawn of autoclaved *S. aureus* RN4220.

III.3.2. Isolation of a novel endolysin Lys109

The random library containing 480 clones were co-transformed into *E. coli* containing SPN1S lysRz-harboring vector and applied to the agar plate containing *S. aureus* for screening. The clones displaying clear lysis zone were sequenced to determine the combination of the EADs (Table III-2). All selected clones contained a CHAP domain from LysSA12 or LysSA11, which showed high staphylolytic activity (Chang, Kim, et al., 2017; Chang, Yoon, et al., 2017). Especially, LysSA12 CHAP domain-containing clones, which account for 68% of selected clones, showed a large and clear lysis zone. There was also a single clone containing LysSAP4 CHAP domain. These results suggest that CHAP domain is necessary to degrade *S. aureus* cell wall peptidoglycan, which is consistent with previous reports that a CHAP domain has mainly used as a donor for the catalytic domain of chimeric endolysins (Daniel et al., 2010; Schmelcher, Powell, et al., 2012; Yang et al., 2014). Among LysSA12 CHAP domain-containing clones, five promising chimeric endolysins were selected for the further comparative analysis (Figure III-3). All selected proteins were expressed in *E. coli* as a soluble form and evaluated for their lytic activity against *S. aureus*. As a result, a chimeric endolysin, consisting of a LysSA12 CHAP domain in the N-terminal region, a LysSA97 amidase domain at the central

and a LysSA97 CBD in the C-terminal region showed the highest lytic activity among the five candidates and was designated as Lys109. BLAST analysis revealed that Lys109 has 78% overall amino acid sequence identity with an amidase from StauST398-1 *S. aureus* phage (Van Der Mee-Marquet et al., 2013) and 80% with endolysins from ΦB166 and ΦB236 *S. aureus* phage (Botka et al., 2015) (Figure III-4). Even though the three endolysins showed high similarity with Lys109, they have not been studied yet, indicating that further research on Lys109 will be meaningful. Moreover, since the lytic activity of *S. aureus* endolysin depends mostly on a CHAP domain and several LysSA12 homologs, such as LysH5 of *S. aureus* phage vB_SauS_phiIPLA88 (98% identity to LysSA12) and *S. aureus* Φ11 endolysin (96% identity to lysSA12) are well documented (García et al., 2010; Sass & Bierbaum, 2007) (Figure III-5), I decided to characterize Lys109 to see how the domain substitutions affect the activity of the endolysin.

Table III-2. Identification of the selected chimeric endolysins

Clone	CHAP	Amidase	CBD
1	SA12		SA11
2	SA12		SA12
3	SA12		SA97
4	SA12	SA12	SA97
5	SA12		SAP4
6	SA12	SA97	SA12
7	SA12	SA97	SA97
8	SA12	SA12	SAP4
9	SA12	SA97	SAP4
10	SA12	SAP4	SA12
11	SA12	SAP4	SAP4
12	SA11	SA12	SAP4
13	SA11		SA12
14	SAP4	SA12	SA12
15	SA11	SA12	SA12
16	SA11		SA11
17	SA12	SA12	SA12
18	SA11	SA12(CHAP)	SA11
19	SA12	SA97	SA11

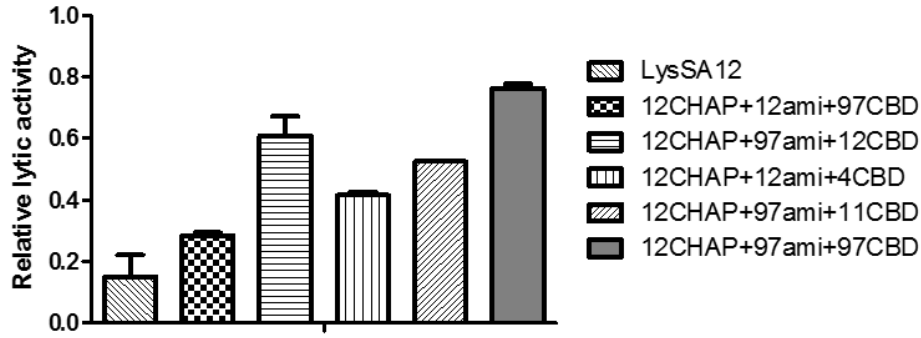

Figure III-3. Lytic activity comaprison of Lys109 with other lysins.

Comparison of relative lytic activity among four other chimeric endolysins and LysSA12 with Lys109 (300 nM each) against *S. aureus* CCARM 3090.

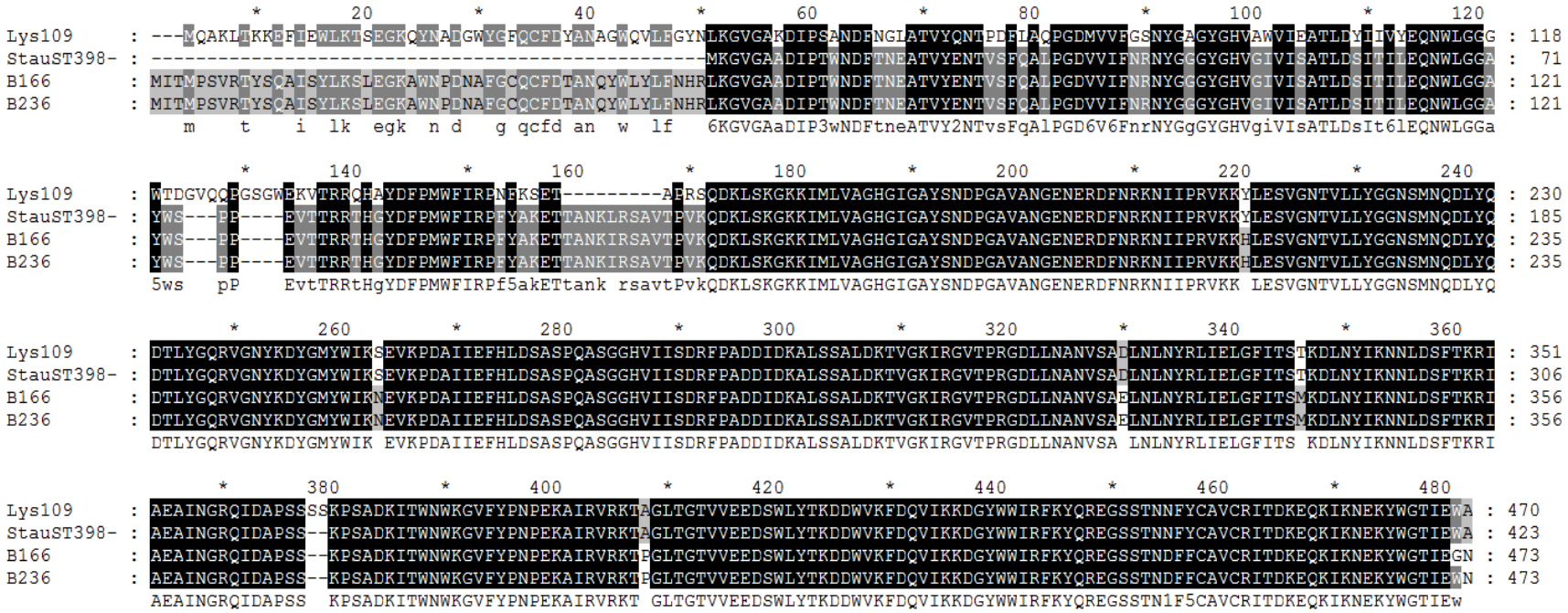

Figure III-4. Sequence alignment of Lys109 with other related endolysins.

StauST398, *S. aureus* phage StauST398 endolysin; B166, *S. aureus* phage ΦB166 endolysin; B236, *S. aureus* phage ΦB236 endolysin. Conserved and identical residues are shaded in gray (dark gray, >70% conserved; light gray, >40% conserved) and black, respectively.

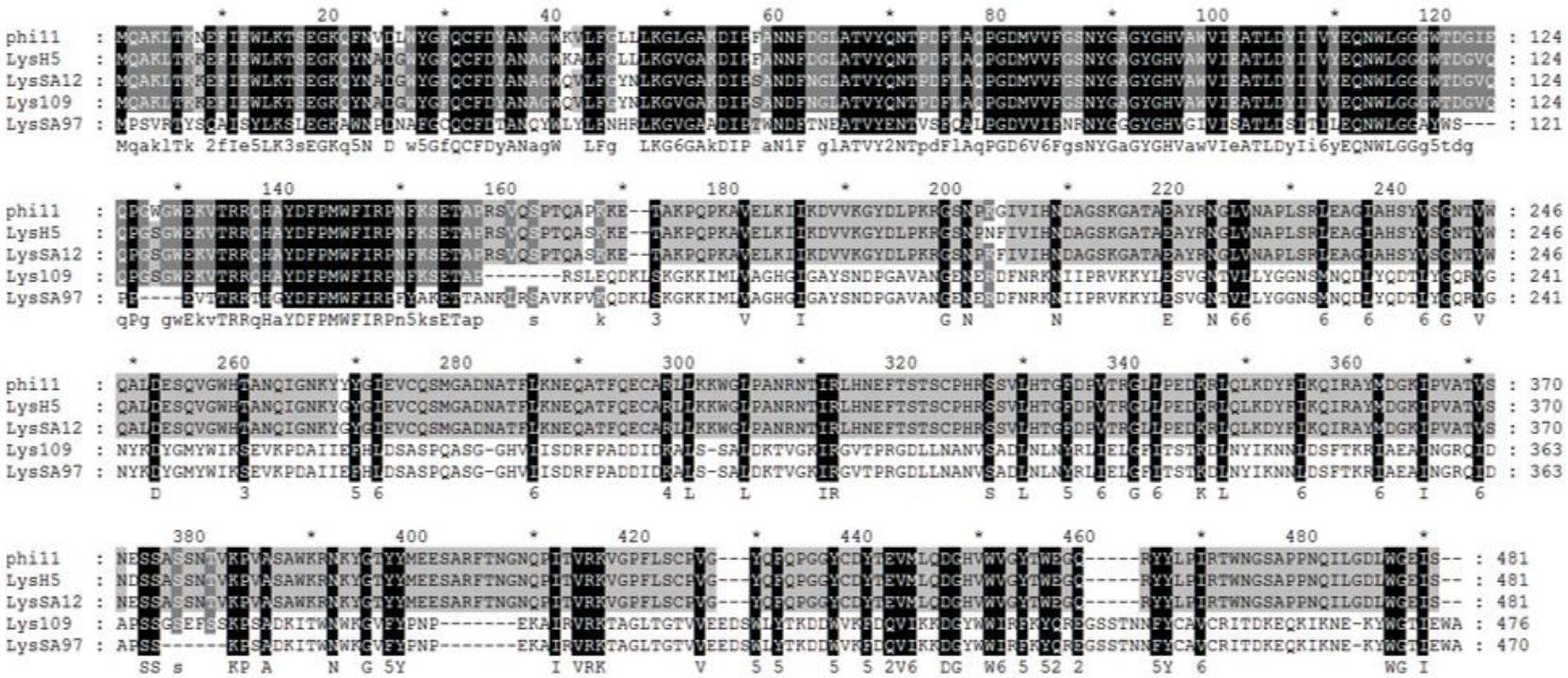

Figure III-5. Sequence alignment of Lys109 with LysSA12 homologs.

phi11, *S. aureus* phage phi11 endolysin; LysH5, *S. aureus* phage vB_SauS-phiIPLA88 endolysin; LysSA12, *S. aureus* phage SA12 endolysin; LysSA97, *S. aureus* phage SA97 endolysin. Conserved and identical residues are shaded in gray (dark gray, >70% conserved; light gray, >40% conserved) and black, respectively.

III.3.3. Lytic activity of Lys109 in comparison with its parental endolysins

Lys109 was highly expressed as a soluble form in *E. coli* and purified via Ni-NTA affinity chromatography (Figure III-6). The antibacterial activity of Lys109 was examined in comparison with its parental endolysins, LysSA12 and LysSA97 at various concentrations (Figure III-7). Lys109 exhibited clear cell lysis against *S. aureus* CCARM 3090, displaying at least 2-folds higher lytic activity than that of LysSA12 and LysSA97 at all tested concentrations. LysSA12 did not show any activity at concentrations below 30 nM and LysSA97 has barely exhibited staphylolytic activity at all tested concentrations. These results indicate the superiority of LysSA12 CHAP over LysSA97 CHAP in the lytic activity despite their sequence similarity (44% identity). The comparative analysis of lytic activity of Lys109 with its parental endolysins against other *S. aureus* strains including clinical isolates and MRSA also showed the evident improvement of lytic activity of Lys109 (Figure III-7).

The MIC of Lys109 was compared with those of its parental endolysins. LysSA97, a donor for the amidase domain and CBD of Lys109, did not show inhibition of cell growth at the maximum concentrations available (5.85 μM), leading us to exclude LysSA97 in the following

experiments (Figure III-7). LysSA12 inhibited the growth of *S. aureus* CCARM 3090 at concentration of 0.843 μM. The MIC of Lys109 was 0.375 μM, which was at least 2.25-fold lower than that of LysSA12, indicating the antimicrobial activity of Lys109 has significantly improved compared to its parental endolysins.

Then, how Lys109 has superior lytic activity to its parental endolysins? One possible reason is that increased binding ability of endolysin led to improvement of antibacterial activity (B. Son, Kong, & Ryu, 2018). Indeed, LysSA97 amidase plus CBD displayed higher binding affinity to the target bacteria than LysSA12 amidase plus CBD (Figure III-8), suggesting that LysSA97 amidase plus CBD might increase the lytic activity of LysSA12 CHAP by enhancing accessibility to the target bacteria. Alternatively, peptidoglycan fragment generated by the initial LysSA12 CHAP digestion could be more sensitive to LysSA97 amidase domain plus CBD than LysSA12 amidase plus CBD as speculated by Becker and colleagues (Becker, Dong, et al., 2009). Further structural and biophysical studies of Lys109 are needed and will help to verify the exact molecular mechanism of enhanced lytic activity provided by domain swapping.

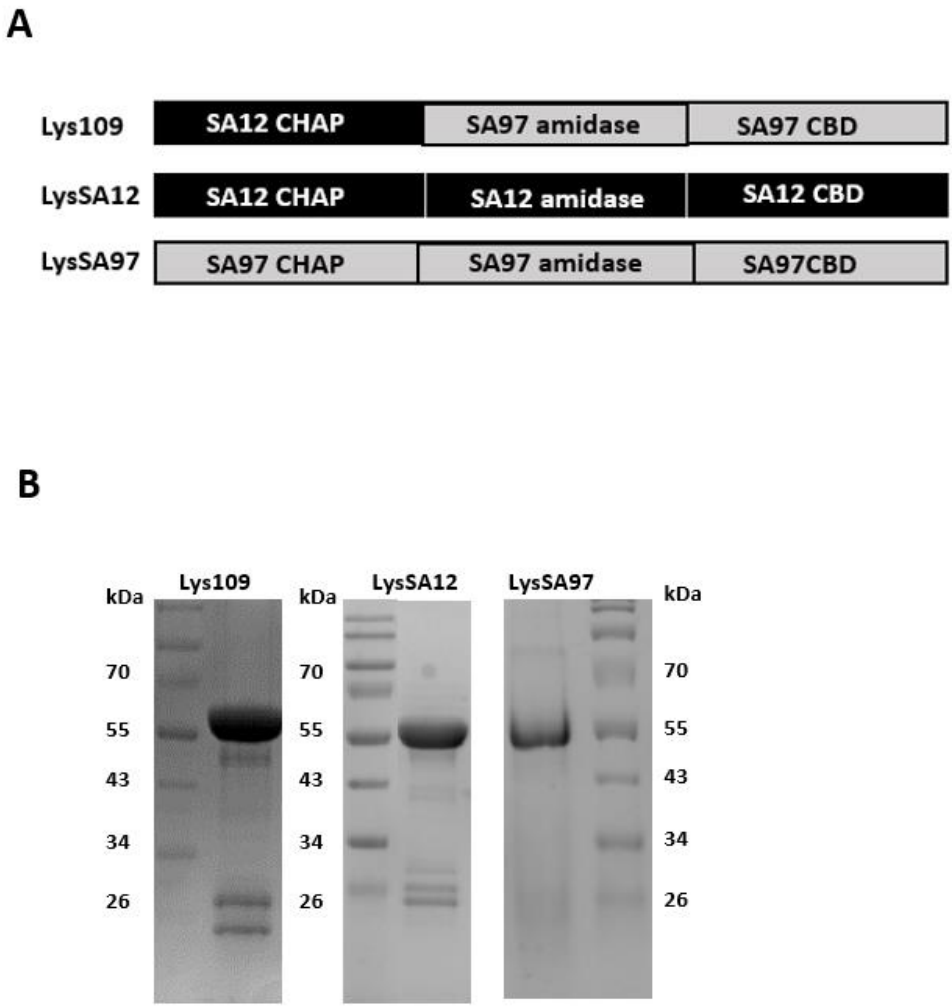

Figure III-6. Modular structure of Lys109, LysSA12 and LysSA97.

(A) Schematic representation of Lys109 and its parental endolysins, LysSA12 and LysSA97. (B) Ni-NTA-purified Lys109, LysSA12 and LysSA97.

A

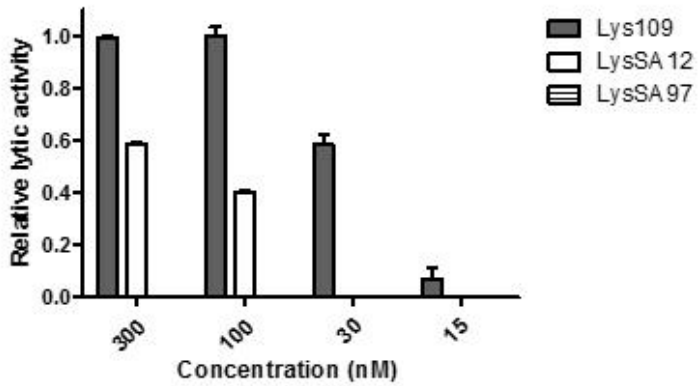
Relative lytic activity
1.0
0.8
0.6
0.4
0.2
0.0
300
100
30
15
Concentration (nM)
Lys109
LysSA12
LysSA97

B

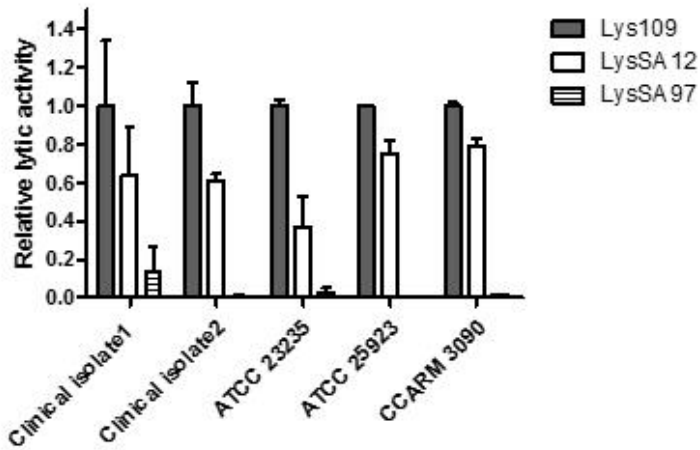
Relative lytic activity
1.4
1.2
1.0
0.8
0.6
0.4
0.2
0.0
Clinical isolate1
Clinical isolate2
ATCC 23235
ATCC 25923
CCARM 3090
Lys109
LysSA12
LysSA97

C

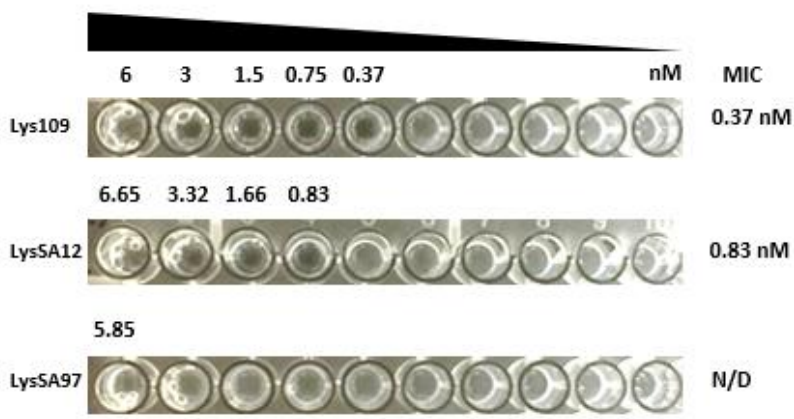
6
3
1.5
0.75
0.37
nM
MIC
Lys109
0.37 nM
6.65
3.32
1.66
0.83
LysSA12
0.83 nM
5.85
LysSA97
N/D

Figure III-7. Lytic activity of Lys109, LysSA12 and LysSA97.

(A) Relative lytic activity of Lys109, LysSA12 and LysSA97 against *S. aureus* CCARM 3090 at different concentrations. (B) Relative lytic activity of Lys109, LysSA12 and LysSA97 (300 nM each) against various *S. aureus* strains. (C) MIC of Lys109, LysSA12 and LysSA97 against *S. aureus* CCARM 3090.

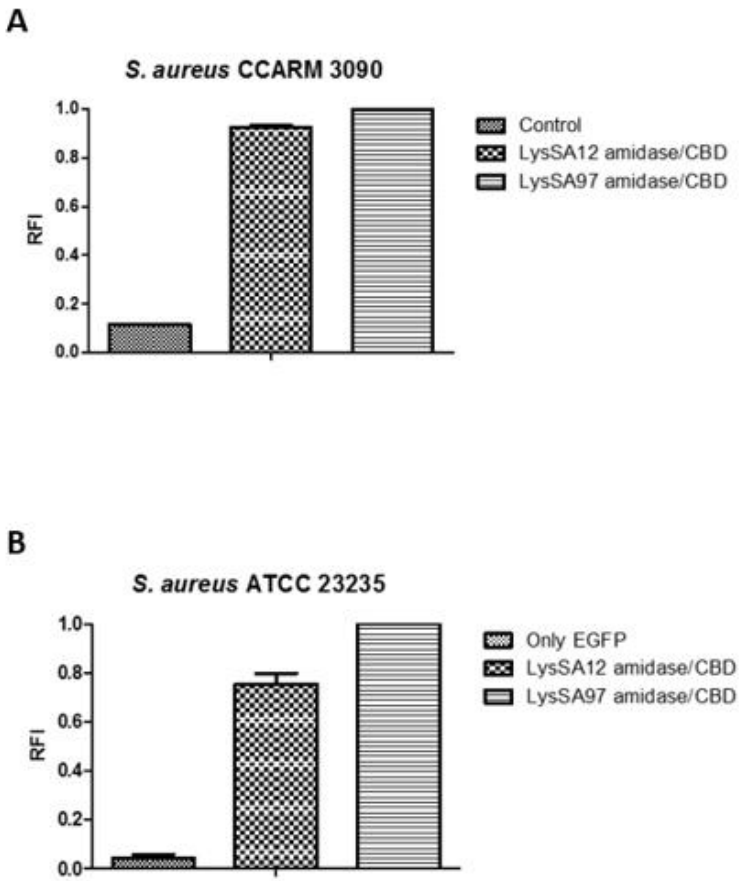

Figure III-8. Binding activity comparison among EGFP_LysSA12 amidase plus CBD and EGFP_LysSA97 amidase plus CBD.

The relative binding activity of 1 μM of EGFP_LysSA12 amidase plus CBD and EGFP_LysSA97 amidase plus CBD toward (A) *S. aureus* CCARM 3090 and (B) S. aureus ATCC 23235. EGFP only did not show binding to *S. aureus.*

III.3.4. Biofilm reduction activity of Lys109

It has been known that more than 60% of bacterial infections in human are involved in biofilms (Lewis, 2001). Biofilms significantly contribute to the resistance of pathogenic bacteria to conventional antibiotic treatment (Abee, Kovács, Kuipers, & Van der Veen, 2011). Several previous studies have shown the ability of endolysins to degrade staphylococcal biofilms (Gutierrez, Ruas-Madiedo, Martínez, Rodríguez, & García, 2014; Sass & Bierbaum, 2007; J.-S. Son et al., 2010). I also evaluated biofilm reduction efficacy by Lys109 against biofilms formed by *S. aureus* CCARM 3090 and *S. aureus* RN4220 by a crystal violet staining based assay (Figure III-9). All biofilms showed high susceptibility to Lys109 in a dose dependent manner. Moreover, Lys109 appeared to have a higher biofilm reduction efficacy than LysSA12 at most concentrations tested. When 300 nM of endolysins were treated to the biofilms, Lys109 exhibited more than 3-fold enhanced efficacy to remove biofilm compared to LysSA12. These results demonstrate that Lys109 has strong lytic activity against not only planktonic cells but also biofilms, which are an important contributing factor for many treatment failures (Otto, 2013).

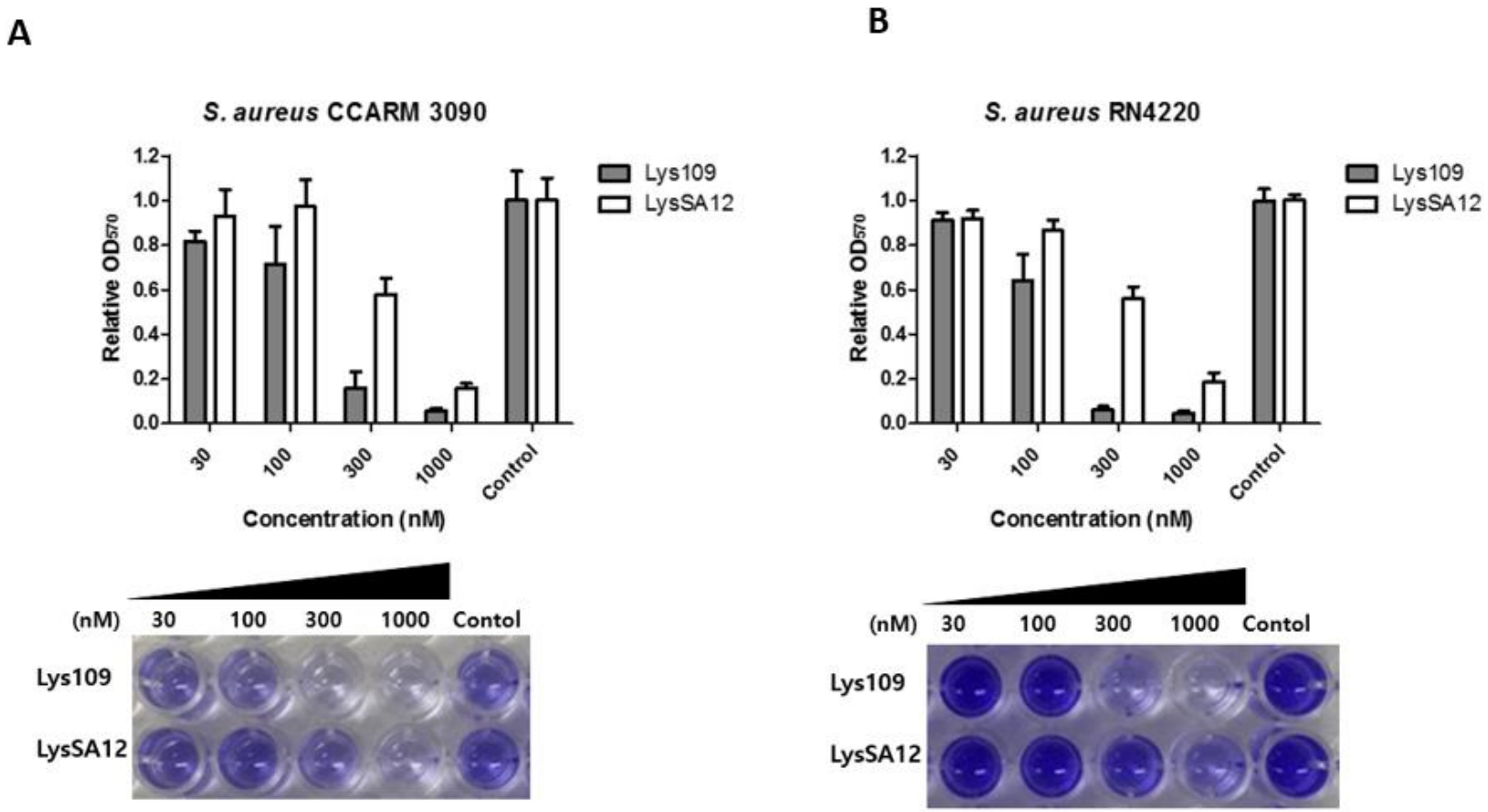
A
S. aureus CCARM 3090
Relative OD570
1.2
1.0
0.8
0.6
0.4
0.2
0.0
Lys109
LysSA12
30
100
300
1000
Control
Concentration (nM)
(nM) 30 100 300 1000 Contol
Lys109
LysSA12
B
S. aureus RN4220
Relative OD570
1.2
1.0
0.8
0.6
0.4
0.2
0.0
Lys109
LysSA12
30
100
300
1000
Control
Concentration (nM)
(nM) 30 100 300 1000 Contol
Lys109
LysSA12

Figure III-9. Biofilm reduction activity of Lys109 and LysSA12.

Biofilms formed by (A) *S. aureus* CCARM 3090 and (B) *S. aureus* RN4220 were treated with various concentrations of Lys109 and LysSA12 and visualized by staining biofilms with crystal violet. Dark staining indicates the biofilm that was maintained after treatment of endolysins and light or no staining indicates successful removal of the biofilm. Control indicates the sample treated with buffer without endolysins.

III.3.5. Temperature and pH effects on the enzymatic activity of Lys109

The thermostability of endolysins was determined (Figure III-10A). Lys109 retained over 95% of its activity after 1 h incubation at 4 to 37 ℃ and the lytic activity of Lys109 started to decrease at 45℃. Approximately 40% decrease of its hydrolytic activity was observed at 50 °C and the higher temperatures, 55 and 65 ℃ caused a complete inactivation of Lys109. LysSA12 showed similar pattern of thermal stability to LysSA109, indicating that the structural stabilization by the fusion of LysSA12 CHAP to LysSA97 amidase domain plus CBD might not be the reason of the enzymatic improvement of Lys109.

The effect of temperature and pH on the lytic activity of Lys109 was evaluated to determine the optimum working condition of Lys109 (Figure III-10B and C). The maximal activity was exhibited at 25-37 ℃ and pH 6.5-9.0. The wide optimum pH range of Lys109 suggest that Lys109 can be applied to many foods associated with a high risk for *S. aureus* contamination, such as milk or meat products (Korkeala, Mäki-Petäys, Alanko, & Sorvettula, 1986; Marino et al., 2000).

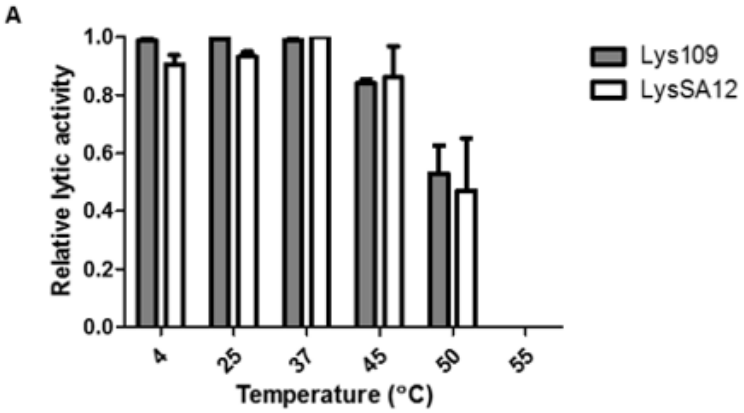
A
Relative lytic activity
1.0
0.8
0.6
0.4
0.2
0.0
4
25
37
45
50
55
Temperature (°C)
Lys109
LysSA12

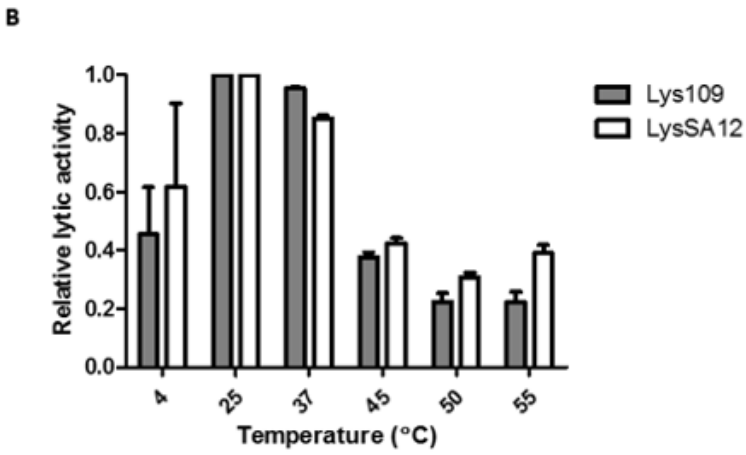
B
Relative lytic activity
1.0
0.8
0.6
0.4
0.2
0.0
4
25
37
45
50
55
Temperature (°C)
Lys109
LysSA12

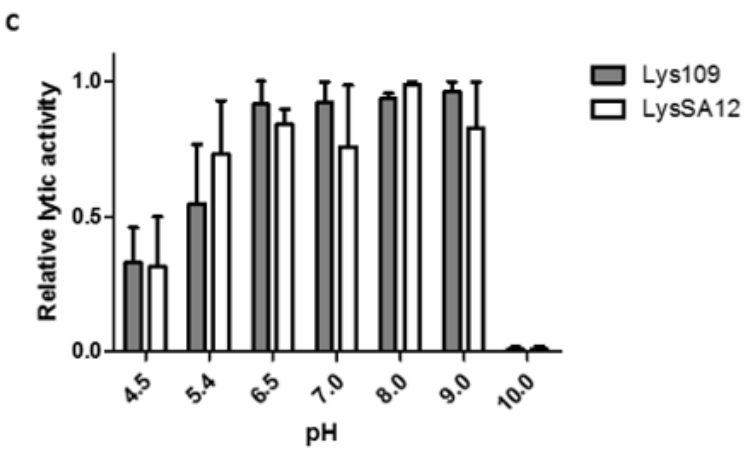
C
Relative lytic activity
1.0
0.5
0.0
4.5
5.4
6.5
7.0
8.0
9.0
10.0
pH
Lys109
LysSA12

Figure III-10. The effect of temperature and pH on the lytic activity of Lys109 and LysSA12.

For evaluation of thermal stability (A), enzymes were incubated at different temperatures for 30 min prior to the lysis assay that was performed against *S. aureus* CCARM 3090 at 25℃. Optimum temperature (B) and pH (C) of Lys109 and LysSA12 was examined by incubating enzymes with target cells at different temperatures and in different pH buffers, respectively.

III.3.6. Antibacterial spectrum of Lys109

Antimicrobial activity against several *S. aureus* and other species of staphylococci was examined by plate lysis method (Table III-3). Thirty-six different bacterial strains including *S. aureus, S. hominis, S. saprophyticus, S. heamolyticus, S. capitis, S. warneri, S. xylosis and S. epidermidis* were tested with different amount of endolysins (167 and 16.7 pmol). Lys109 displayed effective lytic activity against all tested staphylococci strains, but not the other Gram-positive and Gram-negative bacteria, indicating that Lys109 has the same antibacterial spectrum with parental endolysin. However, some of stains were susceptible to 16.7 pmol of Lys109 whereas LysSA12 could not form clear zone at this concentration. These results demonstrated that Lys109 retains the binding specificity of the original endolysin and have superior antimicrobial properties as well.

Table III-3. Antimicrobial spectrum of LysSA12 and Lys109

		LysSA12 (pmol)		Lys109 (pmol)	
		167	**16.7**	**167**	**16.7**
S. aureus	Human isolate 117	+	-	++	+
	Human isolate 81	++	-	++	+
	Human isolate 119	++	-	+++	-
	Plant isolate 37	+	-	++	-
	Plant isolate 8	+	-	++	-
	Plant isolate 13	+	-	+	-
	Animal isolate 154	+	-	+++	-
	Animal isolate 134	+	-	+++	-
	Animal isolate 100	++	-	+++	-
	Animal isolate 99	+	-	++	-
	Clinical isolate 1163	+	-	+++	-
	Clinical isolate FMB1	+	-	++	-
	Clinical isolate FMB2	++	-	+++	-
	Clinical isolate FMB3	++	-	+++	-
	Matitis cow milk isolate FMB4	++	-	+++	+
	ATCC 6538	+	-	++	-
	RN4220	++	-	++	-
	ATCC 23235	+	-	+++	+
	ATCC 13301	++	-	+++	-

	CCARM 3090	+	-	++	-
S. hominis	ATCC 37844	+	-	++	+
S. saprophyticus	ATCC 15305	+	-	++	+
S. heamolyticus	ATCC 29970	+	-	+++	-
S. capitis	ATCC 35661	+	-	++	-
S. warneri	ATCC 10209	+	-	+	-
S. xylosis	ATCC29971	+	-	+	-
S. epidermidis	CCARM 3787	++	+	++	++
Bacillus cereus	KCCM 40133	-	-	-	-
B. subtilis	168	-	-	-	-
Steptococcus thermophilus	ATCC 19258	-	-	-	-
Listeria monocytogenes	ATCC 19114	-	-	-	-
Salmonella Typimurium	LT2	-	-	-	-
Pseudommonas aeruginosa	ATCC 27853	-	-	-	-
Cronobacter sakazakii	ATCC 29544	-	-	-	-
Escherichia coli	MG1655	-	-	-	-

III.3.7. Efficacy of Lys109 against *S. aureus* in food samples

Comparative antibacterial activity of Lys109 and LysSA12 against a MRSA (*S. aureus* CCARM 3090) strain was examined at various concentrations in food samples. Milk and meat products were chosen for the test because they have been frequently implicated in staphyloccocal foodborne illnesses (Kadariya, Smith, & Thapaliya, 2014). In milk artificially contaminated with *S. aureus*, treatment of LysSA12 did not show any CFU reduction at all tested concentrations even though LysSA12 has exerted lytic activity with 100 nM in buffer condition (Figure III-11), demonstrating the importance of in vivo experiment to evaluate the potential of a new antimicrobial. LysH5, a LysSA12 homolog, also could not decrease bacteria cells in milk with 0.15 μM and 1-log reduction was observe with 0.8 μM LysH5 (García et al., 2010; Obeso, Martínez, Rodríguez, & García, 2008). On the other hand, the treatment with 300 nM of Lys109 showed apparent inhibitory effect of *S. aureus* within 15 min and resulted in 2 log reduction of bacterial cells after 1h (Figure III-11). In addition, 900 nM of Lys109 completely eliminated *S. aureus* from the milk within 45 min (Figure III-12).

Previously, some peptidoglycan hydrolases have shown the antimicrobial activity in milk. CHAPK_CWT-LST consisting of CHAP

endopeptidase domain of phage endolysin LysK and the SH3b CBD of lysotaphin has been reported to have the strong staphylolytic activity in milk, showing that 106.5 nM of CHAPK_CWT-LST yielded 2.37 log unit reduction of *S. aureus* after 3 h (Verbree et al., 2018). The treatment with 9 μM of LysSA11 from *S. aureus* phage SA11 resulted in complete elimination of staphylococcal cells from the milk within 30 min (Chang, Kim, et al., 2017). Considering the fact that other staphylococcal peptidoglycan hydrolases have kown to appear only low lytic activity in milk, our results indicate that Lys109 has high staphylolytic activity in milk (Verbree et al., 2018; Yang, Zhang, Wang, Yu, & Wei, 2017).

The treatment of 50 nM Lys109 on surface of pork and beef for 1 h reduced bacterial numbers by 3 log CFU/cm^2 and 2 log CFU/cm^2, respectively (Figure III-12B and C). Lytic activity of Lys109 was decreased at a concentration of 500 nM even though reduction of bacterial numbers on the surface of meat products has been observed by treatment of Lys109. Lys109 might be rapidly inactivated or reduced in its availability within the complex environment of meat during the assay, which is in accordance with a previous report that higher concentrations of enzymes is more likely to be aggregated (Zettlmeissl, Rudolph, & Jaenicke, 1979). A solution for this problem could be a repeated administration of the enzyme with low doses.

It is worth to note that the lytic activity of Lys109 was less effective on beef

than pork. One of the possible reasons is that beef might protect bacterial cells from antimicrobial agents by coating cell surface with the constituents such as fat, thereby making endolysin difficult to reach the bacterial cells (Cutter, 2000; Larson et al., 1996). On the other hand, after the treatment of LysSA12, the bacterial cells count was reduced only 1-log CFU/ cm^2 at all tested concentrations. In a previous report, LysSA97, which is an another parental endolysin of Lys109, has shown negligible antimicrobial activity on beef, and only the treatment of LysSA97 and carvacrol in combination exhibited approximately 2 log CFU/cm^2 decrease in *S. aureus* cell count, indicating Lys109 can exert higher lytic activity on meat products than its original endolysins (Chang, Yoon, et al., 2017). These findings showed that Lys109 has high staphylolytic activity in the complex bio-matrix as well as in the buffer condition and suggested Lys109 has a great potential for uses as a food antimicrobial to control *S. aureus* from dairy and meat products.

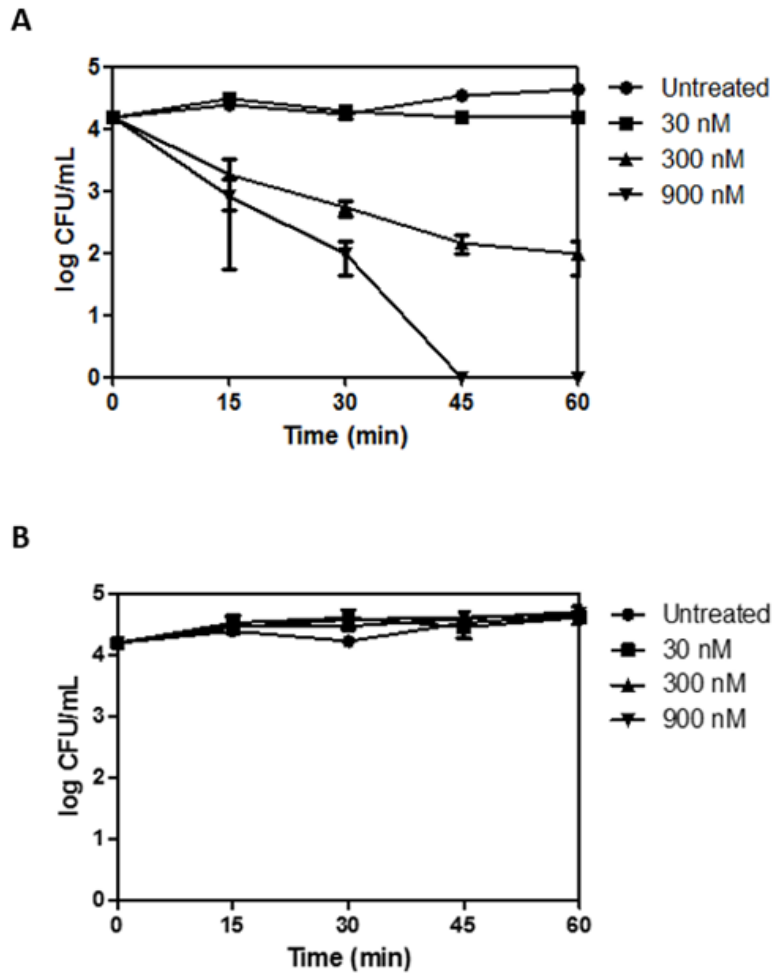

Figure III-11. Antibacterial activity of Lys109 and LysSA12 against *S. aureus* CCARM 3090 in milk.

Lys109 (A) and LysSA12 (B) were treated to milk artificially contaminated with *S. aureus* CCARM 3090 at different concentrations. Bacterial cells were counted every 15 min for 1h.

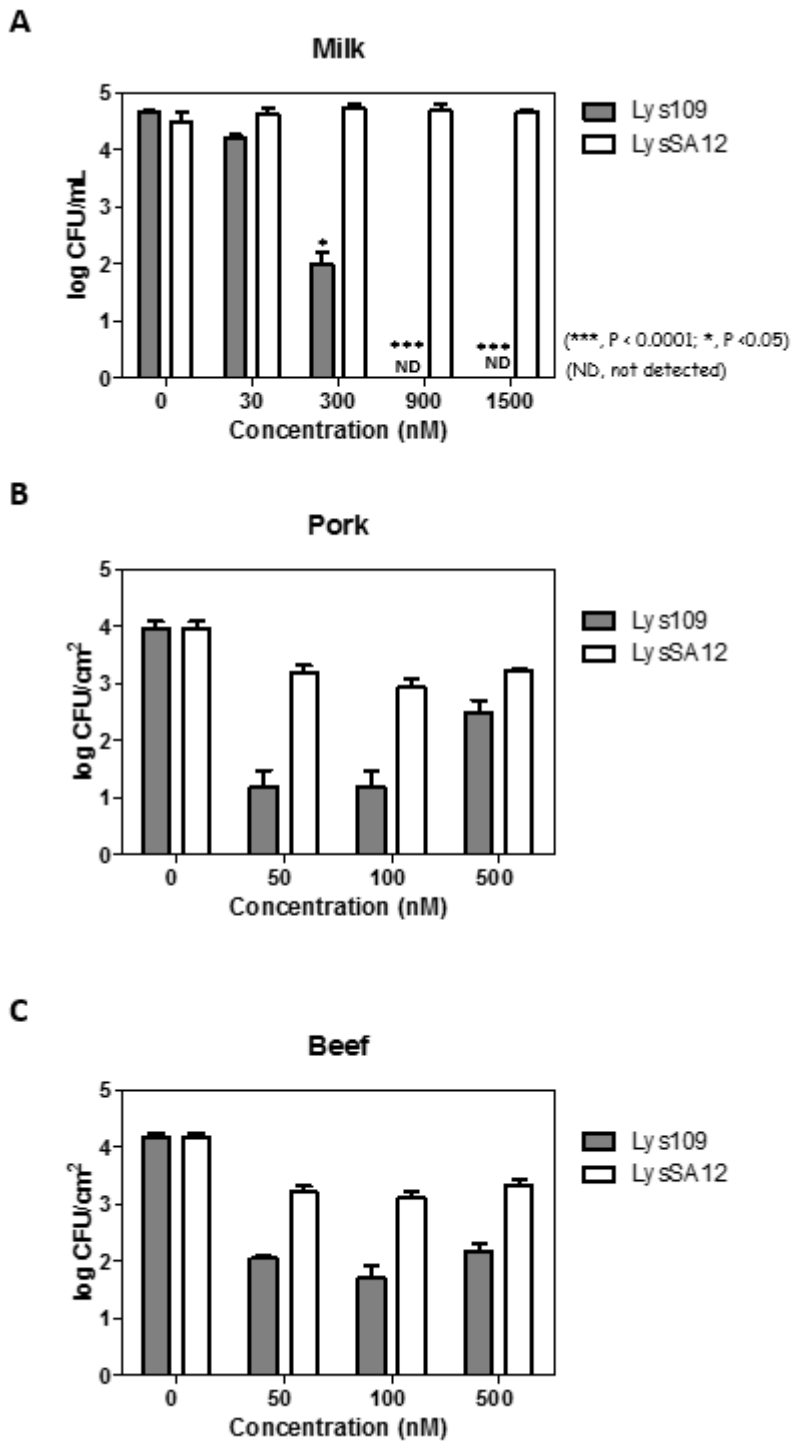
A
Milk
log CFU/mL
Concentration (nM)
0
30
300
900
1500
*
***
ND
***
ND
Lys109
LysSA12
(***, P < 0.0001; *, P <0.05)
(ND, not detected)
B
Pork
log CFU/cm2
Concentration (nM)
0
50
100
500
Lys109
LysSA12
C
Beef
log CFU/cm2
Concentration (nM)
0
50
100
500
Lys109
LysSA12

Figure III-12. Antibacterial activity of Lys109 and LysSA12 against *S. aureus* CCARM 3090 in food samples.

The number of *S. aureus* CCARM 3090 cells in milk (A), pork (B), and (C) beef were counted after treatment of Lys109 and LysSA12 at concentration of 0 nM (negative control), 50 nM, 100 nM, and 500 nM. Each *column* represents the mean standard deviations of triplicate assays. The *asterisks* indicate significant differences (***$P < 0.001$, *$P < 0.05$)

III.3.8. Efficacy of Lys109 against *S. aureus* in stainless steel

S. aureus contamination in food can occur from the environment during handling and processing of food as well. These cross-contaminations contribute to high number of food borne illness outbreaks (Bennett et al., 2013). Stainless steel is a common cooking utensil which can be problem by an improper cleaning and handling. Stainless steel was artificially contaminated with *S. aureus* CCARM 3090 to evaluate the staphylolytic efficacy of Lys109 (**Figure III-13**). At 100 nM, treatment of Lys109 on the surface of stainless steel coupon caused bacterial cell decrease below the detection limit, whereas its parental endolysin was less effective at the same concentration, resulting in only 1-log bacterial reduction after 1 h. Recently, LysSA11 has shown its potential for use as a disinfectant (Chang, Kim, et al., 2017). The lytic activity of Lys109 was similar to that of the higher concentration of LysSA11, suggesting that Lys109 can be used as both an antimicrobial and a sanitizer for utensils.

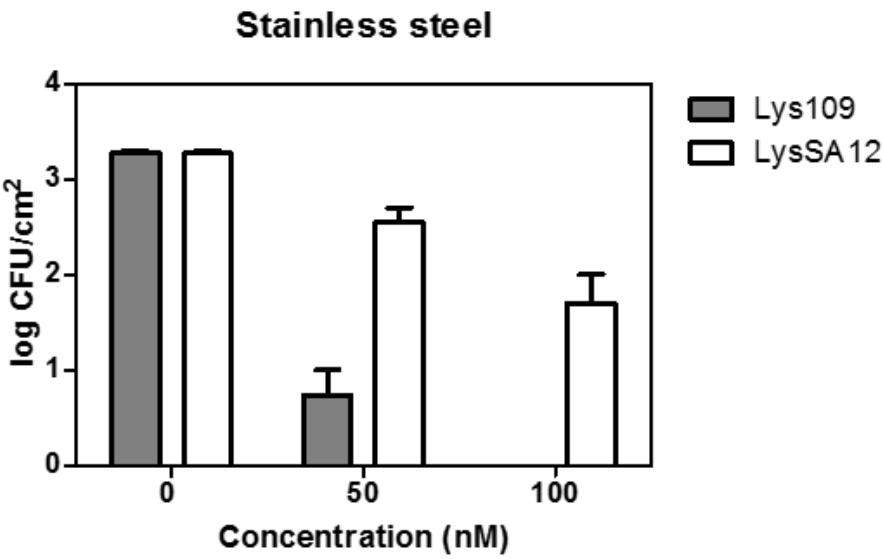

Figure III-13. Antibacterial activity of Lys109 and LysSA12 against *S. aureus* CCARM 3090 on stainless steel.

The number of *S. aureus* CCARM 3090 cells were counted after treatment of Lys109 and LysSA12 at concentration of 0 nM (negative control), 50 nM and 100 nM.

IV. Simultaneous control of *Staphylococcus aureus* and *Bacillus cereus* using fusion protein containing two endolysins

IV.1. Introduction

Food poisoning outbreaks caused by bacterial pathogens are one of the major concerns worldwide. In the United States, approximately 9.4 million cases of foodborne illness with about 56,000 hospitalizations and 1,300 deaths caused by major food-borne pathogens have been reported every year (Scallan et al., 2011). In particular, 300,000 cases are caused by *Bacillus cereus* or *Staphylococcus aureus* which is considered as an important bacteria regarding their frequency and seriousness of the disease (Scallan et al., 2011). Their coexistence in food appears to be dominant since *B. cereus* and *S. aureus* can cause an outbreak in similar food products (Kumar, Murali, & Batra, 2009). Moreover, symptoms caused by *B. cereus* and *S. aureus* food poisoning highly resembles and also overlaps with other foodborne infections. Due to this symptomatic similarities, *B. cereus* food poisonings are occasionally misdiagnosed to *S. aureus* intoxication (Bennett et al., 2013). In previous studies, simultaneous detection of pathogens including *B. cereus* and *S. aureus* has been conducted (Kim et al., 2007; Kumar et al., 2009). For these reasons, simultaneous control of both *S. aureus* and *B. cereus* would be highly meaningful.

Generally, the treatment of antibiotics was the only option to control

these bacteria. However, as the incidence of antibiotic-resistant bacteria is increasing, phage endolysins have been attracted attention as promising alternatives to antibacterial agents (Fischetti, 2008; Loessner, 2005). Most endolysins from the phages infecting Gram-positive bacteria have a modular structure, in which one or several enzymatically active domains (EAD) and a cell wall binding domain (CBD) are functionally separated by a short linker (Callewaert, Walmagh, Michiels, & Lavigne, 2011; Fischetti, 2010; Schmelcher, Donovan, et al., 2012). In the case of staphylococcal phage endolysins, they typically consist of a CHAP domain and an amidase domain as an EAD and a SH3b type CBD (Kashani et al., 2018). The modular structure of the phage endolysins facilitates the endolysin engineering to alter lytic activity, target specificity, protein solubility and other properties (Gutiérrez et al., 2018). A variety of protein engineering strategies such as an exchange of domains, combination of two heterologous CBDs, duplication of a CBD, random mutagenesis and site directed mutagenesis have been attempted to optimize endolysins for specific applications (Schmelcher, Donovan, et al., 2012).

There has been a trial to extend lytic spectrum and increase activity by constructing fusion proteins with two full-length enzymes. In a previous study, the full-length and C-terminally truncated phage endolysin from *Streptococcus agalactiae* bacteriophage B30 were fused to the lysostaphin

protein of *S. simulans*. These proteins degraded both streptococcal and staphylococcal cells and their activities were tested in milk (Donovan, Dong, et al., 2006). This research group also created the fusion proteins with the endopeptidase of streptococcal phage λSA2 endolysin with the *Staphylococcus*-specific CBDs of either the endolysin LysK or lysostaphin. The altered CBDs conferred lytic activity against staphylococci and streptococci on the streptococcal enzyme (Becker, Foster-Frey, et al., 2009).

This is the first study of the fusion proteins consisting of two different endolysins targeting *S. aureus* and *B. cereus*. The full-length and C-terminally truncated LysB4 (LysB4EAD), an endolysin from *B. cereus*-infecting phage B4 were fused to LysSA11, an endolysin of *S. aureus*-infecting phage SA11 via a helical linker in both orientation. The fusion proteins maintained lytic activity of their parental endolysins against both *S. aureus* and *B. cereus*, showing successfully extended antimicrobial spectrum. All fusion proteins exhibited higher thermal stability than LysSA11, and LysB4-LySA11 and LysB4EAD-LysSA11 also had improved thermal stability compared to LysB4. In particular, LysB4EAD-LysSA11 exhibited significantly increased thermal stability compared with its parental endolysins and was selected for further study. The strong antimicrobial activity of the LysB4EAD-LysSA11 was observed in the boiled rice.

These proteins will be potent antimicrobial agents for simultaneous

control of multiple pathogenic bacteria. Moreover, this approach will be helpful to design highly specific antimicrobials but multifunctional antimicrobials.

IV.2. Materials and methods

IV.2.1. Bacterial strains and growth conditions.

All *Staphylococcus* strains were grown in TSB broth at 37 ℃. All *Bacillus, Listeria, Streptococcus* were grown in BHI broth at 37 ℃. Gram-negative bacteria were grown in LB broth at 37 ℃. All tested bacteria was grown under the aerobic condition. *Escherichia coli* DH5α and BL21 (DE3) star strains were used in cloning and expression of proteins, respectively. Baird-Parker agar plates with egg yolk tellurite (BPA; Difco) were used for selective enumeration of *S. aureus* and *Bacillus cereus* selective agar plate with egg yolk emulsion and polymyxin B supplement (Oxoid) was used for enumeration of *B. cereus*.

IV.2.2. Construction of recombinant proteins

LysSA11 and LysB4 or LysSA11 and LysB4EAD was connected by a helical linker $(EAAAK)_4$ according to the previous study (Arai, Ueda, Kitayama, Kamiya, & Nagamune, 2001). Fusion proteins were constructed by an overlapping extension PCR described previously (Nelson & Fitch, 2012). Plasmids and primers used in this study were listed in Table. *lysSA11* gene was amplified from the pET29b_LysSA11 (Chang, Kim, et al., 2017).

lysB4 and *lysB4EAD* genes were amplified from the pET15b_LysB4 (B. Son et al., 2012). The two overlapping PCR fragments containing a helical linker (HL) were used for the second PCR step to generate the *lysB4-lysSA11* or *lysB4EAD-lysSA11* in both orientations. The resultant PCR product was inserted between BamHI/SalI restriction enzyme sites of pET28a. The cloned plasmid was transformed into *E. coli* BL21 (DE3).

Table IV-1. Plasmids and primers used in this chapter

Plasmids		
	Description	**Reference**
pET28a	Kan^r, T7 promoter, His-tagged expression vector	Novagen, Wisconsin, SA
pET15b-LysB4	pE15b with LSA12CBD	(B. Son et al., 2012)
pET29b-LysSA11	pET29a with LSA97CBD	(Chang, Kim, et al., 2017)
Primers (5'→3')		
	Sequence	
B4EAD_HL_overl_R	TTT TGC CGC AGC TTC TTT TGC CGC AGC TTC TTT TGC CGC AGC TTC TTT TGC CGC AGC TTC TCC ACC TGT AGA GCC ACC TCC	
SA11EAD_Sal1_R	TTT GTC GAC TTG TAC CTC GTC TTT GAA ATT	

	AGG
SA11EAD_HL_overl_R	TTT TGC CGC AGC TTC TTT TGC CGC AGC TTC
	TTT TGC CGC AGC TTC TTT TGC CGC AGC TTC
	TTG TAC CTC GTC TTT GAA ATT AGG
B4EAD_Sal1_R	TTT GTC GAC TCC ACC TGT AGA GCC ACC TCC
BamH1_B4_F	AAA GGA TCC ATG GCA ATG GCA TTA CAA ACT
	T
B4_HL_overl_R	TTT TGC CGC AGC TTC TTT TGC CGC AGC TTC
	TTT TGC CGC AGC TTC TTT TGC CGC AGC TTC
	TTT GAA CGT ACC CCA GTA GTT C
SA11_Sal1_R	TTT GTC GAC TTT CCA GTT AAT ACG ACC CCA
	A

BamH1_SA11_F	AAA GGA TCC ATG AAA GCA TCG ATG ACT AGA A
SA11_HL_overl_R	TTT TGC CGC AGC TTC TTT TGC CGC AGC TTC TTT TGC CGC AGC TTC TTT TGC CGC AGC TTC TTT CCA GTT AAT ACG ACC CCA A
HL_B4_overl_F	GAA GCT GCG GCA AAA GAA GCT GCG GCA AAA GAA GCT GCG GCA AAA GAA GCT GCG GCA AAA ATG GCA ATG GCA TTA CAA ACT TT
B4_Sal1_R	TTT GTC GAC TTT GAA CGT ACC CCA GTA GTT C

IV.2.3. Protein expression and purification

The transformed cells were expressed with 0.5 mM IPTG (isopropyl-β-D-thiogalactopyranoside) at OD_{600} (optical density at 600 nm) = 0.7, followed by incubation for additional 20 h at 18 ℃. Bacterial cells were suspended in lysis buffer (50 mM Tris-HCl, 300 mM sodium chloride and 30 % glycerol; pH 8.0) and disrupted by sonication at a duty cycle of 25% and output control of 5 (BRANSON ULTRASONICS). After centrifugation (20,000 x g, 30 min), the supernatant passed through a Ni-nitrilotriacetic acid (NTA) superflow column (Qiagen), and purification of the recombinant proteins was performed according to the manufacturer's instruction. The purified protein was stored at – 80 ℃ until use after buffer was changed to the storage buffer (50 mM Tris-HCl, 300 mM NaCl and 30 % glycerol; pH 8.0) using PD Miditrap G-25 (GE healthcare). The molecular weight and isoelectric point of the proteins were calculated using the Compute pI/Mw program (http://www.expasy.ch/tools/pi_tool.html) (Gasteiger et al., 2005).

IV.2.4. Lytic activity assay

The lysis of the fusion endolysins was assessed by turbidity reduction assay (B. Son et al., 2012). Bacterial cells grown to exponential phase were re-suspended with the reaction buffer (20 mM Tris-HCl, pH 8.0).

Then, purified proteins were added to the cell suspension at a final concentration of 300 nM, and the OD_{600} reduction of cells was measured over time at room temperature by using a SpectraMax i3 multimode microplate reader at 600 nm. The relative lytic activity was calculated after 60 min as follows; (ΔOD_{600} test (endolysin added) - ΔOD_{600} control (buffer only)) /initial OD_{600}. Antimicrobial spectrum was tested by plate lysis assay as previously described (Chang, Kim, et al., 2017). In brief, 10 μL of diluted endolysin (167, 16.7 and 1.67 pmol) was spotted onto a freshly prepared bacterial lawn on TSA agar plates. Spotted plates were air-dried in a laminar flow hood for 15 min and incubated overnight at 37 ℃.

IV.2.5. Effect of pH and temperature on endolysin activity

For the temperature stability assay of the fusion proteins, the lytic activity was measured at 25℃ for 60 min after enzyme was incubated at various temperatures (4-65℃) for 30 min. To study the effect of temperature on enzymatic activity of the fusion proteins, 300 nM of each protein was added into target cell suspension and the mixture was incubated at different temperatures (4–65℃) for 60 min for reaction. To test the effect of pH on the lytic activity of the fusion proteins, 300 nM of each protein was added to the *S. aureus* RN4220 and *B. cereus* ATCC 21768 cells suspended in the

following buffers: 50 mM sodium acetate (pH 4.5 and 5.4), 50 mM Tris–HCl (pH 6.5 -8.0), 50 mM glycine (pH 9.0), and 50 mM N-cyclohexyl-3-aminopropanesulfonic acid (pH 10.0).

IV.2.6. Antimicrobial activity in food samples.

The fusion proteins were evaluated for their lytic activity in boiled rice because rice is frequently implicated as a source of *S. aureus* and *B. cereus* food poisoning (Grande et al., 2006; Pillsbury, Chiew, Bates, & Sheppeard, 2013). The samples were prepared as described previously (Minsuk Kong & Ryu, 2015). Briefly, sterilized instant rice was purchased at local market and heated using the microwave. The resulting cooked rice (10 g) was homogenized in 40 ml distilled water. Then, the slurry samples were artificially contaminated with MRSA RN4220 (10^5 CFU/mL) and *B. cereus* ATCC 21768 (10^4 CFU/ml) separately or in combination. Before the addition of the proteins at 0, 300, and 3000 nM, the samples were pre-incubated with bacteria at 25℃ for 1 h to allow them to adapt to boiled rice samples. Each sample was then incubated at 25℃ for 4 h. The viable bacterial cells (CFU/mL) were counted every 1 h after the addition of the fusion proteins by plating each sample on a BPA for *S. aureus* or *Bacillus cereus* selective agar plate for *B. cereus*.

IV.2.7. Statistical analysis

All experiments were replicated three times. GraphPad Prism (version 5.01) was used to conduct statistical analysis. The one-way analysis of variance (ANOVA) followed by Tukey's multiple comparison test (95% confidence interval) were performed. Significant differences were determined at a significance level of P-value < 0.05.

IV.3. Results and discussion

IV.3.1. Construction and expression of the fusion protein

I aimed to control *S. aureus* and *B. cereus* simultaneously. First, I selected LysSA11 and LysB4 for construction of fusion proteins. LysSA11 is an endolysin derived from the virulent *S. aureus* phage SA11 (Chang, Kim, et al., 2017). This protein is composed of two functional domains: a CHAP domain at its N-terminal region and a CBD at its C-terminal region and has strong lytic activity against *S. aureus* stains. More importantly, it is the only endolysin that contains two domains among the *S. aureus* endolysins in my laboratory, indicating LysSA11 is small in size and is suitable to be fused with other endolysins. LysB4 is a *B. cereus* phage endolysin which exhibited the enzymatic activity of an L-alanoly-D-glutamate endopeptidase on peptidoglycans (B. Son et al., 2012). LysB4 has strong lytic activity against broad range of pathogenic bacteria including *Bacillus* species and *Listeria monocytogenes.*

Using LysSA11 and the full-length or C-terminally truncated LysB4, I created several types of endolysin fusion proteins connected by a helical linker in both orientations; LysSA11-LysB4, LysB4-LysSA11, LysSA11-LysB4EAD and LysB4EAD-LysSA11 (Figure IV-1). The 20 amino acids-

long linkers ((EAAAK)$_4$ were introduced to maintain a reasonable distance between two endolysins, minimizing the steric hindrance. The proteins were overexpressed in soluble form in *E. coli* and purified proteins were visualized as a single band of the expected molecular mass on SDS-PAGE (Figure IV-1).

A

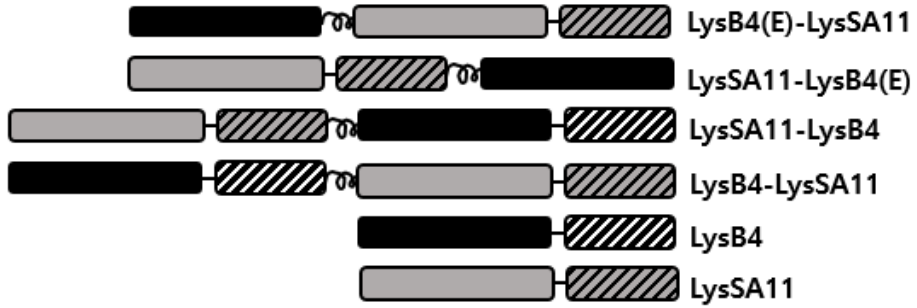
LysB4(E)-LysSA11
LysSA11-LysB4(E)
LysSA11-LysB4
LysB4-LysSA11
LysB4
LysSA11

B

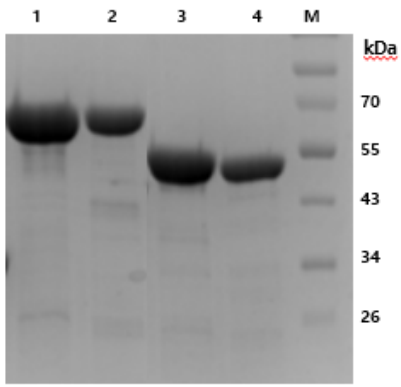
1
2
3
4
M
kDa
70
55
43
34
26

Figure IV-1. Modular structure of the fusion protein with LysSA11 and LysB4.

(A) Schematic representation of fusion proteins with LysSA11, LysB4 and LysB4EAD. (B) SDS-PAGE analysis. Lane 1, LysSA11-LysB4; Lane 2, LysB4-LysSA11; Lane 3, LysSA11-LysB4EAD; Lane 4, LysB4EAD-LysSA11.

IV.3.2. Lytic activity of the fusion proteins

First, the lytic activity of two fusion proteins fused with full-length LysSA11 and LysB4 was evaluated against *S. aureus* and *B. cereus* (Figure IV-2). Both proteins was as active as their parental endolysins in 30 min after the enzymatic reaction, indicating the fusion did not interfere with the activity of their parental endolysins. Interestingly, the lytic activity of LysB4-LysSA11 against *B. cereus* was faster than that of LysSA11-LysB4. LysSA11-LysB4 showed faster lytic activity against *S. aureus* than LysB4-LysSA11. These results indicate the importance of the orientation of the proteins to be fused and both fusion proteins have strong lytic activity for *S. aureus* and *B. cereus*, maintaining their parental specificities. Previously, Yang et el. reported Ply187N-V12C, a chimeric endolysin composed of a CHAP domain of Ply187 of *S. aureus* phage 187 and SH3-5 of enterococcal phage Φ1 endolysin (Loessner, Gaeng, & Scherer, 1999; Yoong, Schuch, Nelson, & Fischetti, 2004). The study showed that the replacement of Ply187CBD to other CBD of phage Φ1 endolysin, which has broad antimicrobial spectrum, increased antimicrobial spectrum of Ply187. However, this is the first time with the fusion of two full-length endolysins which target different genera to expand the antimicrobial spectrum.

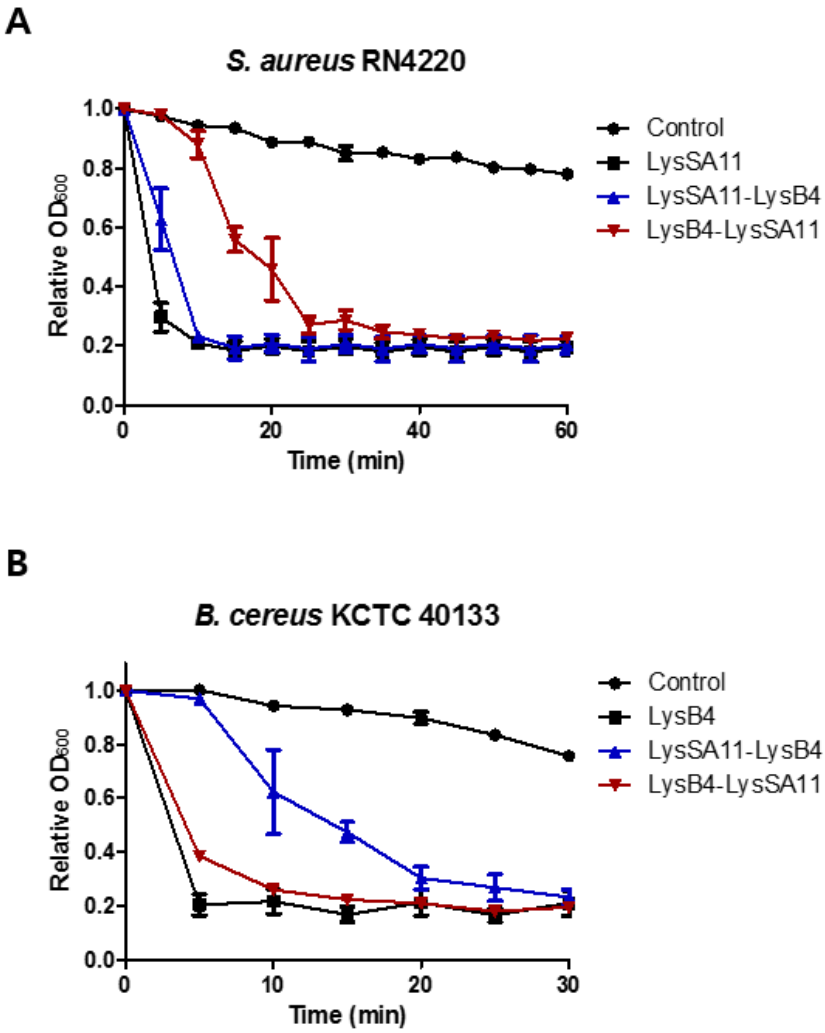

Figure IV-2. The lytic activities of LysSA11, LysB4, LysSA11-LysB4 and LysB4-LysSA11.

Equimolar concentrations (300 nM) of the proteins were added to the suspension of *S. aureus* RN 4220 (A) and *B. cereus* ATCC 21768 (B). Then, the decrease of turbidity was monitored.

IV.3.3. Antibacterial spectrum of the fusion proteins

Antimicrobial activity of the fusion proteins was evaluated against Gram-positive and Gram-negative bacteria (Table IV-2). As previously reported, LysSA11 exhibited lytic activity against all staphylococcal strains tested and had no effect on *B. cereus* and other Gram-positive bacteria. Similarly, LysB4 was active against *B. cereus*, *B. subtilis*, *L. monocytogens* and Gram-negative bacteria when proteins when cells were washed with 0.1 M EDTA to increase the cell wall permeability. LysB4 was not active against staphylococcal strains. On the other hand, LysSA11-LysB4 and LysB4-LysSA11 appeared to have the same antibacterial spectrum, killing not only staphylococcal strains but also *B. cereus*, *B. subtilis* and *L. monocytogens*. In addition, Gram-negative bacteria were susceptible to the fusion proteins. These results demonstrate that the antimicrobial spectrum of two fusion proteins was extended compared to their parental endolysins and the fusion proteins maintain the specificity of LysSA11 and LysB4 which targets A1γ type and A3α type of peptidoglycan, respectively (Schleifer & Kandler, 1972).

Table IV-2. Antimicrobial spectrum of fusion proteins

	Stains		**LysSA11**	**LsySA11-LysB4**	**LysB4-LysSA11**	**LysB4**
Gram-positive bacteria	*Staphylococcus aureus*	ATCC 33586	+	+	+	
		ATCC 6538	+	+	+	
		Newman	+	+	+	
		RN4220	+	+	+	
		ATCC 23235	+	+	+	
		ATCC 29213	+	+	+	
		ATCC 12600	+	+	+	
		ATCC 33593	+	+	+	
		ATCC 35983	+	+	+	
		ATCC 13301	+	+	+	
		CCARM 3793	+	+	+	
		CCARM 3090	+	+	+	
	S. hominis	ATCC 37844	+	+	+	
	S. saprophyticus	ATCC 15305	+	+	+	

	S. heamolyticus	ATCC 29970	+	+	+	
	S. capitis	ATCC 35661	+	+	+	
	S. warneri	ATCC 10209	+	+	+	
	S. xylosis	ATCC29971	+	+	+	
	S. epidermidis	CCARM 3787	+	+	+	
	Bacillus cereus	KCCM 40133		+	+	+
	B. cereus	ATCC 27348		+	+	+
	B. subtilis	168		+	+	+
	Steptococcus thermophilus	ATCC 19258		+	+	+
	Listeria monocytogenes	ATCC 19114		+	+	+
Gram-negative bacteria	*Salmonella Typimurium*	LT2		+	+	+
	Pseudommonas aeruginosa	ATCC 27853		+	+	+
	Cronobacter sakazakii	ATCC 29544		+	+	+
	Shigella flexineri	2a strain 2457 T		+	+	+
	Escherichia coli	MG1655		+	+	+

IV.3.4. Construction of truncated variant of the fusion proteins and their lytic efficacy

A previous study reported that C-terminal domain of the endolysin, PlyL encoded by the *B. anthracis* genome could inhibit the enzymatic activity of its EAD in the absence of the cognate target (Low et al., 2011; Low et al., 2005). In this respect, I have constructed C-terminally truncated version of endolysins, LysSA11EAD (1-159 amino acids) and LysB4EAD (1-176 amino acids) to confirm the possibility for their lytic efficacy (Figure IV-3). The turbidity reduction assay revealed that LysSA11EAD has significantly decreased lytic activity compared to full-length LysSA11 against *S. aureus* when the same molar concentration (300 nM) was treated. Moreover, the lytic activity of higher amount of LysSA11EAD (1000 nM) was also not comparable to that of 300 nM LysSA11. This result suggested that CBD is essential for the lytic activity of LysSA11. Similarly, LysPBC1 endolysin from *B. cereus*-infecting phage PBC1 showed higher lytic activity against *B. cereus* than LysPBC1EAD (Minsuk Kong & Ryu, 2015). Porter et al. reported that the reduction of the lytic activity in absence of CBD is attributed to the lack of affinity for the cell wall (Porter et al., 2007). On the other hand, LysB4EAD exhibited an almost equal lytic activity to LysB4, indicating that LysB4CBD could be useless or play an inhibitory role in the

lytic activity of LysB4. Considering that the CBD-dependence of endolysins is high associated to the charge of a catalytic domain (Low et al., 2011), the high theoretical isoelectric point of LysB4EAD (8.9) supports this explanation.

Based on these results, I constructed two more fusion proteins containing C-terminally truncated LysB4; LysSA11-LysB4EAD and LysB4EAD-LysSA11. A helical linker was introduced described above. All proteins constructed were overexpressed in soluble form in *E. coli* and purified proteins were presented as a single band of the expected molecular mass on SDS-PAGE (Figure IV-1). The lytic activities of the newly constructed fusion proteins were compared to LysSA11-LysB4, LyB4-LysSA11 and their parental proteins. LysSA11-LysB4EAD and LysB4EAD-LysSA11 have showed the similar lytic activity compared with full-length fusion proteins against both *S. aureus* and *B. cereus* (Figure IV-4).

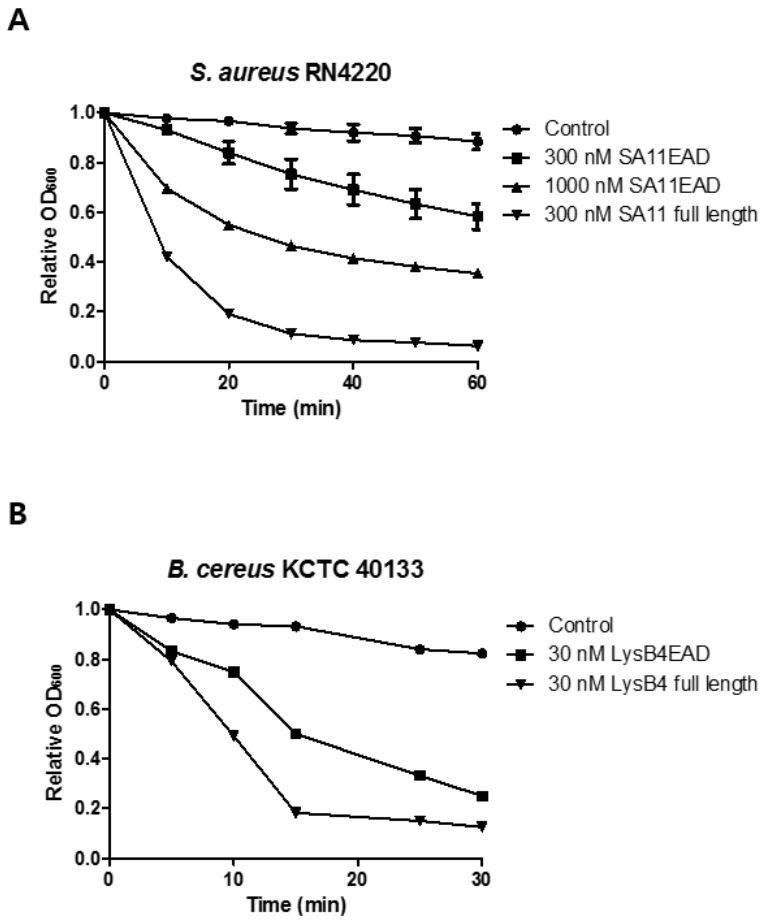

Figure IV-3. The lytic activity of LysSA11, LysB4 and their EADs.

(A) LysSA11 and LysSA11-EAD were added to the suspension of *S. aureus* RN 4220. (B) LysB4 and LysB4-EAD were added to the suspension of *B. cereus* ATCC 21768, and the decrease of turbidity was monitored.

A

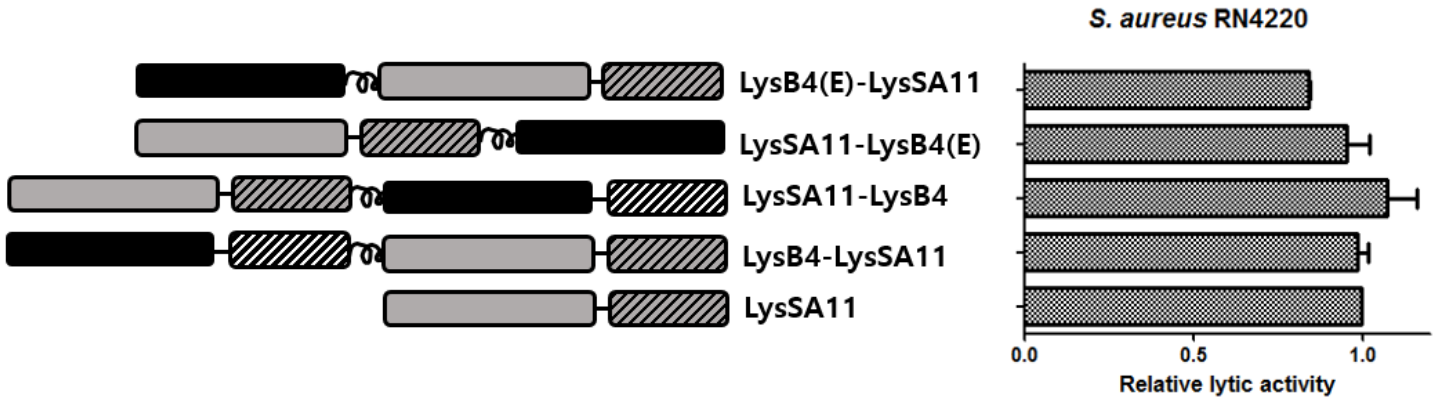
S. aureus RN4220
LysB4(E)-LysSA11
LysSA11-LysB4(E)
LysSA11-LysB4
LysB4-LysSA11
LysSA11
0.0
0.5
1.0
Relative lytic activity

B

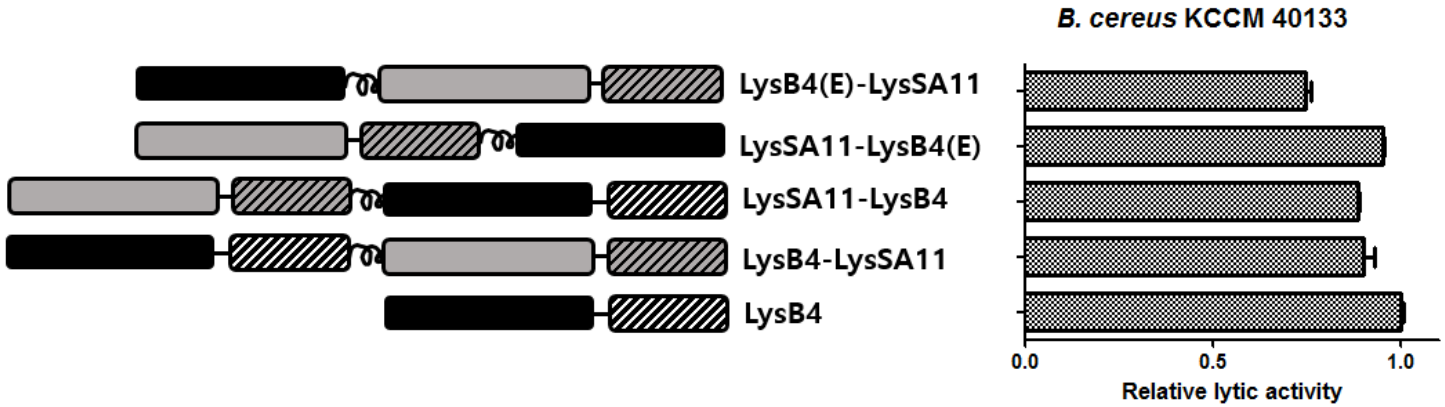
B. cereus KCCM 40133
LysB4(E)-LysSA11
LysSA11-LysB4(E)
LysSA11-LysB4
LysB4-LysSA11
LysB4
0.0
0.5
1.0
Relative lytic activity

Figure IV-4. The relative lytic activities of the fusion proteins against *S. aureus* and *B. cereus*.

Equimolar concentrations (300 nM) of LysSA11, LysB4, LysSA11-LysB4, LysB4-LysSA11, LysSA11-LysB4EAD (LysSA11-LysB4(E)), and LysB4EAD-LysSA11 (LysB4(E)-LysSA11) were added to the suspension of *S. aureus* RN4220 (A) and *B. cereus* ATCC 21768 (B). The relative lytic activity was calculated after 1h against *S. aureus* and 30 min against *B. cereus.*

IV.3.5. Thermal stability determination

Thermal stability of the endolysins is an important factor for development of biocontrol agents since it is correlated with the shelf-life (Gerstmans, Criel, & Briers, 2017). In general, most phage endolysins are not stable to heat and most lose their activity above 50-60 ℃ (Lavigne, Briers, Hertveldt, Robben, & Volckaert, 2004). The thermal stability assay showed that the lytic activity of LysSA11 was significantly decreased at 45 ℃ against *S. aureus* (Figure IV-5A) However, all fusion proteins constructed in this study showed strong lytic activity at 45 ℃ and had residual activity even at 55 ℃, demonstrating the fusion proteins have enhanced thermal stability compared to LysSA11.

LysB4 was relatively stable to heat, showing residual lytic activity up to 65 ℃ (Figure IV-5B). LysSA11-LysB4 and LysSA11-LysB4EAD exhibited an 80% reduction in lytic activity at 55 ℃ compared to LysB4. However, LysB4-LysSA11 and LysB4EAD-LysSA11 constructs showed similar thermal stability with LysB4 against *B. cereus*. In particular, the lytic activity of LysB4EAD-LysSA11 at 65 ℃ was higher than LysB4, and LysB4EAD-LysSA11 was selected for further study.

It has been reported that fusion proteins are used not only to facilitate purification, but also to improve the production, solubility and

stability of target proteins (Janczak et al., 2015). The position of the fusion partner and the properties of a peptide linker are important factors to be considered for successful production and stability of the fusion proteins (Arai et al., 2001; Japrung, Chusacultanachai, Yuvaniyama, Wilairat, & Yuthavong, 2005). In this study, the fusion proteins showed higher thermal stability than LysSA11 regardless of the position, and LysB4 fusion proteins showed increased thermal stability compared to LysB4 when the fusion partner was positioned at the C-terminal of LysB4.

A

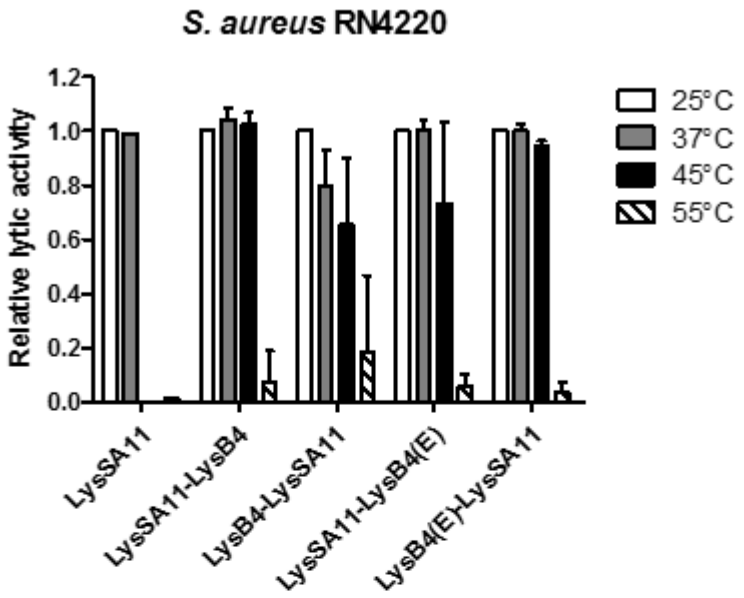
S. aureus RN4220
Relative lytic activity
1.2
1.0
0.8
0.6
0.4
0.2
0.0
25°C
37°C
45°C
55°C
LysSA11
LysSA11-LysB4
LysB4-LysSA11
LysSA11-LysB4(E)
LysB4(E)-LysSA11

B

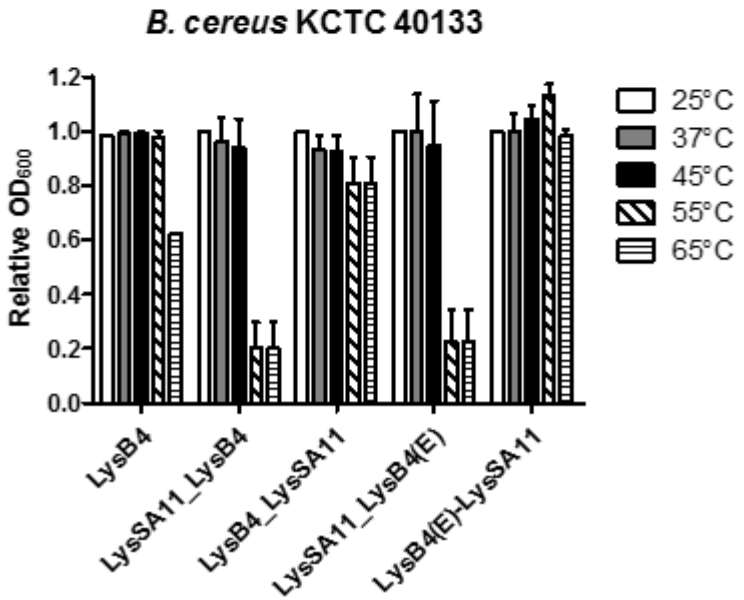
B. cereus KCTC 40133
Relative OD600
1.2
1.0
0.8
0.6
0.4
0.2
0.0
25°C
37°C
45°C
55°C
65°C
LysB4
LysSA11_LysB4
LysB4_LysSA11
LysSA11_LysB4(E)
LysB4(E)-LysSA11

Figure IV-5. The thermal stability of the fusion proteins.

Equimolar concentrations (300 nM) of LysSA11, LysB4, LysSA11-LysB4, LysB4-LysSA11, LysSA11-LysB4EAD (LysSA11-LysB4(E)), and LysB4EAD-LysSA11 (LysB4(E)-LysSA11) were incubated at different temperatures for 30 min. Relative lytic activities are calculated using the activity of enzyme stored at 25 ℃, which showed the maximal activity.

IV.3.6. Effect of pH and NaCl on the lytic activity of LysB4EAD-LysSA11

The influence of pH on the lytic activity of LysB4EAD-LysSA11 was determined (Figure IV-6). Analysis of lytic activity at different pHs showed that LysB4EAD-LysSA11 had more than 80% residual activity at pH 8.0-9.0 against *S. aureus*. Meanwhile, LysB4EAD-LysSA11 was relatively stable under the broad range of pH conditions between pH 5.5-9.0 against *B. cereus,* showing more than 70% residual activity. These results could be attributed to the different behavior of *S. aureus and B. cereus* under the pH conditions (Walkenhorst, Klein, Vo, & Wimley, 2013). *S. aureus* contains teichoic acids in the PG layer, and the teichoic acids have ribitol phosphates which make the PG of *S. aureus* negatively charged. However, the positive charges from the amino groups of D-alanine reduce the charge on the PG of *S. aureus* so that the PG become slightly negative at neutral pH. According to the previous study, the PG of *S. aureus* becomes neutral or even slightly positive charge at low pHs and much more negative charge at high pHs. Therefore, in acidic condition, the fusion protein (pI =9.20) was more likely to be positively charged and thereby the lytic activity might be decreased by repelling of the proteins and the PG of *S. aureus*. Meanwhile, *B. cereus* contain uncharged polysaccharide branch rather than teichoic acid

(Leoff et al., 2008). The presence of diaminopimelic acid (DAP) and glutamic acid makes *B. cereus* cell wall more negatively charged, allowing the protein to be more active under broad range of pHs compared to *S. aureus*.

The influence of NaCl on the lytic activity of LysB4EAD-LysSA11 was determined (Figure IV-7). The lytic activity of LysB4EAD-LysSA11 against both *S. aureus* and *B. cereus* was decreased even in the presence of 50 mM NaCl, indicating that LysB4EAD-LysSA11 is sensitive to NaCl.

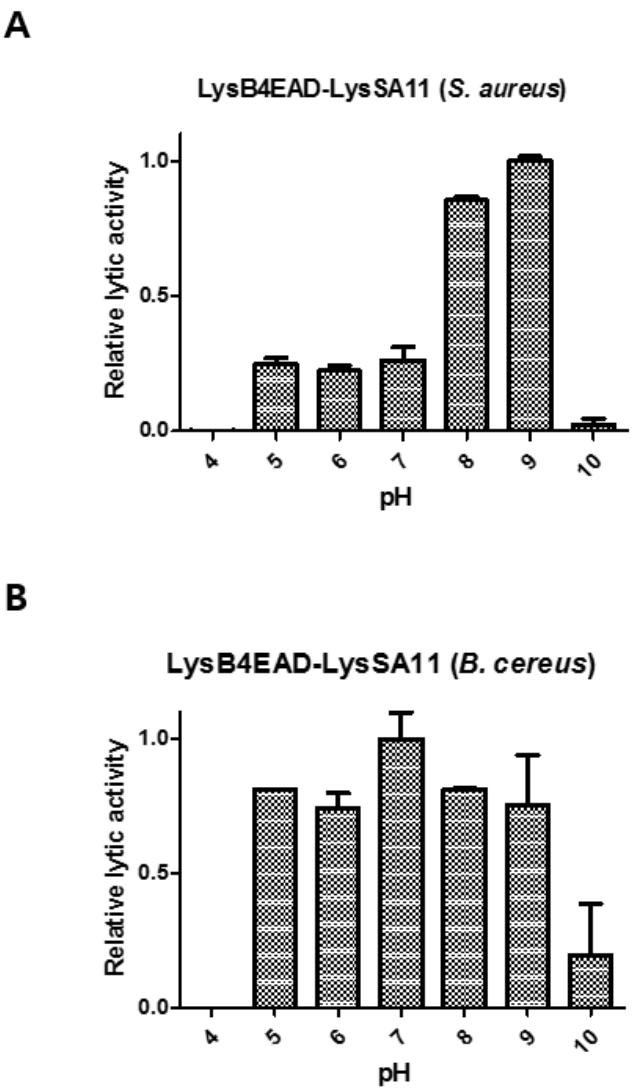

Figure IV-6. The effect of pH on the lytic activity of LysB4EAD-LysSA11.

The lytic activity of LysB4EAD-LysSA11 against (A) *S. aureus* RN4220 and (B) *B. cereus* ATCC 21768 was evaluated under the different pH conditions.

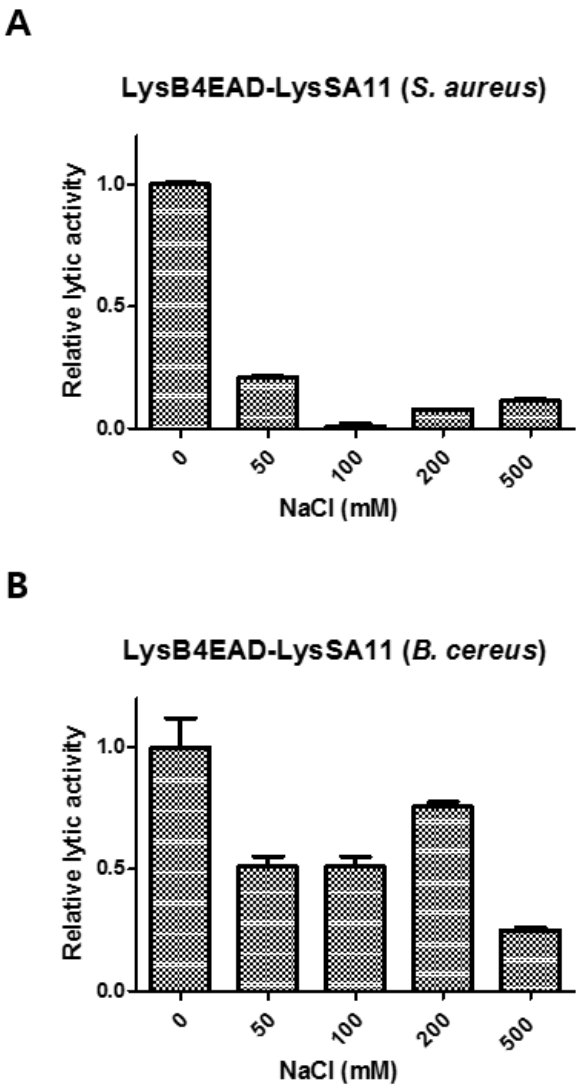

Figure IV-7. The effect of NaCl on the lytic activity of LysB4EAD-LysSA11.

The lytic activity of LysB4EAD-LysSA11 against (A) *S. aureus* RN4220 and (B) *B. cereus* ATCC 21768 was evaluated under the different NaCl concentrations.

IV.3.7. Antimicrobial activity of LysB4EAD-LysSA11 in food

To confirm the potential of LysB4EAD-LysSA11 as a biocontrol agent, the protein was applied in boiled rice artificially contaminated with *S. aureus* or *B. cereus* (Figure IV-8). The pH of the boiled rice was 8.0, which corresponds quite well to the optimum pH of LysB4EAD-LysSA11. When 0.3 μM of the protein were added to boiled rice contaminated with *S. aureus*, 2 log reduction of the bacterial cells were observed after 4h. Higher amount of LysB4EAD-LysSA11 (3.0 μM) removed the staphylococcal cells by 2 log after 1h and killed all bacterial cells in boiled rice after 4h. The lytic activity of LysB4EAD-LysSA11 maintained for 4 h. In the case of *B. cereus*-contaminated boiled rice, the protein rarely lysed *B. cereus* cells even after 4 h of treatment with 0.3 μM. However, viable cells were reduced to the undetectable levels within 2 h after treatment with 3.0 μM of LysB4EAD-LysSA11.

Next, I added LysB4EAD-LysSA11 to the boiled rice simultaneously contaminated with *S. aureus* and *B. cereus* to mimic the natural contamination of the bacteria (Figure IV-9). LysB4EAD-LysSA11 showed effective lytic activity in consistent with the results when the proteins were treated to the boiled rice contaminated separately with *S. aureus* or *B. cereus*. When 3 μM of LysSA11 and LysB4 were added to the boiled rice

simultaneously contaminated with *S. aureus* and *B. cereus*, *S. aureus* decreased by 2 log/ml after 3 h (Figure IV-10A) and *B. cereus* were completely eliminated within 1 h (Figure IV-10B). When 3 μM of LysSA11 and LysB4EAD were added to the boiled rice simultaneously contaminated with *S. aureus* and *B. cereus*, *S. aureus* was reduced to undetectable level within 1h (Figure IV-10C) and the number of *B. cereus* cells were decreased by 1 log/ml after 3 h (Figure IV-10D). In conclusion, the treatment of the fusion endolysin showed higher lytic activity against *B. cereus* than that of two parental endolysins separately. The fusion protein still showed an effective lytic activity despite the lower rate of the lytic activity against *S. aureus*. These results suggest that all fusion proteins constructed can be used as effective biocontrol agents to eliminate both *B. cereus* and *S. aureus* in food matrix.

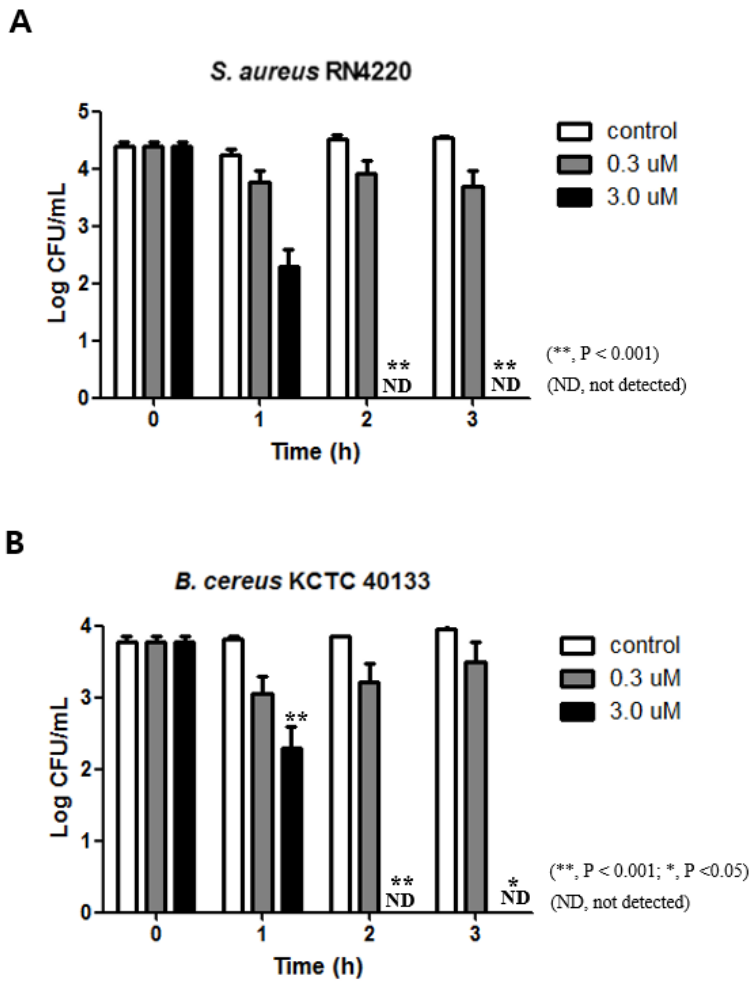

Figure IV-8. Antimicrobial activity of LysB4EAD in boiled rice.

The numbers of (A) *S. aureus* RN4220 and (B) *B. cereus* ATCC 21768 cells in boiled rice were counted after treatment of the different concentrations (0.3 μM and 3.0 μM) of LysB4EAD-LysSA11. ND, not detected. Each *column* represents the mean standard deviations of triplicate assays. The *asterisks* indicate significant differences (***$P < 0.001$, **$P < 0.01$ and *$P < 0.05$)

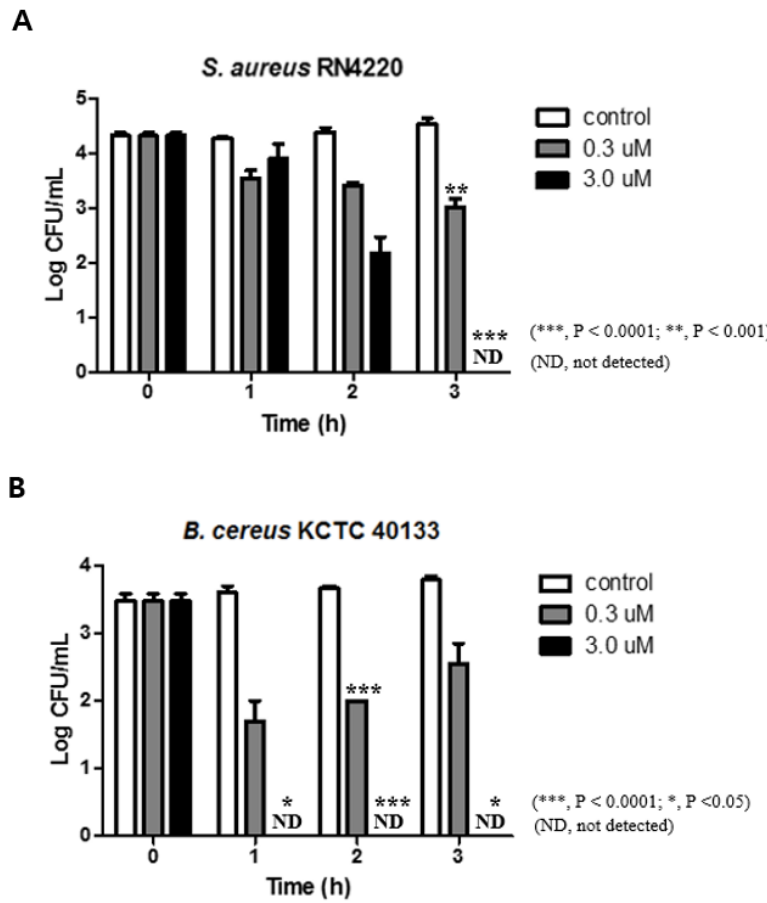

Figure IV-9. Antimicrobial activity of LysB4EAD-LysSA11 in boiled rice contaminated simultaneously with *S. aureus* and *B. cereus*.

The numbers of (A) *S. aureus* RN4220 and (B) *B. cereus* ATCC 21768 cells in boiled rice were counted after treatment of the different concentrations (0.3 μM and 3.0 μM) of LysB4EAD-LysSA11. ND, not detected. Each *column* represents the mean standard deviations of triplicate assays. The *asterisks* indicate significant differences (***$P < 0.001$, **$P < 0.01$ and *$P < 0.05$)

A

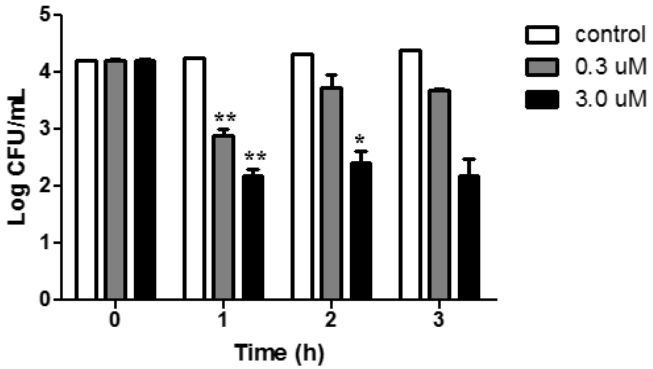
LysSA11 and LysB4 (S. aureus)
Log CFU/mL
Time (h)
control
0.3 uM
3.0 uM
**
**
*

B

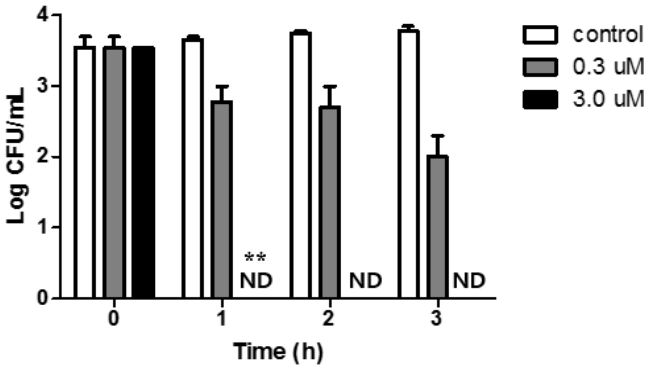
LysSA11 and LysB4 (B. cereus)
Log CFU/mL
Time (h)
control
0.3 uM
3.0 uM
**
ND
ND
ND

C

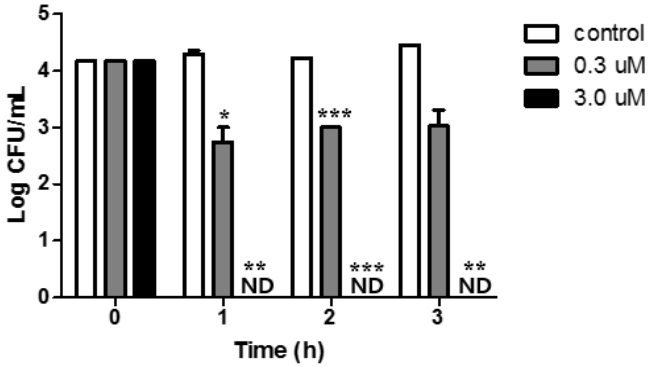
LysSA11 and LysB4EAD (S. aureus)
Log CFU/mL
Time (h)
control
0.3 uM
3.0 uM
*
**
ND
***
***
ND
**
ND

D

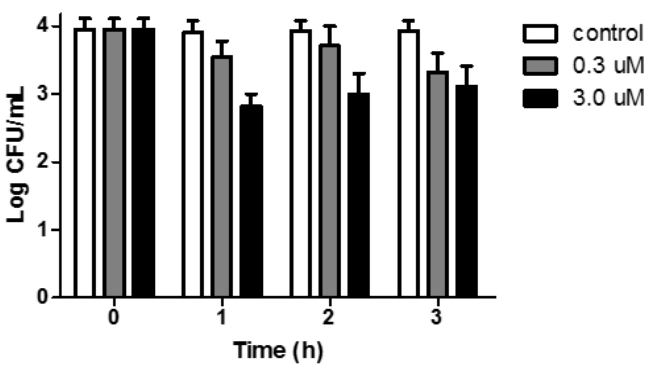
LysSA11 and LysB4EAD (B. cereus)
Log CFU/mL
Time (h)
control
0.3 uM
3.0 uM

Figure IV-10. Antimicrobial activity of LysSA11, LysB4 and LysB4EAD in boiled rice contaminated simultaneously with *S. aureus* and *B. cereus*.

The numbers of (A) *S. aureus* RN4220 and (B) *B. cereus* ATCC 21768 cells in boiled rice were counted after treatment of the different concentrations (0.3 μM and 3.0 μM) of LysSA11 and LysB4. The numbers of (C) *S. aureus* RN4220 and (D) *B. cereus* ATCC 21768 cells in boiled rice were counted after treatment of the different concentrations (0.3 μM and 3.0 μM) of LysSA11 and LysB4EAD. ND, not detected. Each column represents the mean standard deviations of triplicate assays. The asterisks indicate significant differences (***$P < 0.001$, **$P < 0.01$ and *$P < 0.05$)

V. Engineering of cell wall binding domain of the phage endolysin using phage display technique

V.1. Introduction

Several strategies have been developed to tailor the enzyme properties (Fernandez-Gacio, Uguen, & Fastrez, 2003). Although designed mutations guided by molecular modelling or hypothesis about natural evolution could result in novel proteins with expected properties, sometimes they have limitation to guarantee the successful selection for interesting mutants (Cedrone, Ménez, & Quéméneur, 2000). In this regards, creating libraries and screening desired mutants has been increasingly introduced.

Phage display is a powerful technique for the selection of peptides or proteins with specific binding properties (Aghebati-Maleki et al., 2016). This technique is based on the presentation of peptides or proteins on the surface of bacteriophages, especially filamentous phage, M13 (Hoess, 2001; Smith, 1985). M13 phage which infect *E. coli* strains with the F-pilus is not a lytic phage and consists of a single stranded circular DNA encapsulated in a long helical capsid proteins (Marvin, 1998). The major coat proteins of M13 phage are g3p, g6p, g7p, g8p and g9p. The g8p covered the length of the phage. The g3p which is one of the major coat protein of M13 presents in 3-5 copies and is responsible for phage infectivity. Most of the displayed enzymes are fused by their C-terminal to g3p protein through a linker

(Soumillion & Fastrez, 2002). M13 phages are resistant to harsh conditions such as acid pH, high temperatures, detergents and enzymatic cleavage, allowing the selection to be conducted under harsh condition (Aghebati-Maleki et al., 2016; Deutscher, 2010).

To construct a library, phage display system should be selected for the desired results. There are different types of phage display systems including natural phage genome-based system and phagemid-based system. Phagemid-based system is the most widely used. Phagemid is plasmid, consisting of replication origin, selective marker, intergenic region, promoter and signal sequence. Sequences of protein to be displayed are present in phagemid and all other major genes necessary for phage assembly are present in the helper phage which has deficient phage packaging signal. Phagemid particle production is occurred by infection with a helper phage (Soumillion & Fastrez, 2002). After helper phages inject their DNA into the host cells containing phagemid, the fusion protein encoded by phagemid is produced. When phage assembly begins, phage virions preferentially assembled using phagemid DNA which carries a fully functional packaging signal.

Phage display allows easy cloning of DNA sequences for random peptide libraries into a phage vector and rapid identification of selected peptides by sequencing of the DNA encoding the peptide inserts due to

physical linkage between the phenotype and genotype of the expressed protein (Fernandez-Gacio et al., 2003). However, it is necessary that the phage particle should be able to be assembled and that the desired protein can be displayed on the finished phage particle.

The screening of phage display libraries is based on an affinity selection process (also called bio-panning or panning) (Hoogenboom, 1997). Library of variant DNA sequence encoding peptide or proteins is created using random mutagenesis and cloned into phage or phagemid genome. The resultant phage library displaying variant proteins or peptides is exposed to target molecules. Unbound phages are washed off and bound phages are eluted which are further used to infect host cells and amplified. Finally, selected phages are analyzed for identification of their sequences.

Phage display basically consists of DNA manipulation, phage packaging and panning. The advantage of this technique is that it can display a large number of different proteins and can easily change the screening format. It is also simple, economical and does not require special equipment. Proteins can be fused to all coat proteins, but it can affect coat protein function (e.g., infectivity), and phage viability.

In this study, I tried to engineer the cell wall binding domain (CBD) for the efficient detection of *B. cereus* using a phage display technique as a promising approach for random screening. The CBD of LysPBC1 from

*Bacillus cere*us phage PBC1 were randomly mutated and successfully displayed on the capsid surface of M13 phage via fusion with the pIII coat protein, g3p protein. Displayed LsyPBC1_CBD retained its binding ability to *B. cereus*. Whole-cell phage display panning using *B. cereus* cells was conducted. Among the several selected clones from the library, a LysPBC1_CBD Q47H mutant showed approximately 2-fold increase in cell wall binding ability compared to LysPBC1_CBD. However, this approach was insufficient to reduce the number of nonspecifically binding clones at the panning steps. In order to successfully identify CBD with high affinity through a phage display system, an optimization of the experimental conditions is required.

V.2. Materials and Methods

V.2.1. Bacterial strains, media, and growth conditions

E. coli XL-1 Blue were used in cloning of phagemid and as the bacterial host for recombinant phage amplification using VCSAM13 or Hyperphage M13 K07ΔpIII (PROGEN Biotechnik GmbH, Heidelberg, Germany). This strain were grown in 2xYT (16 g tryptone, 10 g yeast extract, 5 g NaCl) media containing 10 μg/ml tetracycline at 37 ℃. *Bacillus cereus* ATCC 21768 was grown in BHI medium at 37 ℃ with shaking.

V.2.2. Helper phage and phagemid virion production

To prepare VCSM13 helper phage stock, *E. coli* XL1-Bue cells were grown to a mid-log phase (OD_{600} = 0.5) at 37 ℃ and infected with helper phage at a ratio of 1:20. The mixture was incubated at 37 ℃ for 30 min without shaking for phage infection, followed by overnight incubation after adding 25 μg/ml kanamycin.

To prepare phagemid virions, phagemid-harboring *E. coli* XL1-Blue was grown in 2xYT containing 100 μg/ml ampicillin and 0.1 μM glucose to a mid-log phase and infected with helper phage at MOI 20. After infection at 37 ℃ for 30 min without shaking, bacteria were centrifugated 10 min at

3,220g and resuspended in 2xYT medium containing 100 μg/ml ampicillin and 20 μg/ml kanamycin. Infected bacteria were grown overnight at 37 ℃, followed by PEG/NaCl precipitation.

V.2.3. Construction of phagemid vector, pSEX81

The CBD gene of LysPBC1, an endolysin from *B. cereus*-infecting PBC1 phage was amplified by PCR from the PBC1 phage genome using primers containing trypsin cleavage site (NcoI_PBC1CBD_F, AAA CCA TGG GCA AAG CAG TAA ATG TTG AT; PBC1_CBD_GGGGS_Trypsin_BamHI_R, TTT GGA TCC TCT GAT ATC TTT GGA GCC ACC GCC ACC ATA CTC AAT CAC TTC TTC TTG ATA CCA C) (Minsuk Kong & Ryu, 2015). The gene product was digested with NcoI and BamHI and cloned into the pSEX81 phagemid vector (PROGEN Biotechnik GmbH), followed by electroporation into *E. coli* XL1-Blue cells.

V.2.4. Construction of phage display library

The random mutation of LysPBC1CBD gene was amplified by an error-prone PCR-based method using GeneMorph® II Random Mutagenesis Kit (Stratagene, CA, USA). *E. coli* XL1-Blue competent cells were transformed with the library DNA. Recovered cells were plated on LB agar

containing 50 μg/ml tetracycline, 100 μg/ml ampicillin and 0.1 μM glucose. Phage propagation was performed with the cells harboring the library DNA as described above.

V.2.5. Western blotting assay

Phage samples were dissolved in Laemmli sample buffer and boiled for 10 min. The samples loaded onto 12% SDS-PAGE gels were separated based on molecular weights, and transferred to a polyvinylidene difluoride membrane. The membrane was blocked with 5% non-fat dry milk in 1× Tris-buffered saline-Tween 20 (TBS-T) buffer and probed with anti-pIII (g3p) antibody (3:2,000 dilution; MoBiTec GmbH, Göttingen, Germany) as a primary antibody. Anti-mouse IgG conjugated with peroxidase (3:5,000 dilution; Santa Cruz Biotechnology, Santa Cruz, CA, USA) was used as the secondary antibody in all Western blots. The chemiluminescent signals were developed with a West-Zol plus Western blot.

V.2.6. Panning procedure

Library screening was performed using an affinity selection. Mixtures of displayed phages with *B. cereus* cells were formed in solution and then separated from unbound phages by centrifugation. Prior to panning

steps, *B. cereus* cells were prepared by fixation in 4% paraformaldehyde for 30 min, followed by incubating with PBS containing 2% skim milk for 1h at room temperature. Then, phage particles were added to the cells in PBS with 2% skim milk and rotated for an additional 5 min to allow the phages to bind to the cells. Unbound cells were removed by washing 5 times with PBS containing 0.05% Tween-20 followed by an additional washing with PBS. After final centrifugation, the cell pellet was resuspended in 200 μl of 1 mg/ml trypsin and rotated at room temperature for 30 min to elute the bound phages. The mixture was centrifuged for 2 min at 16,000g and the supernatant containing bound phages was stored on ice. *E. coli* XL1-Blue cells grown to mid-log were infected with the eluted phage for 30 min and the cells were plated on an LB containing 50 μg/ml tetracycline, 100 μg/ml ampicillin. After incubation overnight at 37 ℃, the cells harboring the genomes of phage recovered from the panning were grown to mid log phase and infected with VCSM13 helper phage at MOI 20 for phage propagation. The enriched phage library was used in the next round of panning. After each round of panning, the cells harboring the genome of phage recovered were randomly picked and identified by a sequence analysis.

A subtractive panning strategy was introduced to effectively reduce the number of nonspecific clones. Phage particles were added to *Salmonella* Typhimurium, as an unwanted target, and the mixture was incubated for 1 h

at room temperature. After centrifugation, the supernatant was transferred into a fresh tube and incubate *B. cereus* cells for selection of the binding phages. Reinfection and identification of selected clones were conducted as described above.

V.2.7. EGFP fusion protein binding assay.

Some of clones were selected to test their cell wall binding ability after panning step. The binding of each EGFP fusion protein to *B. cereus* cells was measured as previously described (Loessner et al., 2002). Bacterial cells, cultivated to early exponential phase, were harvested and re-suspended in Dulbecco's phosphate-buffered saline (PBS). The cells were incubated with EGFP fusion protein for 5 min at room temperature. The mixture was washed twice with PBS to remove unbound protein and was transferred to a 96-well plate to measure fluorescence using a SpectraMax i3 multimode microplate reader with excitation at 485 nm and emission at 535 nm. The OD_{600} of cells was measured, and fluorescence was normalized by calculating the whole-cell fluorescence per OD_{600}. Relative binding capacity was derived by comparing to the highest measured value and is presented as relative fluorescence intensity (RFI). In addition, target bacteria labelled with EGFP fusion protein were examined by fluorescence microscopy

(DE/Axio Imager A1 microscope, Carl Zeiss, Oberkochen, Germany) using a GFP filter set (470/40 nm excitation, 495 nm dichroic, 525/50 nm emission).

V.3. Results and discussion

V.3.1. Establishment of a screening system using phage display

In this study, pSEX81, a phagemid surface expression vector was used for screening LysPBC1_CBD with higher binding affinity. This vector contains the M13 phage coat protein pIII gene, the pelB gene that directs the fusion protein to the periplasmic space, the strong promoter regulated by IPTG, the T7 terminator, the ColE1 origin, the F1 phage intergenic region, and the ampicillin antibiotic resistance recognition moiety. The total size is 4,882 bp and the phage host strain to be amplified using this phagemid vector is *E. coli* XL1-Blue (recA1 endA1 gyrA96 thi-1 hsdR17 supE44 relA1 lac^- F'[$proAB^+$ $lacI^q$ ZΔM15 Tn10 (tet^R)]. To construct phagemid vector containing LysPBC1_CBD, LysPBC1_CBD was introduced between NcoI and BamHI restriction enzyme sites in pSEX81. Trypsin cleavage site was inserted in front of pIII in pSEX81 for the trypsin cleavage elution of recombinant phages from the target cells after panning. The overall phage display and selection procedure of using helper phage and pSEX81 phagemid is described in Figure V-1. After the phages displaying LysPBC1_CBD are exposed to *B. cereus* cells, bound phages are eluted and used to re-infect *E.coli* to be amplified. The phage populations may be

randomly selected and individually analyzed for identification of their sequences. Finally, *E. coli* cells containing constructed phagemid vector will be superinfected with helper phage VCSM13.

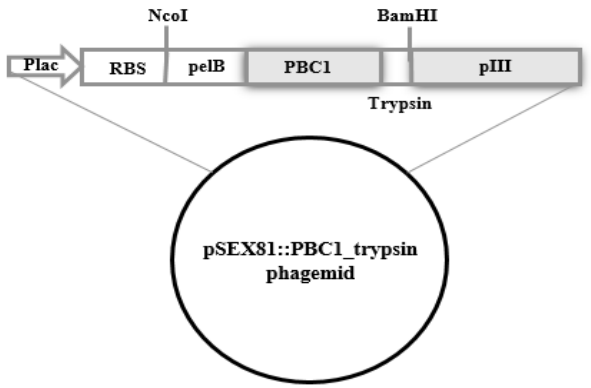

1. Transform *E. coli* XL1-Blue
2. Superinfect with helper phage

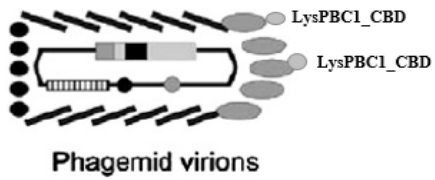

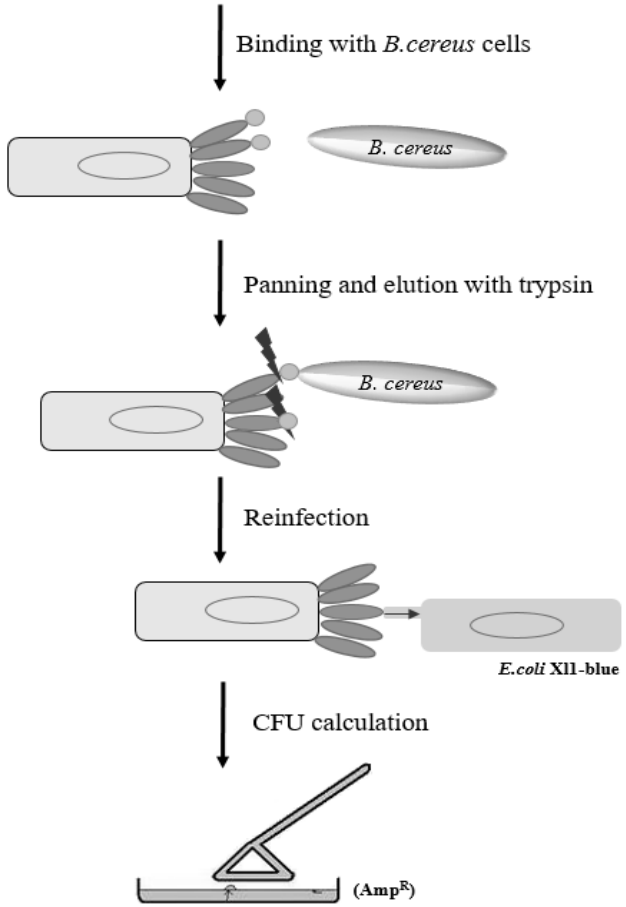

Figure V-1. The overall scheme of the affinity selection process.

VCSM phage was used for packaging of LysPBC1_CBD display phagemid pSEX81 in E. coli XL1-Blue. The resulting recombinant phage contains several copies of the LysPBC1_CBD. The trypsin cleavage site connecting LysPBC1_CBD and pIII would be used for protease elution after panning, and resultant wild-type of pIII can allow the recombinant phage to re-infect *E. coli*.

V.3.2. Confirmation of displayed LysPBC1_CBD on VCSM13 phage and its binding ability to *B. cereus.*

The display levels of LysPBC1_CBD were analyzed by western blot analysis using anti-pIII mAb after harvesting the recombinant phage virions. As expected, the bands corresponding to both pIII protein fused with LysPBC1_CBD and pIII protein were detected in the sample of VCSM13 phage particles obtained by superinfecting *E. coli* cells carrying pSEX81_LysPBC1_CBD phagemid (pSEX81_LysPBC1_CBD/VCSM13 phage), indicating that expressed LysPBC1_CBD was migrated to periplasmic space by pelB sequence, folding and assembling with VCSM13 phage. However, pIII protein was predominant in wild-type VCSM13 phages, (**Figure V-2**A). These results show LysPBC1_CBD is successfully displayed on the surface of VCSM13 phages.

The binding ability of displayed LysPBC1_CBD to *B. cereus* cells was evaluated. After binding and washing steps, trypsin was treated to elute phages that bound to *B. cereus* cells. *E. coli* were infected with the eluted phages, and the number of displayed phages was measured by spreading the infected *E. coli* on the agar plate containing ampicillin. *E. coli* cells were obtained when VCSM13 phage displaying LysPBC1_CBD were incubated with *B. cereus* cells whereas no colonies appeared when wild-type VCSM13

phage were incubated with *B. cereus* cells, indicating LysPBC1_CBD maintains its binding cell wall binding ability when displayed on the surface of the phage (Figure V-2B).

To determine the binding specificity of the displayed LysPBC1_CBD, LysPBC1-CBD displayed phages were incubated with *B. cereus* and Gram-negative, *Salmonella* Typhimurium (Figure V-2C). The binding ability of the phages displaying LysPBC1_CBD to *S.* Typhimurium was negligible compared to *B. cereus*. These results demonstrated that LysPBC1_CBD could bind to *B. cereus* cells specifically and maintain its function after displayed on the surface of the phages.

A

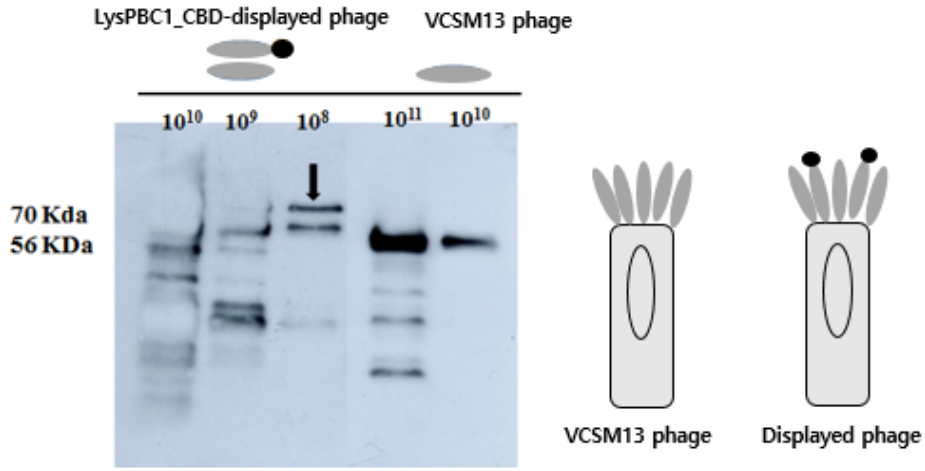

B

E. coli cells infected with phages after elution (Amp^R, CFU/mL)	
VCSM13 phage	LysPBC1_CBD displayed VCSM13 phage
-	3×10^7

C

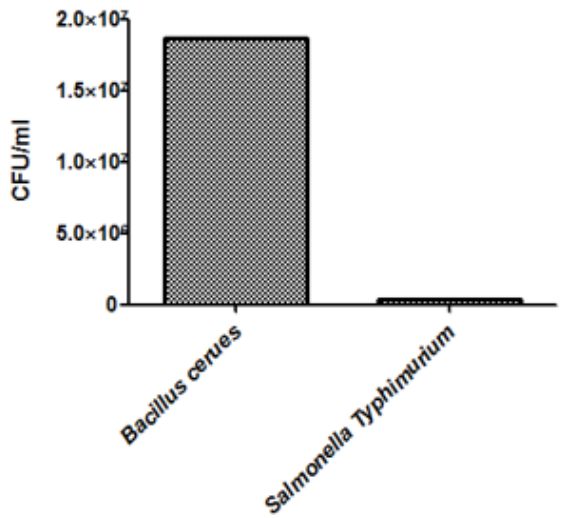

Figure V-2. Western blot analysis of LysPBC1_CBD-pIII fusion proteins displayed on VCSM13 phage and the binding ability of the displayed protein.

(A) Protein extracts of LysPBC1_CBD displayed phage and wild-type phage were separated by loading different concentrations of phages in 12% SDS-PAGE gels. Immunoblot was carried out with anti-pIII mAb to determine the amount of LysPBC1_CBD-pIII fusion proteins displayed on the surfaced of phage particles. Anti-mouse IgG conjugated with peroxidase was used as the secondary antibody. (B) The number of *E. coli* infected with the eluted phages was counted by spreading of the infected *E. coli* on the agar plate containing ampicillin. (C) The recombinant phages displaying LysPBC1_CBD were incubated with *B. cereus* and S. Typhimurium.

V.3.3. Contruction of phage display library through random mutagenesis

LysPBC1_CBD DNA was randomly mutated by error-prone PCR using GeneMorph II random mutagenesis kit, which can control the mutation frequencies (mutations/kb) as desired by controlling the amount of initial target DNA and the number of PCR cycles. To achieve high mutation rate, the initial DNA amount was 10 ng and 30 cycles of PCR were performed. Sequence analysis revealed that mutation frequencies of 1-3 mutations/gene were observed as shown in **Table V-1**, and 90% mutation efficiency. Mutation bias was found to be 35% for changing AT to CG and 52% for changing GC to AT. Deletion or insertion was not confirmed. Prepared genes were inserted into pSEX81 phagemid vector as described in V.3.1

Table V-1. Mutation frequency of selected colonies

Clones	Mutation frequency (mutations/gene)	
1	2	
2	1	
3	3	
4	1	
5	3	Mutation bias AT → CG 35% GC → AT 52%
6	0	
7	3	
8	1	
9	1	
10	1	
	90%	

V.3.4. Selection for isolating CBD with higher binding affinity

Considering the fact that the intact cell panning procedure commonly sufferes from a large number of non-specific binding phage at the screening step (Eisenhardt, Schwarz, Bassler, & Peter, 2007; Hoogenboom et al., 1999; Mutuberria, Hoogenboom, van der Linden, de Bruïne, & Roovers, 1999), other stategies rather than classical panning procedure have been required. Subtractive panning is widely used to reduce non-specific binding in phage display based screening system (Eisenhardt et al., 2007). This strategy includes a depletion step against unwanted epitopes, followed by a selection step for the target epitope, allowing a highly specific selection for the target. In this study, subtractive panning was performed using *Salmonella* Typhimurium cells as unwanted epitopes and *B. cereus* cells as the target epitope every panning round. However, the sequence analysis of randomly selected 10 colonies revealed that there was no selective amplification of LysPBC1_CBD mutants after several rounds of panning steps. This approach was insufficient to reduce the number of nonspecifically binding clones despite subtractive panning. In order to identify CBD with high cell wall binding affinity through phage display system, optimization of experimental conditions is required. Meanwhile, a previous study showed that net charge of endolysin can alter the lytic

activity EAD of endolysin (Low et al., 2011). In this regard, 10 colonies were selected from the first panning round (**Table V-2**), and three out of 10 selected clones were assayed for their binding ability to *B. cereus* (Figure V-3). Among them, LysPBC1_CBD Q47H mutant has higher bindnig abiltiy compare to the wild-type LysPBC1_CBD. LysPBC1_CBD Q25K and LysPBC1_CBD E69K showed similar binding ability to wild-type LysPBC1_CBD. These results indicate that the phage display technique enables engineering a CBD to have a higher cell wall binding affinity and thus has a great potential to develop an effective bioprobe using an engineered CBD.

Table V-2. Sequence analysis of selected clones after panning step

Clones	Sequence analysis
1	AAG(K)-> TAG(E), GAT(D)-> GGA(E), TTA(L)-> TCA(S)
2	WT
3	GCG(A)-> GCT(A), GAA(E)-> AAA(K)
4	deletion
5	deletion
6	deletion
7	CAA(Q)-> CAT(H)
8	CAG(Q)-> AAG(K)
9	AAA(K)-> TAA(stop)
10	-

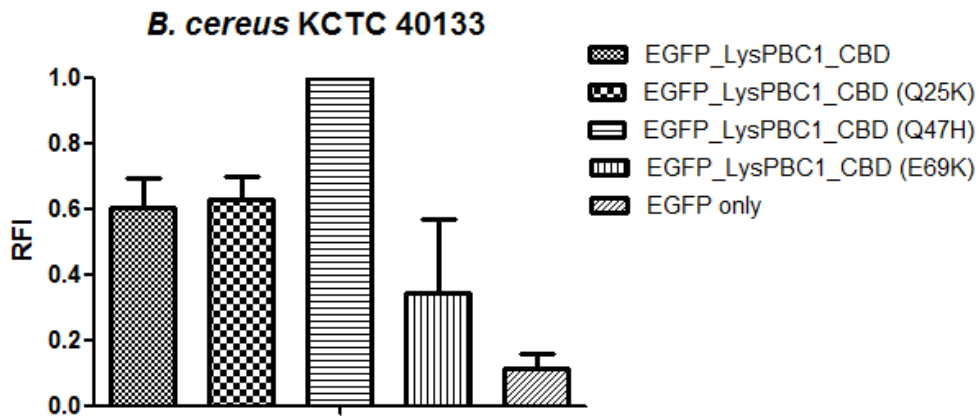

Figure V-3. Binding activity comparison among EGFP-fused LysPBC1-CBD mutants.

Relative cell binding activities of 1 μM of EGFP_LysPBC1_CBD, EGFP_LysPBC1_CBD (Q25K), EGFP_LysPBC1_CBD (Q47H), EGFP_LysPBC1_CBD (E69K) toward *B. cereus* ATCC 21768 were measured.

References

Abaev, I., Foster-Frey, J., Korobova, O., Shishkova, N., Kiseleva, N., Kopylov, P., Pryamchuk, S., Schmelcher, M., Becker, S. C., & Donovan, D. M. (2013). Staphylococcal phage 2638A endolysin is lytic for *Staphylococcus aureus* and harbors an inter-lytic-domain secondary translational start site. *Applied microbiology and biotechnology, 97*(8), 3449-3456.

Abee, T., Kovács, Á. T., Kuipers, O. P., & Van der Veen, S. (2011). Biofilm formation and dispersal in Gram-positive bacteria. *Current opinion in biotechnology, 22*(2), 172-179.

Aghebati-Maleki, L., Bakhshinejad, B., Baradaran, B., Motallebnezhad, M., Aghebati-Maleki, A., Nickho, H., Yousefi, M., & Majidi, J. (2016). Phage display as a promising approach for vaccine development. *Journal of biomedical science, 23*(1), 66.

Altschul, S. F., Gish, W., Miller, W., Myers, E. W., & Lipman, D. J. (1990). Basic local alignment search tool. *Journal of molecular biology, 215*(3), 403-410.

Altschul, S. F., Madden, T. L., Schäffer, A. A., Zhang, J., Zhang, Z., Miller, W., & Lipman, D. J. (1997). Gapped BLAST and PSI-BLAST: a new generation of protein database search programs. *Nucleic acids research*, *25*(17), 3389-3402.

Andrews, J. M. (2001). Determination of minimum inhibitory concentrations. *Journal of Antimicrobial Chemotherapy*, *48*(suppl_1), 5-16.

Arai, R., Ueda, H., Kitayama, A., Kamiya, N., & Nagamune, T. (2001). Design of the linkers which effectively separate domains of a bifunctional fusion protein. *Protein engineering*, *14*(8), 529-532.

Atanassova, V., Meindl, A., & Ring, C. (2001). Prevalence of Staphylococcus aureus and staphylococcal enterotoxins in raw pork and uncooked smoked ham—a comparison of classical culturing detection and RFLP-PCR. *International journal of food microbiology*, *68*(1), 105-113.

Baba, T., Takeuchi, F., Kuroda, M., Yuzawa, H., Aoki, K.-i., Oguchi, A., Nagai, Y., Iwama, N., Asano, K., & Naimi, T. (2002). Genome and

virulence determinants of high virulence community-acquired MRSA. *The Lancet, 359*(9320), 1819-1827.

Bai, J., Kim, Y.-T., Ryu, S., & Lee, J.-H. (2016). Biocontrol and rapid detection of food-borne pathogens using bacteriophages and endolysins. *Frontiers in microbiology, 7*, 474.

Becker, S. C., Dong, S., Baker, J. R., Foster-Frey, J., Pritchard, D. G., & Donovan, D. M. (2009). LysK CHAP endopeptidase domain is required for lysis of live staphylococcal cells. *FEMS microbiology letters, 294*(1), 52-60.

Becker, S. C., Foster-Frey, J., & Donovan, D. M. (2008). The phage K lytic enzyme LysK and lysostaphin act synergistically to kill MRSA. *FEMS microbiology letters, 287*(2), 185-191.

Becker, S. C., Foster-Frey, J., Stodola, A. J., Anacker, D., & Donovan, D. M. (2009). Differentially conserved staphylococcal SH3b_5 cell wall binding domains confer increased staphylolytic and streptolytic activity to a streptococcal prophage endolysin domain. *Gene, 443*(1), 32-41.

Becker, S. C., Swift, S., Korobova, O., Schischkova, N., Kopylov, P., Donovan, D. M., & Abaev, I. (2015). Lytic activity of the staphylolytic Twort phage endolysin CHAP domain is enhanced by the SH3b cell wall binding domain. *FEMS microbiology letters*, *362*(1), 1.

Bennett, S. D., Walsh, K. A., & Gould, L. H. (2013). Foodborne disease outbreaks caused by Bacillus cereus, Clostridium perfringens, and Staphylococcus aureus—United States, 1998–2008. *Clinical Infectious Diseases*, *57*(3), 425-433.

Bhavsar, A. P., & Brown, E. D. (2006). Cell wall assembly in Bacillus subtilis: how spirals and spaces challenge paradigms. *Mol Microbiol*, *60*(5), 1077-1090. doi:10.1111/j.1365-2958.2006.05169.x

Borysowski, J., Weber-Dąbrowska, B., & Górski, A. (2006). Bacteriophage endolysins as a novel class of antibacterial agents. *Experimental Biology and Medicine*, *231*(4), 366-377.

Botka, T., Růžičková, V., Konečná, H., Pantůček, R., Rychlík, I., Zdráhal, Z., Petráš, P., & Doškař, J. (2015). Complete genome analysis of two

new bacteriophages isolated from impetigo strains of Staphylococcus aureus. *Virus genes, 51*(1), 122-131.

Briers, Y., & Lavigne, R. (2015). Breaking barriers: expansion of the use of endolysins as novel antibacterials against Gram-negative bacteria. *Future microbiology, 10*(3), 377-390.

Briers, Y., Volckaert, G., Cornelissen, A., Lagaert, S., Michiels, C. W., Hertveldt, K., & Lavigne, R. (2007). Muralytic activity and modular structure of the endolysins of Pseudomonas aeruginosa bacteriophages φKZ and EL. *Molecular microbiology, 65*(5), 1334-1344.

Briers, Y., Walmagh, M., Van Puyenbroeck, V., Cornelissen, A., Cenens, W., Aertsen, A., Oliveira, H., Azeredo, J., Verween, G., & Pirnay, J.-P. (2014). Engineered endolysin-based "Artilysins" to combat multidrug-resistant gram-negative pathogens. *mBio, 5*(4), e01379-01314.

Brüssow, H., & Hendrix, R. W. (2002). Phage genomics: small is beautiful. *Cell, 108*(1), 13-16.

Callewaert, L., Walmagh, M., Michiels, C. W., & Lavigne, R. (2011). Food applications of bacterial cell wall hydrolases. *Current opinion in biotechnology*, *22*(2), 164-171.

Carlton, R. M. (1999). Phage therapy: past history and future prospects. *ARCHIVUM IMMUNOLOGIAE ET THERAPIAE EXPERIMENTALIS-ENGLISH EDITION-*, *47*, 267-274.

Catalao, M. J., Gil, F., Moniz-Pereira, J., Sao-Jose, C., & Pimentel, M. (2013). Diversity in bacterial lysis systems: bacteriophages show the way. *FEMS microbiology reviews*, *37*(4), 554-571.

Cedrone, F., Ménez, A., & Quéméneur, E. (2000). Tailoring new enzyme functions by rational redesign. *Current opinion in structural biology*, *10*(4), 405-410.

Chambers, H. F., & DeLeo, F. R. (2009). Waves of resistance: Staphylococcus aureus in the antibiotic era. *Nature reviews microbiology*, *7*(9), 629.

Chan, B. K., Abedon, S. T., & Loc-Carrillo, C. (2013). Phage cocktails and

the future of phage therapy. *Future microbiology, 8*(6), 769-783.

Chang, Y., Kim, M., & Ryu, S. (2017). Characterization of a novel endolysin LysSA11 and its utility as a potent biocontrol agent against *Staphylococcus aureus* on food and utensils. *Food Microbiology, 68*, 112-120.

Chang, Y., Lee, J.-H., Shin, H., Heu, S., & Ryu, S. (2013). Characterization and complete genome sequence analysis of *Staphylococcus aureus* bacteriophage SA12. *Virus genes, 47*(2), 389-393.

Chang, Y., & Ryu, S. (2017). Characterization of a novel cell wall binding domain-containing *Staphylococcus aureus* endolysin LysSA97. *Applied microbiology and biotechnology, 101*(1), 147-158.

Chang, Y., Shin, H., Lee, J.-H., Park, C. J., Paik, S.-Y., & Ryu, S. (2015). Isolation and genome characterization of the virulent *Staphylococcus aureus* bacteriophage SA97. *Viruses, 7*(10), 5225-5242.

Chang, Y., Yoon, H., Kang, D.-H., Chang, P.-S., & Ryu, S. (2017). Endolysin LysSA97 is synergistic with carvacrol in controlling

Staphylococcus aureus in foods. *International journal of food microbiology, 244*, 19-26.

Cheng, Q., & Fischetti, V. A. (2007). Mutagenesis of a bacteriophage lytic enzyme PlyGBS significantly increases its antibacterial activity against group B streptococci. *Applied microbiology and biotechnology, 74*(6), 1284-1291.

Cutter, C. N. (2000). Antimicrobial effect of herb extracts against Escherichia coli O157: H7, Listeria monocytogenes, and Salmonella typhimurium associated with beef. *Journal of Food Protection, 63*(5), 601-607.

Daniel, A., Euler, C., Collin, M., Chahales, P., Gorelick, K. J., & Fischetti, V. A. (2010). Synergism between a novel chimeric lysin and oxacillin protects against infection by methicillin-resistant Staphylococcus aureus. *Antimicrobial agents and chemotherapy, 54*(4), 1603-1612.

De Lencastre, H., Oliveira, D., & Tomasz, A. (2007). Antibiotic resistant Staphylococcus aureus: a paradigm of adaptive power. *Current opinion in microbiology, 10*(5), 428-435.

Deutscher, S. L. (2010). Phage display in molecular imaging and diagnosis of cancer. *Chemical Reviews, 110*(5), 3196-3211.

Díez-Martínez, R., de Paz, H., Bustamante, N., García, E., Menéndez, M., & García, P. (2013). Improving the lethal effect of Cpl-7, a pneumococcal phage lysozyme with broad bactericidal activity, by inverting the net charge of its cell wall-binding module. *Antimicrobial agents and chemotherapy, 57*(11), 5355-5365.

Donovan, D. M., Dong, S., Garrett, W., Rousseau, G. M., Moineau, S., & Pritchard, D. G. (2006). Peptidoglycan hydrolase fusions maintain their parental specificities. *Applied and environmental microbiology, 72*(4), 2988-2996.

Donovan, D. M., & Foster-Frey, J. (2008). LambdaSa2 prophage endolysin requires Cpl-7-binding domains and amidase-5 domain for antimicrobial lysis of streptococci. *FEMS microbiology letters, 287*(1), 22-33.

Donovan, D. M., Foster-Frey, J., Dong, S., Rousseau, G. M., Moineau, S., & Pritchard, D. G. (2006). The cell lysis activity of the Streptococcus

agalactiae bacteriophage B30 endolysin relies on the cysteine, histidine-dependent amidohydrolase/peptidase domain. *Applied and environmental microbiology, 72*(7), 5108-5112.

Eisenhardt, S. U., Schwarz, M., Bassler, N., & Peter, K. (2007). Subtractive single-chain antibody (scFv) phage-display: tailoring phage-display for high specificity against function-specific conformations of cell membrane molecules. *Nature protocols, 2*(12), 3063.

Enright, M. C., Robinson, D. A., Randle, G., Feil, E. J., Grundmann, H., & Spratt, B. G. (2002). The evolutionary history of methicillin-resistant Staphylococcus aureus (MRSA). *Proceedings of the National Academy of Sciences, 99*(11), 7687-7692.

Eugster, M. R., & Loessner, M. J. (2012). Wall teichoic acids restrict access of bacteriophage endolysin Ply118, Ply511, and PlyP40 cell wall binding domains to the *Listeria monocytogenes* peptidoglycan. *Journal of bacteriology, 194*(23), 6498-6506.

Fenton, M., Casey, P. G., Hill, C., Gahan, C. G., McAuliffe, O., O'Mahony, J., Maher, F., & Coffey, A. (2010). The truncated phage lysin

CHAPk eliminates Staphylococcus aureus in the nares of mice. *Bioengineered bugs, 1*(6), 404-407.

Fernandes, S., Proença, D., Cantante, C., Silva, F. A., Leandro, C., Lourenço, S., Milheiriço, C., de Lencastre, H., Cavaco-Silva, P., & Pimentel, M. (2012). Novel chimerical endolysins with broad antimicrobial activity against methicillin-resistant Staphylococcus aureus. *Microbial drug resistance, 18*(3), 333-343.

Fernandez-Gacio, A., Uguen, M., & Fastrez, J. (2003). Phage display as a tool for the directed evolution of enzymes. *Trends in biotechnology, 21*(9), 408-414.

Fetsch, A., Contzen, M., Hartelt, K., Kleiser, A., Maassen, S., Rau, J., Kraushaar, B., Layer, F., & Strommenger, B. (2014). Staphylococcus aureus food-poisoning outbreak associated with the consumption of ice-cream. *International journal of food microbiology, 187*, 1-6.

Finn, R. D., Bateman, A., Clements, J., Coggill, P., Eberhardt, R. Y., Eddy, S. R., Heger, A., Hetherington, K., Holm, L., & Mistry, J. (2013). Pfam: the protein families database. *Nucleic acids research, 42*(D1), D222-

D230.

Fischetti, V. A. (2006). *Using phage lytic enzymes to control pathogenic bacteria.* Paper presented at the BMC oral health.

Fischetti, V. A. (2008). Bacteriophage lysins as effective antibacterials. *Current opinion in microbiology, 11*(5), 393-400.

Fischetti, V. A. (2010). Bacteriophage endolysins: a novel anti-infective to control Gram-positive pathogens. *International Journal of Medical Microbiology, 300*(6), 357-362.

Foster, T. J. (2004). The Staphylococcus aureus "superbug". *The Journal of clinical investigation, 114*(12), 1693-1696.

Fujikawa, H., & Sakha, M. Z. (2014). Prediction of competitive microbial growth in mixed culture at dynamic temperature patterns. *Biocontrol science, 19*(3), 121-127.

Furuno, J. P., Perencevich, E. N., Johnson, J. A., Wright, M.-O., McGregor, J. C., Morris Jr, J. G., Strauss, S. M., Roghman, M.-C., Nemoy, L. L.,

& Standiford, H. C. (2005). Methicillin-resistant *Staphylococcus aureus* and vancomycin-resistant enterococci co-colonization. *Emerging infectious diseases, 11*(10), 1539.

García, P., Martínez, B., Rodríguez, L., & Rodríguez, A. (2010). Synergy between the phage endolysin LysH5 and nisin to kill Staphylococcus aureus in pasteurized milk. *International journal of food microbiology, 141*(3), 151-155.

Gasteiger, E., Hoogland, C., Gattiker, A., Wilkins, M. R., Appel, R. D., & Bairoch, A. (2005). Protein identification and analysis tools on the ExPASy server *The proteomics protocols handbook* (pp. 571-607): Springer.

Gerstmans, H., Criel, B., & Briers, Y. (2017). Synthetic biology of modular endolysins. *Biotechnology advances*.

Grande, M. J., Lucas, R., Abriouel, H., Valdivia, E., Omar, N. B., Maqueda, M., Martínez-Bueno, M., Martínez-Cañamero, M., & Gálvez, A. (2006). Inhibition of toxicogenic Bacillus cereus in rice-based foods by enterocin AS-48. *International journal of food microbiology,*

106(2), 185-194.

Gu, J., Xu, W., Lei, L., Huang, J., Feng, X., Sun, C., Du, C., Zuo, J., Li, Y., & Du, T. (2011). LysGH15, a novel bacteriophage lysin, protects a murine bacteremia model efficiently against lethal methicillin-resistant Staphylococcus aureus infection. *Journal of clinical microbiology, 49*(1), 111-117.

Gutiérrez, D., Fernández, L., Rodríguez, A., & García, P. (2018). Are Phage Lytic Proteins the Secret Weapon To Kill Staphylococcus aureus? *mBio, 9*(1), e01923-01917.

Gutierrez, D., Ruas-Madiedo, P., Martínez, B., Rodríguez, A., & García, P. (2014). Effective removal of staphylococcal biofilms by the endolysin LysH5. *PLoS One, 9*(9), e107307.

Hoess, R. H. (2001). Protein design and phage display. *Chemical Reviews, 101*(10), 3205-3218.

Hoogenboom, H. R. (1997). Designing and optimizing library selection strategies for generating high-affinity antibodies. *Trends in*

biotechnology, 15(2), 62-70.

Hoogenboom, H. R., Lutgerink, J. T., Pelsers, M. M., Rousch, M. J., Coote, J., van Neer, N., de Bruïne, A., van Nieuwenhoven, F. A., Glatz, J. F., & Arends, J. W. (1999). Selection-dominant and nonaccessible epitopes on cell-surface receptors revealed by cell-panning with a large phage antibody library. *European journal of biochemistry, 260*(3), 774-784.

Idelevich, E. A., von Eiff, C., Friedrich, A. W., Iannelli, D., Xia, G., Peters, G., Peschel, A., Wanninger, I., & Becker, K. (2011). In vitro activity against Staphylococcus aureus of a novel antimicrobial agent, PRF-119, a recombinant chimeric bacteriophage endolysin. *Antimicrobial agents and chemotherapy, 55*(9), 4416-4419.

Jado, I., López, R., García, E., Fenoll, A., Casal, J., & García, P. (2003). Phage lytic enzymes as therapy for antibiotic-resistant Streptococcus pneumoniae infection in a murine sepsis model. *Journal of Antimicrobial Chemotherapy, 52*(6), 967-973.

Janczak, M., Bukowski, M., Górecki, A., Dubin, G., Dubin, A., & Wladyka,

B. (2015). A systematic investigation of the stability of green fluorescent protein fusion proteins. *Acta Biochimica Polonica, 62*(3).

Japrung, D., Chusacultanachai, S., Yuvaniyama, J., Wilairat, P., & Yuthavong, Y. (2005). A simple dual selection for functionally active mutants of Plasmodium falciparum dihydrofolate reductase with improved solubility. *Protein Engineering Design and Selection, 18*(10), 457-464.

Jørgensen, H., Mørk, T., & Rørvik, L. (2005). The occurrence of Staphylococcus aureus on a farm with small-scale production of raw milk cheese. *Journal of Dairy Science, 88*(11), 3810-3817.

Kadariya, J., Smith, T. C., & Thapaliya, D. (2014). Staphylococcus aureus and staphylococcal food-borne disease: an ongoing challenge in public health. *BioMed research international, 2014*.

Kashani, H. H., Schmelcher, M., Sabzalipoor, H., Hosseini, E. S., & Moniri, R. (2018). Recombinant endolysins as potential therapeutics against antibiotic-resistant Staphylococcus aureus: Current status of research and novel delivery strategies. *Clinical microbiology reviews, 31*(1),

e00071-00017.

Kerr, D. E., Plaut, K., Bramley, A. J., Williamson, C. M., Lax, A. J., Moore, K., Wells, K. D., & Wall, R. J. (2001). Lysostaphin expression in mammary glands confers protection against staphylococcal infection in transgenic mice. *Nature biotechnology, 19*(1), 66-70.

Kim, J. S., Lee, G. G., Park, J. S., Jung, Y. H., Kwak, H. S., Kim, S. B., Nam, Y. S., & Kwon, S.-T. (2007). A novel multiplex PCR assay for rapid and simultaneous detection of five pathogenic bacteria: Escherichia coli O157: H7, Salmonella, Staphylococcus aureus, Listeria monocytogenes, and Vibrio parahaemolyticus. *Journal of Food Protection, 70*(7), 1656-1662.

Kong, M., & Ryu, S. (2015). Bacteriophage PBC1 and its endolysin as an antimicrobial agent against Bacillus cereus. *Applied and environmental microbiology, 81*(7), 2274-2283.

Kong, M., Sim, J., Kang, T., Nguyen, H. H., Park, H. K., Chung, B. H., & Ryu, S. (2015). A novel and highly specific phage endolysin cell wall binding domain for detection of Bacillus cereus. *Eur Biophys J,*

44(6), 437-446. doi:10.1007/s00249-015-1044-7

Korkeala, H., Mäki-Petäys, O., Alanko, T., & Sorvettula, O. (1986). Determination of pH in meat. *Meat science, 18*(2), 121-132.

Kumar, T. K., Murali, H., & Batra, H. (2009). Simultaneous detection of pathogenic B. cereus, S. aureus and L. monocytogenes by multiplex PCR. *Indian journal of microbiology, 49*(3), 283-289.

Kuroda, A., & Sekiguchi, J. (1990). Cloning, sequencing and genetic mapping of a Bacillus subtilis cell wall hydrolase gene. *Microbiology, 136*(11), 2209-2216.

Larkin, M. A., Blackshields, G., Brown, N., Chenna, R., McGettigan, P. A., McWilliam, H., Valentin, F., Wallace, I. M., Wilm, A., & Lopez, R. (2007). Clustal W and Clustal X version 2.0. *bioinformatics, 23*(21), 2947-2948.

Larson, A. E., Rosa, R., Lee, O. A., Price, S., Haas, G. J., & Johnson, E. A. (1996). Antimicrobial activity of hop extracts against Listeria monocytogenes in media and in food. *International journal of food*

microbiology, *33*(2-3), 195-207.

Lavigne, R., Briers, Y., Hertveldt, K., Robben, J., & Volckaert, G. (2004). Identification and characterization of a highly thermostable bacteriophage lysozyme. *Cellular and Molecular Life Sciences CMLS*, *61*(21), 2753-2759.

Leoff, C., Choudhury, B., Saile, E., Quinn, C. P., Carlson, R. W., & Kannenberg, E. L. (2008). Structural Elucidation of the Nonclassical Secondary Cell Wall Polysaccharide from Bacillus cereus ATCC 10987 COMPARISON WITH THE POLYSACCHARIDES FROM BACILLUS ANTHRACIS AND B. CEREUS TYPE STRAIN ATCC 14579 REVEALS BOTH UNIQUE AND COMMON STRUCTURAL FEATURES. *Journal of Biological Chemistry*, *283*(44), 29812-29821.

Lewis, K. (2001). Riddle of biofilm resistance. *Antimicrobial agents and chemotherapy*, *45*(4), 999-1007.

Lim, J.-A., Shin, H., Kang, D.-H., & Ryu, S. (2012). Characterization of endolysin from a Salmonella Typhimurium-infecting bacteriophage

SPN1S. *Research in microbiology, 163*(3), 233-241.

Lindsay, J. A., & Holden, M. T. (2004). *Staphylococcus aureus*: superbug, super genome? *Trends in microbiology, 12*(8), 378-385.

Loeffler, J. M., Djurkovic, S., & Fischetti, V. A. (2003). Phage lytic enzyme Cpl-1 as a novel antimicrobial for pneumococcal bacteremia. *Infection and immunity, 71*(11), 6199-6204.

Loessner, M. J. (2005). Bacteriophage endolysins—current state of research and applications. *Current opinion in microbiology, 8*(4), 480-487.

Loessner, M. J., Gaeng, S., & Scherer, S. (1999). Evidence for a Holin-Like Protein Gene Fully Embedded Out of Frame in the Endolysin Gene of Staphylococcus aureusBacteriophage 187. *Journal of bacteriology, 181*(15), 4452-4460.

Loessner, M. J., Kramer, K., Ebel, F., & Scherer, S. (2002). C-terminal domains of Listeria monocytogenes bacteriophage murein hydrolases determine specific recognition and high-affinity binding to bacterial cell wall carbohydrates. *Molecular microbiology, 44*(2),

335-349.

Low, L. Y., Yang, C., Perego, M., Osterman, A., & Liddington, R. (2011). The role of net charge on the catalytic domain and the influence of the cell-wall binding domain on the bactericidal activity, specificity and host-range of phage lysins. *Journal of Biological Chemistry*, jbc. M111. 244160.

Low, L. Y., Yang, C., Perego, M., Osterman, A., & Liddington, R. C. (2005). Structure and lytic activity of a Bacillus anthracis prophage endolysin. *Journal of Biological Chemistry*.

Lowy, F. D. (1998). Staphylococcus aureus infections. *New England journal of medicine*, *339*(8), 520-532.

Manoharadas, S., Witte, A., & Bläsi, U. (2009). Antimicrobial activity of a chimeric enzybiotic towards Staphylococcus aureus. *Journal of biotechnology*, *139*(1), 118-123.

Mao, J., Schmelcher, M., Harty, W. J., Foster-Frey, J., & Donovan, D. M. (2013). Chimeric Ply187 endolysin kills Staphylococcus aureus

more effectively than the parental enzyme. *FEMS microbiology letters, 342*(1), 30-36.

Marino, T. G., West, L. A., Liewehr, F. R., Mailhot, J. M., Buxton, T. B., Runner, R. R., & McPherson III, J. C. (2000). Determination of periodontal ligament cell viability in long shelf-life milk. *Journal of Endodontics, 26*(12), 699-702.

Marvin, D. (1998). Filamentous phage structure, infection and assembly. *Current opinion in structural biology, 8*(2), 150-158.

Matsuzaki, S., Rashel, M., Uchiyama, J., Sakurai, S., Ujihara, T., Kuroda, M., Ikeuchi, M., Tani, T., Fujieda, M., & Wakiguchi, H. (2005). Bacteriophage therapy: a revitalized therapy against bacterial infectious diseases. *Journal of infection and chemotherapy, 11*(5), 211-219.

Mayer, M. J., Payne, J., Gasson, M. J., & Narbad, A. (2010). Genomic sequence and characterization of the virulent bacteriophage ΦCTP1 from Clostridium tyrobutyricum and heterologous expression of its endolysin. *Applied and environmental microbiology, 76*(16), 5415-

5422.

Mutuberria, R., Hoogenboom, H. R., van der Linden, E., de Bruïne, A. P., & Roovers, R. C. (1999). Model systems to study the parameters determining the success of phage antibody selections on complex antigens. *Journal of immunological methods, 231*(1-2), 65-81.

Navarre, W. W., Ton-That, H., Faull, K. F., & Schneewind, O. (1999). Multiple Enzymatic Activities of the Murein Hydrolase from *Staphylococcal* Phage φ11 IDENTIFICATION OF A d-ALANYL-GLYCINE ENDOPEPTIDASE ACTIVITY. *Journal of Biological Chemistry, 274*(22), 15847-15856.

Nelson, M. D., & Fitch, D. H. (2012). Overlap extension PCR: an efficient method for transgene construction *Molecular Methods for Evolutionary Genetics* (pp. 459-470): Springer.

O'flaherty, S., Coffey, A., Meaney, W., Fitzgerald, G., & Ross, R. (2005). The recombinant phage lysin LysK has a broad spectrum of lytic activity against clinically relevant staphylococci, including methicillin-resistant Staphylococcus aureus. *Journal of bacteriology,*

187(20), 7161-7164.

Obeso, J. M., Martínez, B., Rodríguez, A., & García, P. (2008). Lytic activity of the recombinant staphylococcal bacteriophage ΦH5 endolysin active against Staphylococcus aureus in milk. *International journal of food microbiology, 128*(2), 212-218.

Oliveira, H., Melo, L. D., Santos, S. B., Nóbrega, F. L., Ferreira, E. C., Cerca, N., Azeredo, J., & Kluskens, L. D. (2013). Molecular aspects and comparative genomics of bacteriophage endolysins. *Journal of virology*, JVI. 03277-03212.

Otto, M. (2012). MRSA virulence and spread. *Cellular microbiology, 14*(10), 1513-1521.

Otto, M. (2013). Staphylococcal infections: mechanisms of biofilm maturation and detachment as critical determinants of pathogenicity. *Annual review of medicine, 64*, 175-188.

Pillsbury, A., Chiew, M., Bates, J., & Sheppeard, V. (2013). An outbreak of staphylococcal food poisoning in a commercially catered buffet.

Commun Dis Intell, 37(2), E144-E148.

Porter, C. J., Schuch, R., Pelzek, A. J., Buckle, A. M., McGowan, S., Wilce, M. C., Rossjohn, J., Russell, R., Nelson, D., & Fischetti, V. A. (2007). The 1.6 Å crystal structure of the catalytic domain of PlyB, a bacteriophage lysin active against Bacillus anthracis. *Journal of molecular biology, 366*(2), 540-550.

Pritchard, D. G., Dong, S., Kirk, M. C., Cartee, R. T., & Baker, J. R. (2007). LambdaSa1 and LambdaSa2 prophage lysins of *Streptococcus agalactiae*. *Applied and environmental microbiology, 73*(22), 7150-7154.

Rashel, M., Uchiyama, J., Ujihara, T., Uehara, Y., Kuramoto, S., Sugihara, S., Yagyu, K.-I., Muraoka, A., Sugai, M., & Hiramatsu, K. (2007). Efficient elimination of multidrug-resistant Staphylococcus aureus by cloned lysin derived from bacteriophage ϕMR11. *The Journal of infectious diseases, 196*(8), 1237-1247.

Rodríguez-Rubio, L., Martínez, B., Rodríguez, A., Donovan, D. M., & García, P. (2012). Enhanced staphylolytic activity of the

Staphylococcus aureus bacteriophage vB_SauS-phiIPLA88 HydH5 virion-associated peptidoglycan hydrolase: fusions, deletions, and synergy with LysH5. *Applied and environmental microbiology, 78*(7), 2241-2248.

Rodríguez-Rubio, L., Martínez, B., Rodríguez, A., Donovan, D. M., Götz, F., & García, P. (2013). The phage lytic proteins from the Staphylococcus aureus bacteriophage vB_SauS-phiIPLA88 display multiple active catalytic domains and do not trigger staphylococcal resistance. *PLoS One, 8*(5), e64671.

Sass, P., & Bierbaum, G. (2007). Lytic activity of recombinant bacteriophage φ11 and φ12 endolysins on whole cells and biofilms of Staphylococcus aureus. *Applied and environmental microbiology, 73*(1), 347-352.

Scallan, E., Hoekstra, R. M., Angulo, F. J., Tauxe, R. V., Widdowson, M.-A., Roy, S. L., Jones, J. L., & Griffin, P. M. (2011). Foodborne illness acquired in the United States—major pathogens. *Emerging infectious diseases, 17*(1), 7.

Schlag, M., Biswas, R., Krismer, B., Kohler, T., Zoll, S., Yu, W., Schwarz, H., Peschel, A., & Götz, F. (2010). Role of staphylococcal wall teichoic acid in targeting the major autolysin Atl. *Molecular microbiology, 75*(4), 864-873.

Schleifer, K. H., & Kandler, O. (1972). Peptidoglycan types of bacterial cell walls and their taxonomic implications. *Bacteriological reviews, 36*(4), 407.

Schmelcher, M., Donovan, D. M., & Loessner, M. J. (2012). Bacteriophage endolysins as novel antimicrobials. *Future microbiology, 7*(10), 1147-1171.

Schmelcher, M., & Loessner, M. J. (2016). Bacteriophage endolysins: applications for food safety. *Current opinion in biotechnology, 37*, 76-87.

Schmelcher, M., Powell, A. M., Becker, S. C., Camp, M. J., & Donovan, D. M. (2012). Chimeric phage lysins act synergistically with lysostaphin to kill mastitis-causing Staphylococcus aureus in murine mammary glands. *Applied and environmental microbiology, 78*(7),

2297-2305.

Schmelcher, M., Tchang, V. S., & Loessner, M. J. (2011). Domain shuffling and module engineering of Listeria phage endolysins for enhanced lytic activity and binding affinity. *Microbial biotechnology, 4*(5), 651-662.

Schuch, R., Nelson, D., & Fischetti, V. A. (2002). A bacteriolytic agent that detects and kills Bacillus anthracis. *Nature, 418*(6900), 884.

Seybold, U., Kourbatova, E. V., Johnson, J. G., Halvosa, S. J., Wang, Y. F., King, M. D., Ray, S. M., & Blumberg, H. M. (2006). Emergence of community-associated methicillin-resistant *Staphylococcus aureus* USA300 genotype as a major cause of health care—associated blood stream infections. *Clinical Infectious Diseases, 42*(5), 647-656.

Smith, G. P. (1985). Filamentous fusion phage: novel expression vectors that display cloned antigens on the virion surface. *Science, 228*(4705), 1315-1317.

Solanki, K., Grover, N., Downs, P., Paskaleva, E. E., Mehta, K. K., Lee, L.,

Schadler, L. S., Kane, R. S., & Dordick, J. S. (2013). Enzyme-based listericidal nanocomposites. *Scientific reports, 3*, 1584.

Son, B., Kong, M., & Ryu, S. (2018). The Auxiliary Role of the Amidase Domain in Cell Wall Binding and Exolytic Activity of Staphylococcal Phage Endolysins. *Viruses, 10*(6), 284.

Son, B., Yun, J., Lim, J.-A., Shin, H., Heu, S., & Ryu, S. (2012). Characterization of LysB4, an endolysin from the *Bacillus cereus*-infecting bacteriophage B4. *BMC microbiology, 12*(1), 33.

Son, J.-S., Lee, S.-J., Jun, S. Y., Yoon, S. J., Kang, S. H., Paik, H. R., Kang, J. O., & Choi, Y.-J. (2010). Antibacterial and biofilm removal activity of a podoviridae Staphylococcus aureus bacteriophage SAP-2 and a derived recombinant cell-wall-degrading enzyme. *Applied microbiology and biotechnology, 86*(5), 1439-1449.

Soumillion, P., & Fastrez, J. (2002). Investigation of phage display for the directed evolution of enzymes. *Directed Molecular Evolution of Proteins: or How to Improve Enzymes for Biocatalysis*, 79-110.

Spratt, B. G. (1994). Resistance to antibiotics mediated by target alterations. *Science*, *264*(5157), 388-393.

Sulakvelidze, A., Alavidze, Z., & Morris, J. G. (2001). Bacteriophage therapy. *Antimicrobial agents and chemotherapy*, *45*(3), 649-659.

Swift, S. M., Seal, B. S., Garrish, J. K., Oakley, B. B., Hiett, K., Yeh, H.-Y., Woolsey, R., Schegg, K. M., Line, J. E., & Donovan, D. M. (2015). A thermophilic phage endolysin fusion to a *Clostridium perfringens*-specific cell wall binding domain creates an anti-*Clostridium* antimicrobial with improved thermostability. *Viruses*, *7*(6), 3019-3034.

Syne, S.-M., Ramsubhag, A., & Adesiyun, A. A. (2013). Microbiological hazard analysis of ready-to-eat meats processed at a food plant in Trinidad, West Indies. *Infection ecology & epidemiology*, *3*(1), 20450.

Takano, M., Oshida, T., Yasojima, A., Yamada, M., Okagaki, C., Sugai, M., Suginaka, H., & Matsushita, T. (2000). Modification of autolysis by synthetic peptides derived from the presumptive binding domain of

Staphylococcus aureus autolysin. *Microbiology and immunology, 44*(6), 463-472.

Tong, S. Y., Davis, J. S., Eichenberger, E., Holland, T. L., & Fowler, V. G. (2015). Staphylococcus aureus infections: epidemiology, pathophysiology, clinical manifestations, and management. *Clinical microbiology reviews, 28*(3), 603-661.

Van Der Mee-Marquet, N., Corvaglia, A.-R., Valentin, A.-S., Hernandez, D., Bertrand, X., Girard, M., Kluytmans, J., Donnio, P.-Y., Quentin, R., & Francois, P. (2013). Analysis of prophages harbored by the human-adapted subpopulation of Staphylococcus aureus CC398. *Infection, Genetics and Evolution, 18*, 299-308.

Van Tassell, M. L., Daum, M. A., Kim, J.-S., & Miller, M. J. (2016). Creative lysins: Listeria and the engineering of antimicrobial enzymes. *Current opinion in biotechnology, 37*, 88-96.

Verbree, C. T., Dätwyler, S. M., Meile, S., Eichenseher, F., Donovan, D. M., Loessner, M. J., & Schmelcher, M. (2018). Corrected and Republished from: Identification of Peptidoglycan Hydrolase

Constructs with Synergistic Staphylolytic Activity in Cow's Milk. *Applied and environmental microbiology, 84*(1), e02134-02117.

Viertel, T. M., Ritter, K., & Horz, H.-P. (2014). Viruses versus bacteria—novel approaches to phage therapy as a tool against multidrug-resistant pathogens. *Journal of Antimicrobial Chemotherapy, 69*(9), 2326-2336.

Walkenhorst, W. F., Klein, J. W., Vo, P., & Wimley, W. C. (2013). The pH dependence of microbe sterilization by cationic antimicrobial peptides: not just the usual suspects. *Antimicrobial agents and chemotherapy*, AAC. 00063-00013.

Wu, J. A., Kusuma, C., Mond, J. J., & Kokai-Kun, J. F. (2003). Lysostaphin disrupts Staphylococcus aureus and Staphylococcus epidermidis biofilms on artificial surfaces. *Antimicrobial agents and chemotherapy, 47*(11), 3407-3414.

Yang, H., Linden, S. B., Wang, J., Yu, J., Nelson, D. C., & Wei, H. (2015). A chimeolysin with extended-spectrum streptococcal host range found by an induced lysis-based rapid screening method. *Scientific reports,*

5, 17257.

Yang, H., Zhang, H., Wang, J., Yu, J., & Wei, H. (2017). A novel chimeric lysin with robust antibacterial activity against planktonic and biofilm methicillin-resistant Staphylococcus aureus. *Scientific reports*, *7*, 40182.

Yang, H., Zhang, Y., Yu, J., Huang, Y., Zhang, X.-E., & Wei, H. (2014). Novel chimeric lysin with high-level antimicrobial activity against methicillin-resistant Staphylococcus aureus in vitro and in vivo. *Antimicrobial agents and chemotherapy, 58*(1), 536-542.

Yoong, P., Schuch, R., Nelson, D., & Fischetti, V. A. (2004). Identification of a broadly active phage lytic enzyme with lethal activity against antibiotic-resistant Enterococcus faecalis and Enterococcus faecium. *Journal of bacteriology, 186*(14), 4808-4812.

Young, R. (2013). Phage lysis: do we have the hole story yet? *Current opinion in microbiology, 16*(6), 790-797.

Zettlmeissl, G., Rudolph, R., & Jaenicke, R. (1979). Reconstitution of lactic

dehydrogenase. Noncovalent aggregation vs. reactivation. 1. Physical properties and kinetics of aggregation. *Biochemistry, 18*(25), 5567-5571.

Zhang, H., Bao, H., Billington, C., Hudson, J. A., & Wang, R. (2012). Isolation and lytic activity of the Listeria bacteriophage endolysin LysZ5 against Listeria monocytogenes in soya milk. *Food Microbiology, 31*(1), 133-136.

국문 초록

항생제 내성 세균의 발생률이 증가함에 따라, 박테리오파지 (bacteriophage, 파지)에서 유래된 엔도라이신 (endolysin)은 항생제에 대한 유망한 대안 중 하나로서 상당한 주목을 받아오고 있다. 그러나 강력한 능력을 갖는 엔도라이신을 발견하는 것은 시간이 많이 걸리고, 매우 노동 집약적인 작업을 필요로 하며, 용균 활성이 높으면서 가용성 형태의 단백질을 얻는데 어려움이 있다. 이와 관련하여, 엔도라이신이 효소적 활성 도메인 (enzymatic active domain, EAD)과 세포벽 결합 도메인 (cell wall binding domain, CBD)으로 이루어진 모듈형 구조라는 점은 무작위 돌연변이 또는 도메인 교체와 같은 엔도라이신의 engineering을 가능하게 하며, 원하는 특성을 갖는 엔도라이신을 얻는데 효과적으로 이용될 수 있다. 대부분의 황색포도상구균(*Staphylococcus aureus*) 유래의 파지 엔도라이신은 N 말단의 histidine-dependent amidohydrolases/peptidase (CHAP) 도메인, 중앙의 아미데이즈 (amidase) 도메인 및 C 말단의 CBD로 구성된 구조를 갖는다. 엔도라이신의 도메인 각각에 대한 연구에도 불구하고,

도메인 중 특히 아미데이즈 도메인의 정확한 기능이 밝혀지지 않았다. 엔도라이신의 성공적인 모듈 engineering을 위해서 고려해야 하는 중요한 요소는 각 도메인의 정확한 기능을 이해하는 것이다. 이러한 이유로, 본 연구에서는 황색포도상구균 파지 엔도라이신의 각 도메인에 대한 기능적 분석이 수행되었다. CHAP 도메인이 주로 엔도라이신의 용균 활성을 부여하는 반면, 중앙에 있는 아미데이즈 도메인은 황색포도상구균의 세포벽을 분해하는데 효소 활성을 나타내지 않는 것으로 나타났다. 그러나, 아미데이즈 도메인이 결핍된 엔도라이신은 온전한 엔도라이신에 비해 세포벽 분해 활성이 감소되었다. 녹색 형광 단백질 (EGFP)과 CBD 그리고 EGFP와 아미데이즈 도메인 및 CBD로 구성된 융합 단백질의 세포벽 결합 친화력 비교 실험은 아미데이즈 도메인의 주요 기능이 CBD의 세포벽 결합 친화도를 증가시킨다는 것을 밝혔으며, 이 아미데이즈 도메인의 존재가 엔도라이신의 전체적인 용균 활성을 높여주는데 도움을 준 것을 알 수 있다. 본 연구는 황색포도상구균을 타겟하는 엔도라이신의 아미데이즈 도메인이 CBD의 세포벽 결합에 대한 보조적인 역할을 한다는 것을 제시하였으며, 이는 황생포도상구균을 제어하는데 효과적인 항생제 및 진단 제제를 개발하

는 데 유용한 정보가 될 수 있다. 이러한 결과를 바탕으로 원래의 포도상구균 엔도라이신 보다 더 높은 용균 활성을 갖는 엔도라이신을 얻기 위해서 random domain swapping을 수행하였다. Random library에서 LysSA12 CHAP 도메인, LysSA97 아미데이즈 도메인 및 CBD로 구성된 새로운 키메라 엔도라이신인 Lys109이 선정되었고, 황색포도상구균에 대한 용균 활성을 확인했다. 그 결과, Lys109는 황색포도상구균 종에 대해서 원래의 엔도라이신보다 더 강력한 박테리아 용균 활성을 나타냈다. 또한, Lys109는 황색포도상구균의 바이오 필름을 효과적으로 제거하였다. Lys109의 용균 활성은 황색포도상구균으로 오염된 식품 및 스테인리스에서도 확인되었다. 우유에서 황색포도상구균은 900 nM의 Lys109을 처리했을 때, 45 분 이내에 완전히 사멸되어 검출되지 않았다. 반면 LysSA12는 더 높은 농도의 단백질로도 균 사멸 효과를 보이지 않았다. 돼지 고기와 쇠고기의 표면에 황색포도상구균을 오염시키고 50 nM Lys109를 1 시간 동안 처리했을 때, 황색포도상구균이 각각 3−log/cm^2와 2−log/cm^2 감소되었다. 스테인리스에서 100 nM의 Lys109로 1 시간 처리 한 후에는 완전한 박테리아 사멸이 관찰되었다. 이러한 결과는 새로운 키메라

엔도라이신이 황색포도상구균을 제거하는데 효과적이며, 식품 내 황색포도상구균에 대한 생물 방제제 및 식품 가공이나 조리 과정에서 살균제로 활용 가능성이 높음을 시사한다. 또한 본 연구에서는 황색포도상구균과 바실러스 세레우스 (*Bacillus cereus*)를 동시에 제어할 수 있는 융합 단백질을 만들었다. 이것은 다른 박테리아 속을 목표로 하는 두 개의 엔도라이신의 융합이 시도된 첫 번째 연구이다. 바실러스 세레우스를 감염하는 파지 B4로부터 유래된 엔도라이신 LysB4의 전체 및 C 말단이 절단된 LysB4EAD를 나선형 링커 (helical linker)를 통해 황색포도상구균 감염 파지 SA11의 엔도라이신 LysSA11에 융합시켰다. 만들어진 전체 길이 엔도라이신의 융합 단백질들은 황색포도상구균과 바실러스 세레우스 모두에 대해 배향 (orientation)에 관계없이 원래 엔도라이신의 강력한 용균 활성을 유지하였다. 또한, 절단 된 융합 단백질도 전체 융합 단백질에 필적하는 용균 활성을 갖고 있었다. 특히, 만들어진 4개의 모든 융합 단백질은 LysSA11에 비해서 높은 열 안정성을 보였으며, LysB4-LysSA11과 LysB4EAD-LysSA11은 LysB4에 비해서도 높은 열 안정성을 나타내었다. 특히, LysB4EAD-LysSA11의 열 안정성 개선 정도가 월등히 높았

으므로, 이 단백질을 선정해서 특성 분석 및 응용 연구를 진행하였다. 융합 단백질의 강력한 용균 활성은 밥과 같은 식품에 처리했을 때도 관찰되었으며, 이는 이 단백질이 다중 병원체를 표적하는 효과적인 항균제로의 활용가능성을 시사한다. 본 연구에서는 엔도라이신 engineering의 새로운 방법으로 파지 디스플레이 시스템을 사용하여 바실러스 세레우스를 감염하는 파지 PBC1의 엔도라이신인 LysPBC1의 CBD의 세포벽 결합 친화도를 향상시키기 위한 실험을 진행하였다. LysPBC1_CBD는 pIII 코트 단백질을 통해 M13 filamentous 파지 표면에 성공적으로 디스플레이되었고, 디스플레이 된 단백질은 바실러스 세레우스에 대해서 결합 능력이 유지되는 것을 확인하였다. 그 후, 파지에 디스플레이 된 LysPBC1_CBD 무작위 라이브러리 (random library)를 구축하였다. 라이브러리의 몇몇 선택된 클론들 중에서, LysPBC1_CBD Q47H 돌연변이체는 LysPBC1_CBD 야생형에 비교하여 세포벽 결합 능력이 약 2 배 증가한 것으로 나타났다. 이 결과는 파지 디스플레이 시스템을 사용하여 CBD의 engineering이 가능하며, CBD 기반의 세균 검출 기술 개발에 활용이 가능함을 시사한다. 그러나 본 연구에서, 패닝 (panning) 단계 동안 바실러스 세레우

스균에 비특이적으로 결합하는 클론의 수를 감소 시키는데 한계가 있었다. 파지 디스플레이 시스템을 통해 높은 세포벽 친화성을 갖는 CBD를 성공적으로 선택하기 위해서는 추후에 실험 조건의 최적화가 필요하다. 본 연구는 식중독균을 표적으로 하는 박테리오파지 엔도라이신을 다양한 방법으로 엔지니어링하고 응용함으로써 엔지니어링된 엔도라이신이 생물방제제 및 세균 검출 기술 개발에 활용될 수 있는 가능성을 제시하였다.

주제어: 황색포도상구균, 박테리오파지, 엔도라이신, 단백질 엔지니어링, 생물방제, 검출

학번: 2015-30475